

**Genetic and metabolic analysis of downy mildew
resistance in hops (*Humulus lupulus* L.)**

**Dissertation
zur Erlangung des
Doktorgrades der Agrarwissenschaften (Dr. agr.)**

der

Naturwissenschaftlichen Fakultät III
Agrar- und Ernährungswissenschaften,
Geowissenschaften und Informatik
der Martin-Luther-Universität Halle-Wittenberg

vorgelegt von

Alexander Eduard Feiner

Geb. am 19.08.1985 in Mainburg

Gutachter: 1. Prof. Dr. Klaus Pillen
2. Prof. Dr. Ludger Wessjohann
3. Prof. Dr. Gerd Weber

Tag der Verteidigung: 27. Januar 2020

Halle (Saale)

Content

Content	2
List of Figures	5
List of Tables	8
1 Introduction	9
1.1 Hops - <i>Humulus lupulus</i> L.	9
1.2 Downy mildew caused by <i>Pseudoperonospora humuli</i>	10
1.2.1 Characteristics of the fungus	10
1.2.2 Epidemiology.....	11
1.3 Resistance breeding and resistance related metabolites	13
1.3.1 History of hop breeding	13
1.3.2 Resistance to downy mildew in hops	13
1.3.3 Resistance related metabolites in plants	14
1.4 Untargeted metabolomics and secondary metabolites.....	15
1.4.1 The metabolome	15
1.4.2 Untargeted metabolomics.....	16
1.4.3 Metabolomics-assisted breeding	18
1.5 Application of molecular genetics	18
1.5.1 Molecular markers, marker-assisted and genomic selection.....	18
1.5.2 Genotyping-by-sequencing.....	19
1.5.3 Linkage analysis and association study	20
1.6 Objectives of this study and experimental design	21
2 Material and methods	23
2.1 Mapping population	23
2.2 Inoculation with <i>Pseudoperonospora humuli</i>	26
2.2.1 Maintenance of the <i>Pseudoperonospora humuli</i> sporangia	26
2.2.2 Inoculation.....	26
2.3 Phenotyping of downy mildew resistance	27
2.4 Untargeted metabolomics of secondary metabolites	28
2.4.1 Sample preparation for LC-MS measurements.....	28
2.4.2 Analysis of secondary metabolites using mass spectrometry	30
2.4.3 Pathogen-metabolite and metabolite-resistance statistical analysis.....	32
2.5 Downy mildew protection assay	33
2.6 Genotyping and genetic mapping	35
2.6.1 Isolation of genomic DNA and sequencing	35
2.6.2 Single nucleotide polymorphism calling	37
2.6.3 Relatedness of offsprings	38
2.6.4 Linkage mapping of single nucleotide polymorphisms	38

2.6.5	Marker-trait association through genome-wide association mapping	40
2.6.6	Sequence analysis using BLAST	42
3	Results	43
3.1	Phenotyping of downy mildew infection displays large variation	43
3.1.1	Optimization and mapping population for inoculation experiments	43
3.1.2	Phenotyping of the disease	44
3.2	Pre-formed metabolites are correlated with downy mildew resistance	47
3.2.1	Untargeted profiling and annotation of specialized metabolites	47
3.2.2	Downy mildew infection triggers massive mobilization of specialized metabolites.....	52
3.2.3	Downy mildew resistance is correlated to a small set of metabolites with putative protective function	54
3.3	Application of phenylpropanoids mix protects from downy mildew.....	62
3.4	Genetic mapping displays the overlay of specialized metabolites and downy mildew resistance.....	64
3.4.1	Quality filtering of single nucleotide polymorphism markers.....	64
3.4.2	Linkage mapping of single nucleotide polymorphism	66
3.4.3	Genome-wide association of downy mildew resistance	69
3.4.4	Downy mildew resistance and phenylpropanoid levels are regulated by overlapping locus	72
3.4.5	Sequence BLAST of downy mildew resistance association markers	74
4	Discussion	76
4.1	Phenotyping and genetic regulation of downy mildew resistance	76
4.2	Segregation distortion requires new mapping tools	78
4.3	Downy mildew resistance is a metabolic phenomenon	79
4.3.1	Downy mildew resistance is largely prophylactic	79
4.3.2	Phenylpropanoids are the protective compounds	80
4.4	The major downy mildew resistance locus likely confers resistance by regulating the phenylpropanoid biosynthetic pathway.....	82
4.5	Application in breeding and development of bio-fungicides	84
5	Summary.....	86
6	Deutsche Zusammenfassung.....	87
7	References.....	89
8	Supplementary data	107
8.1	Sample list.....	107
8.2	Authentic standards.....	119
8.3	MS/MS spectra of DMR correlated phenylpropanoids	120
8.4	Sequence BLAST of DMR association markers.....	128

9	Paper manuscript, patent application and presentations.....	137
10	Danksagung.....	138
11	Curriculum vitae	139
12	Eidesstattliche Erklärung.....	140

List of Figures

Figure 1: Symptoms of downy mildew infection. A) primary infection, stunted lateral, B) secondary infection on female inflorescence resulted in completely dried out cones.	11
Figure 2: Life cycle of <i>Pseudoperonospora humuli</i> according to Gent et al.(2009).	12
Figure 3: Correlation and association analysis of genetic, metabolic and phenotypic data.	22
Figure 4: Mapping population grown in the incubator, week 9 after germination. Lower-level infected plant set n=192, upper level mock plant set n=192. ...	24
Figure 5: Timeline of preparation of the mapping population, inoculation with <i>P. humuli</i> and leaf sampling.	25
Figure 6: Analysis of the GBS sequencing data using the TASSEL pipeline.....	38
Figure 7: A) Germinated seedlings in Jiffy pots, week 2, B) seedlings week 6, just before cloning, C) cloned genotypes in Oasis wedges, week 6, D) fully developed plants, week 13, just before inoculation.	43
Figure 8: Different levels of downy mildew infection seven days after inoculation across the mapping population. A) resistant=1, B) tolerant =3, C) medium=5, D) susceptible=7, E) highly susceptible=9. Pot size=5 x 5 cm.	44
Figure 9: Frequency of mean values of disease scores of n=142 disease phenotyped hop individuals used for the optimization of the phenotyping experiment.	45
Figure 10: Frequency of mean values of disease scores of n=192 disease phenotyped hop individuals. A) Inoculation experiment 1 and B) inoculation experiment 2.	46
Figure 11: Distribution of disease scores in both independent inoculation experiments (n=192). Lines are medians, boxes are interquartiles and whiskers 1.5x the interquartile range.....	46
Figure 12: Total ion chromatogram of the pool sample in A) positive ion mode and B) negative ion mode. Basepeak chromatogram of the pool sample in C) positive ion mode and D) negative ion mode.....	49
Figure 13: Validation of rutin in a pool sample with authentic standard in positive mode. A) Extracted ion chromatogram of $m/z = 611.1607 \pm 0.005$ Da of pool sample (blue) and rutin (red). B) MS/MS spectrum of pool sample with precursor $m/z=611.1595$, $rt=77.2$, 20.0-50.0 eV and C) MS/MS spectrum of pure rutin standard with precursor $m/z=611.1594$, $rt=76.9$, 20.0-50.0 eV. .	50
Figure 14: <i>Pseudoperonospora humuli</i> -induced phytochemical response in the hop leaf. Log ₂ -fold changes of all basepeaks recorded in A) positive and B) negative ion mode 48 hours after infection. In grey the insignificant responses and in black the significant FDR <0.05 corrected inductions after infection are shown.	52
Figure 15: Log ₂ -fold changes of basepeaks with phytochemical annotation in A) positive and B) negative mode. In grey the insignificant responses and in black the significant FDR <0.05 corrected inductions after infection are shown.	53
Figure 16: Correlation between the DMR-to-metabolite correlation coefficients from the infected plant set (R_{Infected}) and the DMR-to-metabolite correlation coefficients from the mock treated plant set (R_{Mock}) in A) positive and B) negative mode. BP=basepeaks, PP=phenylpropanoid annotations.	55

Figure 17: Correlation between DMR seven days after infection and the power-transformed, scaled and centered ion count of basepeak ID pos6197 quantified in leaves 48 hours after infection. A) infected plant set and the B) mock treated plant set.....	55
Figure 18: MS/MS scan 1314, MS/MS spectrum of [M-H] ⁺ ion of m/z 355.10 at rt=22.6 sec, cosine=0.98, shared peaks=3.....	59
Figure 19: MS/MS scan 1312, MS/MS spectrum of [M-H] ⁺ ion of m/z 355.10 at rt=47.7 sec, cosine=0.98, shared peaks=4.....	60
Figure 20: MS/MS scan 509, MS/MS spectrum of [M-H] ⁻ ion of m/z 353.09 at rt=21.5 sec, cosine=0.94, shared peaks=5.....	60
Figure 21: MS/MS scan 510, MS/MS spectrum of [M-H] ⁻ ion of m/z 353.09 at rt=48.1 sec, cosine=0.96, shared peaks=5.....	61
Figure 22: Phenotypic effects of the four conditions in the DM protection assay on genotype 168. (A) Protection/Infection. (B) Mock/Infection. (C) Protection/Mock. (D) Mock/Mock. Pot size= 5x5 cm.....	63
Figure 23: Boxplots of candidate metabolites protection assay, mock control for either protection or infection solution/suspension. Protection solution with 1mM mix of candidate metabolites, infection suspension with <i>P. humuli</i> . n=10.	63
Figure 24: Relatedness of 192 individuals of F1 mapping population against parents 'Yeoman' x '21588m'.....	64
Figure 25: Minor allele frequency of 1,049,502 SNPs within the 192 F1 genotypes of the mapping population.....	65
Figure 26: Genetic maps. A) paternal map of 259 SNPs ('21588m'), segregation type II and B) maternal map of 161 SNPs ('Yeoman'), segregation type I.	67
Figure 27: Consensus map of maternal and paternal markers, segregation types I, II and III, containing 210 SNP markers.....	68
Figure 28: Log quantile-quantile (QQ) plot of 950,479 association tests (SNPs) for downy mildew resistance in the mapping family. Significant markers after Bonferroni correction were S3_50054921, S3_50054946 and S3_50054950.	70
Figure 29: Linkage group-based (black and grey) Manhattan plots of DMR markers. Significant phenylpropanoid associations are highlighted in red (positive ion mode A),C); negative ion mode B), D)). A, B) 259 paternal ('21588m') segregating DMR markers (Bonferroni p=0.05/259=1.9e-04, blue line). C, D) 161 maternal ('Yeoman') segregating DMR markers (Bonferroni p=0.05/161=3.1e-04, blue line).....	72
Figure 30: Linkage group-based (black and grey) Manhattan plots of 210 DMR markers (Bonferroni p=0.05/210=2.4e-04, blue line) on consensus map of 10 linkage groups. Significant phenylpropanoid associations of positive ion mode A) and negative ion mode B) are highlighted in red.....	74
Figure 31: Phenylpropanoid biosynthesis pathway on KEGG map. DMR correlated metabolites with negative correlation are marked in red, positive correlated compounds are marked in green. Ferulate-5-hydroxylase (F5H) as a DMR associated candidate is marked in blue.....	83
Figure 32: MSMS spectrum of mass ID neg4563, m/z=353.09.....	120
Figure 33: MS/MS spectrum of mass ID pos10896, m/z= 355.10.....	120
Figure 34: MS/MS spectrum of mass ID neg4566, m/z= 353.09.....	121
Figure 35: MS/MS spectrum of mass ID pos10893, m/z= 355.10.....	121
Figure 36: MS/MS spectrum of mass ID neg4564, m/z= 353.09.....	122
Figure 37: MS/MS spectrum of mass ID neg3624, m/z= 325.09.....	122

Figure 38: MS/MS spectrum of mass ID neg4500, $m/z= 351.07$	123
Figure 39: MS/MS spectrum of mass ID neg1121, $m/z= 195.06$	123
Figure 40: MS/MS spectrum of mass ID neg4072, $m/z= 195.07$	124
Figure 41: MS/MS spectra of mass ID pos3313, $m/z= 211.10$	124

List of Tables

Table 1: Rating of sporulation on diseased leaves.....	27
Table 2: Used reagents and equipment for the extraction of polar compounds.....	29
Table 3: Used reagents and equipment for the LC-MS analysis.	31
Table 4: Treatments in the bioassay for activity testing of selected phenylpropanoids.....	33
Table 5: Selected phenylpropanoids tested in bioassay (Kanehisa and Goto 2000).	34
Table 6: Summary of positive and negative peak tables, basepeak annotations and MS/MS spectra of pool sample and authentic standards.....	48
Table 7: Features/annotations up- or down-regulated 24 hours after inoculation with <i>Pseuoperonospora humuli</i> and correlated to disease score seven days after inoculation.	51
Table 8: Correlation of phenylpropanoids extracted from either infected (R_{Infected}) or control (R_{Mock}) plants 48 hours after treatment to DMR in plants seven days after infection ($\text{FDR} < 0.1$).....	58
Table 9: Identified and mapped SNPs of mapping family on consensus map.	69
Table 10: Flanking markers on the DMR significant scaffold LD153786 on the 'Shinshu Wase' reference genome (Natsume et al. 2015). Significant DMR association markers are marked in bold.	71
Table 11: Candidate genes on 'Shinshu Wase' scaffolds containing SNPs in LD with DMR Markers S3_50054921, S3_50054946, S3_50054950 in target organism <i>Arabidopsis thaliana</i> (Lamesch et al. 2012). The complete list of genes and scaffolds is shown in the supplementary data.....	75
Table 12: Sample list including sample type, treatment, sample weight and replicate downy mildew scoring rates of experiment 1.....	107
Table 13: List of authentic standards analyzed in the study.....	119
Table 14: m/z intensities of MS/MS spectra of DMR correlated phenylpropanoids	125
Table 15: Candidate genes on 'Shinshu Wase' scaffolds containing SNPs in LD with DMR Markers S3_50054921, S3_50054946, S3_50054950 in target organism <i>Arabidopsis thaliana</i> (Lamesch et al. 2012).	128

1 Introduction

1.1 Hops - *Humulus lupulus* L.

Hops, *Humulus lupulus* L., is a dioecious perennial member of the *Cannabaceae* family and originates from Asia (Murakami et al. 2006). The two genera of the *Cannabaceae* family, represented by *Humulus lupulus* L. and *Cannabis sativa* L. (hemp, marijuana), $2n = 2x = 20$ respectively (van Bakel et al. 2011), hypothetically diverged about 27.8 million years ago (Laurson 2015).

Hops was classified into three species which are *H. lupulus*, *H. scandens* and *H. yunnanensis* (Small 1978; Barrie 2011). *Humulus lupulus* is entirely spread in the Northern Hemisphere (Small 1978; Neve 1991). Furthermore, *H. lupulus* has been subdivided into five different taxonomic varieties: 1) var. *lupulus* for wild hops and cultivars with European origin, 2) var. *cordifolius* for Japanese wild hops, and 3) var. *neomexicanus*, 4) *pubescens* and 5) *lupuloides*, for wild hops from North America. Distinctive morphological characteristics, such as hairs on the bine and number of lobes on the leaf, can be detected between the different varieties (Small 1978). Molecular markers used for cladistic analyses support the five species delineation, with some caveats (Reeves and Richards 2011).

The history of cultivation and domestication of hops in Europe is unknown. Nevertheless, historical records suggest that hops were already used by the Romans (Wilson 1975). The origin of European cultivars descended either from the cultivation of native wild hops or from migrated plants from the East (Moir 2000). But only little is known about their migration routes and origin or their phylogenetic relationships (Neve 1991; Pillay and Kenny 1996; Murakami 2000).

Only the female plants (Figure 1B) are economically important and mainly used for beer brewing as a flavoring as well as bittering agent and because of their antibacterial properties ensuring proper yeast fermentation. They are grown for unfertilized, ripe, female inflorescences (hop cones). Because of its complex pool of secondary metabolites, hops are used as a source of pharmaceuticals in modern applications such as biofuel production and animal fodder (Ososki and Kennelly 2003; Stevens and Page 2004; Nagel et al. 2008; Siragusa et al. 2008; Miranda et al. 2016).

The earliest written evidence of hop cultivation mentions a hop garden in Germany in 736 (Neve 1991). It was found in a rule book of a Benedictine monastery in France that hops were used in beer in the year 822 (Eyck and Gehring 2015). Nowadays the hop production takes place on both the Southern and Northern hemispheres between 35th and 55th latitude due to strong photoperiodism requirements for flowering (Neve 1991) and encompassed 60,672 ha with a production of about 116,200 mt in crop 2018 (Hopsteiner 2018).

1.2 Downy mildew caused by *Pseudoperonospora humuli*

1.2.1 Characteristics of the fungus

Pseudoperonospora humuli, the causal organism of hop downy mildew, is an obligate biotrophic oomycete pathogen and has been a serious threat in hop growing areas in recent years (Gent et al. 2017). Especially in humid hop growing areas it is one of the most severe disease. Resulting losses in yield and quality vary depending on susceptibility of the variety, timing of infection and weather conditions. The damage can range from non-detectable in hot and dry years to heavy crop losses in quantity and quality as well as plant death in humid seasons.

It was first described from diseased hop tissue in Japan by Miyabe and Takahashi in 1906 as *Peronoplasmopara humuli* n. sp. and later revised systematically by Wilson in 1914 (Miyabe and Takahashi 1906; Skotland and Romanko 1964; Mitchell 2010). *P. humuli* primarily reproduces asexually through sporangia in a polycyclic manner throughout the growing season. By the late 1920s, additional hop growing regions including British Columbia, England, Germany, and the Pacific Northwest reported downy mildew infection. One explanation for the rapid expansion of the distribution of the disease may be the movement of plant materials across international borders during establishment of regional hop breeding programs.

1.2.2 Epidemiology

Under high disease pressure during flowering, leaves and cones are infected and become dark brown and dry out completely (Figure 1B). Systemically infected shoots or laterals referred to as “spikes” emerge in spring following the cessation of dormancy (Figure 1A). These diseased shoots display stunted growth and symptoms of chlorosis. An uneven distribution of the infection can lead to both healthy and infected shoots growing on the same plant.

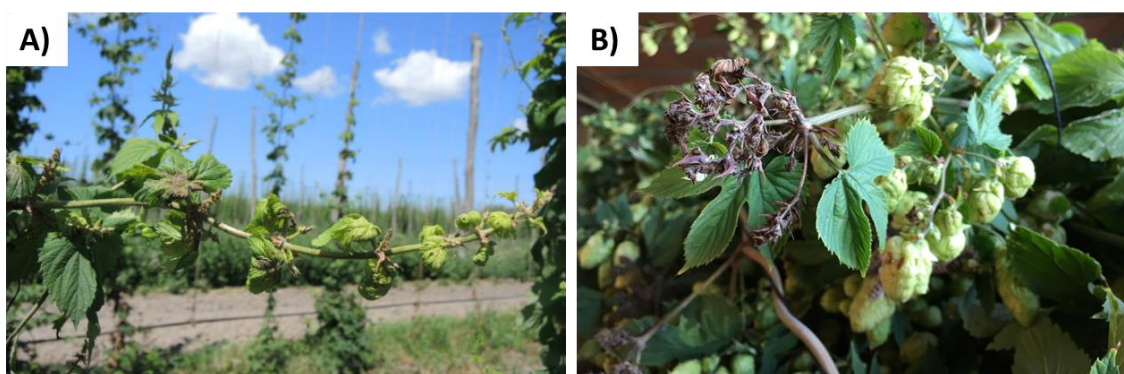


Figure 1: Symptoms of downy mildew infection. A) primary infection, stunted lateral, B) secondary infection on female inflorescence resulted in completely dried out cones.

The mycelium of the downy mildew fungus overwinters on material left in the field or within the plant (Figure 2). As the plant starts to grow in spring, young shoots are already infected with this overwintering mycelium. The mycelium produces a microscopic spore-bearing structure, called a sporangiophore, on the underside of leaves of stunted shoots. This structure causes an asexual type of spores, called zoospores, which infect cones and leaves.

Sporulation occurs on the abaxial surface with sporangiophores emerging in the early morning hours when temperatures during night are above 6°C and relative humidity is greater than 90% (Royle 1970; Royle and Thomas 1973; Royle and Kremheller 1981). Once temperature is favorable (10 to 21°C) and free water is present, sporangia release swimming zoospores which enter open stomata. The infection can become systemic and infected meristem tissue causes growth abnormalities such as spikes (basal and lateral) (Skotland 1961; Royle and Kremheller 1981).

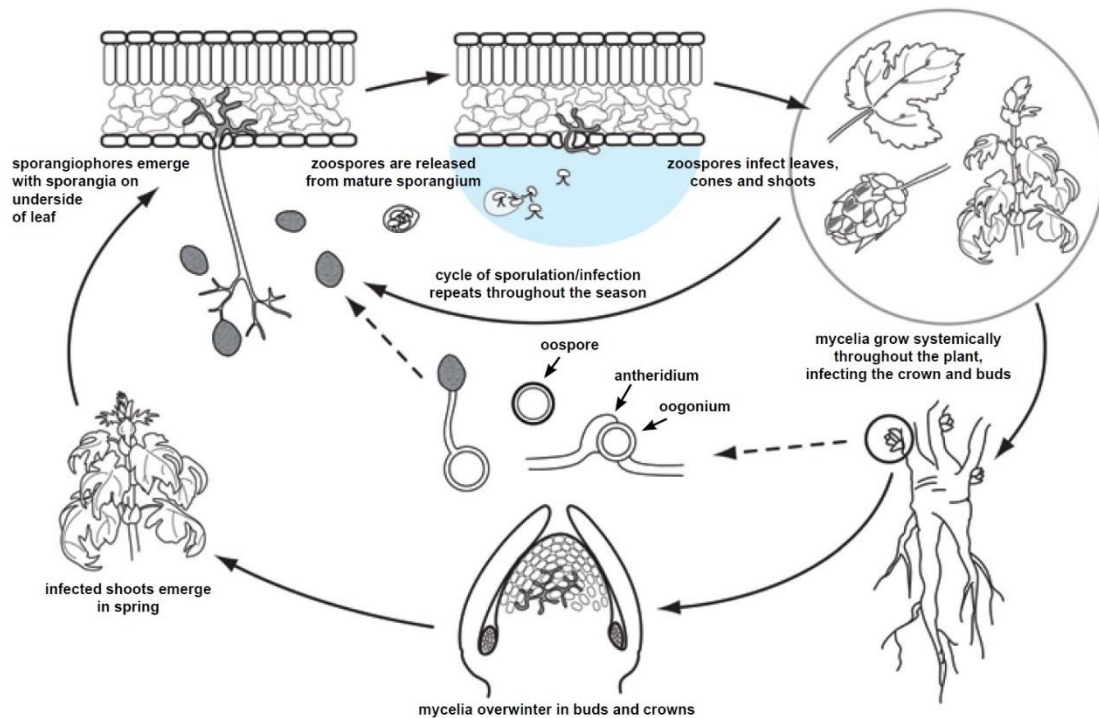


Figure 2: Life cycle of *Pseudoperonospora humuli* according to Gent et al.(2009).

The foliar phase of the disease primarily functions as a mechanism of secondary spread of the pathogen between plants in a hop yard. The crown rot phase is primarily associated with production of basal spikes or crown death, which may occur in highly susceptible cultivars (Royle and Kremheller 1981; Woods and Gent 2016). Lastly, infection of the cone is of primary, industrial concern, due to loss of yield or quality (Royle and Kremheller 1981).

The role of oospores, the sexual spores of the pathogen in the disease cycle, is unclear. While oospores can be found in necrotic tissues, their overall importance in the epidemiology and life cycle of *P. humuli* has yet to be determined (Parker 2007; Mitchell 2010; Gent et al. 2017).

1.3 Resistance breeding and resistance related metabolites

1.3.1 History of hop breeding

At the beginning of the 20th century the first organized hop breeding program started at Wye College in Kent, England, and was established to release new cultivars for beer production (Neve 1986; Darby 2006).

Already at that time the requirements for the breeding program were to develop pathogen resistant varieties with high yield, pleasant aroma and high concentrations of alpha and beta acids (Neve 1986; Patzak 2005). For this purpose hop plants from North America were introduced into European breeding programs because of their high concentrations of prenylated compounds (Neve 1986; Darby 2006).

Other European growing regions established breeding programs after massive devastation of downy mildew caused by the fungal pathogen *Pseudoperonospora humuli*. The first appearance was recorded in Japan in 1906 and shortly thereafter in North America which marked the greatest threat to hop cultivation up to that time. New centers of hop research were founded in Germany, Czech Republic and USA to defy the attack of such pathogens (Biendl et al. 2014).

The reproductive mode of hops affects many aspects of crop management and breeding. Males and female regenerative organs are dimorphic while families are highly heterozygous and phenotypically variable. Genetically diverse genotypes are obtained by single mating followed by phenotypic selection and fixation of desired genotypes by asexual reproduction. Diverse factors such as a high degree of heterozygosity, dioecy and obligate outcrossing, a poorly understood gender-determination system and a large genome size (2.57 Gb according to Natsume et al. 2015) contribute to the difficulty of hop breeding (Neve 1991; Darby 2006; Matthews et al. 2013; Zhang et al. 2017).

1.3.2 Resistance to downy mildew in hops

A natural disease resistance reduces the pathogen growth in or on the plant and protects plants in two ways. On the one hand, by pre-formed structures and chemicals, or on the other hand by infection-induced responses of host immune system (Malamy and Klessig 1992; Mauch-Mani 1996; Dixon 2001).

Breeding for resistance is one of the most important tasks in developing new hop cultivars. Released cultivars like the U.K. 'Yeoman' and 'Challenger' (Neve and Darby 1983; Neve 1991) or the American 'Teamaker' (Henning et al. 2008) are well known varieties with downy mildew resistance and have been used as breeding sources for many decades.

However, the underlying biochemical resistance mechanism in hops has not been completely elucidated, yet. The focus of hop breeding in the past years was the investigation of resistance associated markers within QTL mapping studies (Parker 2007; Henning et al. 2015). Such research provided more evidence for the quantitative nature of downy mildew in hops controlled by multiple loci across the genome, which was hypothesized decades ago (Neve 1991).

Studies in crops also being attacked by oomycetes such as grapevine and cucumbers revealed the accumulation of stilbenoids and specific host transcriptional responses in resistant genotypes (Pezet et al. 2004; Malacarne et al. 2011). This kind of investigations might rise the interest of breeders, if such biochemical processes are also active in resistant hop cultivars.

1.3.3 Resistance related metabolites in plants

Antimicrobial metabolites contribute to resistance against various pathogens mostly in an induced manner (Malamy and Klessig 1992; Dixon 2001; Thordal-Christensen 2003). However, the investigation of secondary metabolites and their complex role in resistance were difficult to assess due to the lack of appropriate tools to exactly determine metabolite localization and transport mechanisms in plant tissues or cells.

Many stress-induced compounds are classified as phytoalexins which are antimicrobial chemicals synthesized in response to pathogen attack. Included are pterocarpan, prenylated isoflavonoids, stilbenes, isoflavans, psoralens, coumarins, 3-deoxyanthocyanidins, flavonols and aurones (Dixon 2001). Higher levels of salicylic acid in response to exposure to UV light and ozone or infection in crops, such as in cucumber, tobacco and Arabidopsis, are part of a signaling process result in systemic acquired resistance (Dixon and Paiva 1995; Dixon 2001).

For example, phenylpropanoids act in multiple aspects of plant responses towards both biotic and abiotic stresses. They are not only key contributors of the plants resistance towards pathogens, but are also indicators of plant stress responses upon variation of mineral treatment or light (La Camera et al. 2004).

Secondary metabolites are well-known disease defense compounds, and, for example, biochemical markers for powdery mildew in hops have been investigated (Cerenak et al. 2009). Testing extremely susceptible or resistance cultivars, a Slovenian research group afforded resistance markers (e.g. santalene, germacrene-D or alpha-selinene) which had a correlation between powdery mildew infection and the abundance of secondary metabolites.

1.4 Untargeted metabolomics and secondary metabolites

1.4.1 The metabolome

The collectivity of all metabolites within an organism is referred to as the metabolome (Fiehn 2002). Primary metabolites relate to amino acids, organic and fatty acids, sterols, sugars and sugar alcohols (Kráľová et al. 2012) whereas secondary metabolites mainly refer to defensive compounds such as phytohormones and chemicals discussed in section 1.3.3 including their precursors, intermediates and derivatives (Croteau et al. 2000; Wasternack 2007; Kráľová et al. 2012; Tiago et al. 2017). Due to their involvement in cellular and physiological energetics, signaling and structure metabolites play an important role in biological systems (Vinayavekhin et al. 2010).

Basically, the metabolome is the result of gene expression (Sumner et al. 2003). Therefore, metabolites are heavily influenced by biotic and abiotic factors and as a corollary: the whole metabolome is affected by such factors (Dixon and Paiva 1995; Kráľová et al. 2012). Biotic factors such as mycorrhizal fungi (Kogel et al. 2010), pathogens (Paranidharan et al. 2008; Cerenak et al. 2009; Chong et al. 2009; Thakur and Sohal 2013; Lazazzara et al. 2018) and herbivores (Kutyniok and Müller 2012) can change the constitution of the metabolome. Moreover, abiotic factors in the environment, perhaps climate change, will have persistent consequences for the plant metabolome (Tiago et al. 2017). Therefore, a major goal

in plant biology is to investigate the biochemical pathways and conditions of plant secondary metabolism to understand their relation to other organisms.

1.4.2 Untargeted metabolomics

Recently, metabolomics has benefited from considerable improvements in mass spectrometry as well as data analysis and interpretation (Carreno-Quintero et al. 2013). Metabolomics is applied to understand complex biological systems on metabolite level using high-throughput quantification, in most cases mass spectrometry, and identification technology combined with statistical methods (Fiehn et al. 2000).

Two main approaches to identify and quantify a complete set of metabolites in biological organisms or objects are (1) targeted and (2) untargeted metabolomics (Fiehn 2002; Patti et al. 2012).

(1) In a targeted approach an hypothesis about the importance of a particular set of metabolites and their biological role already exists (Hollywood et al. 2006; Lokhov and Archakov 2009). Since the identities of the detected metabolites and their belonging to classes is known prior the measurements the analytical workflow can be optimized to measure content of a specific set of compounds. Increased analytical depth due to enhanced sensitivity, higher precision and the possibility to use absolute quantification of metabolite levels are the main advantages of this approach (Fiehn 2002).

(2) In an untargeted metabolomics study on the other hand, the compounds in a given sample are (mostly) unknown. Thus, the focus in such a study is the unbiased detection and quantification of a metabolome with its small molecule constituents as complete as possible with the purpose to generate novel hypotheses about their biological importance (Hollywood et al. 2006; Lokhov and Archakov 2009). The main advantage of an untargeted approach is the possibility to analytically detect novel, unexpected regulations of metabolite levels. Often relative quantification suffices to compare metabolite levels in several groups of biologically variant samples.

Both targeted and untargeted metabolomics are quantitative methods providing limited information about the underlying molecular mechanisms which are re-

sponsible for altered metabolite levels. Since the early works on secondary metabolite profiling in model plants (von Roepenack-Lahaye et al. 2004) untargeted metabolomics has been preferably used as a diagnostic tool (Ellis et al. 2007) for the determination of biomarkers (Shulaev 2006), the unbiased fingerprinting of plant products (Farag et al. 2012), for metabolite based phylogeny (Farag et al. 2013) and also for the determination of developmental stages of organisms (Riewe et al. 2017).

Advantages of modern mass spectrometry (MS) technologies are the detection and quantification of low molecular weight metabolites with high sensitivity even at very low concentrations and the identification of metabolites within a large number of different chemical classes (Riewe et al. 2017; Knoch et al. 2017). Additionally, structural information received from tandem mass spectrometry allows precise identification (Farag et al. 2012). Thus, mass spectrometry plays an important role in many metabolomics studies analyzing the composition of small molecules.

Moreover, the constantly improving MS-based data analysis including mass spectral deconvolution and peak detection is an important tool in metabolomics research. *XCMS* and *CAMERA* are open source freewares containing novel algorithms for efficient Liquid chromatography/mass spectrometry (LC/MS) metabolite data processing (peak-picking and alignment) (Smith 2010; Kuhl et al. 2012). In general, resulting data matrices contain mass-to-charge (m/z) values and corresponding intensities of detected ions. Retention times of preceding separations, like chromatography, can be also used to index metabolites (Riewe et al. 2017).

Untargeted metabolomics on hops has been performed by the Wessjohann group, comparing various analytical methods for the detection of cultivars (Farag et al. 2012, 2014), genetic changes (Gatica-Arias et al. 2012) or medicinal properties (Farag et al. 2013).

1.4.3 Metabolomics-assisted breeding

The plant metabolome is part of the link between the phenome and the genome and can be characterized as the readout of the plant physiological status. Therefore, researchers were highly motivated to unravel the underlying genetic processes of plant metabolism and its natural variation (Wen et al. 2014; W. Chen et al. 2014). Due to the latest technology improvements in genotyping and high-throughput profiling, metabolite-based genome-wide association study (mGWAS) became a capable tool to dissect the biochemical and genetic background of metabolism (Luo 2015).

Researcher have investigated the interdependences between resistance and metabolite levels involved in protecting the plant from pathogen attack (Pezet et al. 2004; Riedelsheimer et al. 2012; Lazazzara et al. 2018). Especially in the process of grape breeding, resistance correlated metabolites, such as, resveratrol and the viniferins, have been used for decades as metabolic markers for selecting genotypes with potential resistance to *Plasmopara viticola*, the downy mildew on grapevines (Pool et al. 1981; Malacarne et al. 2011; Chitarrini et al. 2017).

1.5 Application of molecular genetics

1.5.1 Molecular markers, marker-assisted and genomic selection

Molecular markers are polymorphisms found naturally in populations that reveal variation at DNA sequence level (Semagn et al. 2006). The technology of molecular markers allows plant breeders and geneticists to locate and understand the basics of the numerous gene interactions determining complex traits (Carreno-Quintero et al. 2013). The latest and third generation of detecting molecular markers include single nucleotide polymorphisms (SNP). A SNP occurs when a single nucleotide in the genome of an individual differs between members of a biological population. SNPs are the most abundant molecular markers with higher frequency and far higher prevalence than Simple Sequence Repeats (SSRs). While individual SSRs may have much higher polymorphic information content, SNPs as a class of markers have a high level of polymorphism and because of high density distribution, SNPs can often be found near or within a gene (He et al.

2014). Therefore, SNPs can be used to generate ultra-high-density genetic maps, for phylogenetic analysis, for mapping traits and for fast identification of individuals (He et al. 2014).

Molecular breeding methods, such as marker-assisted selection (MAS) and genomic selection (GS) have the capability to complement conventional breeding selection methods by providing a direct, precise and sophisticated system (He et al. 2014; B. Singh and Singh 2015). Huge advantages afforded by MAS and GS over conventional breeding methods are (1) the possibility of screening large numbers at a very early stage in the selection process and (2) no dependence of marker composition on environmental influences. Furthermore, MAS and GS do not require the pathogen of investigation for selection nor is the breeder dependent on developmental stages (B. Singh and Singh 2015). However, successful application of DNA-based selection requires an understanding of the complex genetic architecture underlying variation in the phenotype. More specifically, GS requires the identification of the marker-trait-association of each individual SNP, which entails the screening of the whole genome of the plant of interest (Gupta et al. 2010; D. Singh et al. 2011; Kumar et al. 2011; J. Chen et al. 2011), while on the other hand, MAS requires targeted selection of genomic regions based on SNPs with large non-additive independent effects.

1.5.2 Genotyping-by-sequencing

The continuously decreasing cost of sequencing technologies and advances in high throughput-screening led to genome-wide SNP genotyping using the method called Genotyping-by-Sequencing (GBS) (Elshire et al. 2011). Recently, Matthews, Coles and Pitra were the first group to apply GBS to hop breeding (Matthews et al. 2013).

Genotyping-by-sequencing is used to identify differences in SNP variation in a given set of individuals and combines existing methods - genotyping and next-generation sequencing (NGS). GBS protocols can have multiple forms but all of them share the following core steps. First step is the sequencing of the DNA from the individuals under observation followed by the second step which maps the sequencing reads to a reference whole genome or transcriptome sequence

(Elshire et al. 2011). Subsequent procedures are SNP calling, filtering, genotyping and imputation, continued by haplotype identification and further downstream analysis (Elshire et al. 2011).

Established applications of GBS are general marker discovery, recombination characterization and haplotype identification to quantitative trait loci (QTL) analysis, genome-wide association studies (GWAS) and genomic selection. In many plant breeding programs GBS has been successfully used in implementing GWAS, genetic linkage analysis, genomic diversity study, genomic selection and molecular marker discovery (He et al. 2014). Zhang et al. (2017) have developed a high-density molecular marker system for *Humulus* spp., using GBS.

1.5.3 Linkage analysis and association study

Genetic association and linkage analysis are the common strategies to unravel the genetic background of specific traits and diseases (Schaid, Chen, and Larson 2018). The main difference between these two approaches is that association analysis concentrates on the relation between a specific allele and the trait within populations whereas linkage analysis explores the relation between the transfer of a genetic locus and the trait within families. Applying both approaches many different types of variants could have been detected (Carlson et al. 2004).

Mainly in human genetics genome-wide association studies helped researcher to investigate common variants underlying complex diseases or traits (Carlson et al. 2004). A genome-wide association study is defined to identify genetic associations with observable traits or the presence or absence of a disease or condition. Furthermore, it relies on the information of millions of SNPs and their pattern of linkage disequilibrium (LD) across the entire genome. In out-crossing species, for example in maize, LD usually extends short distances with less than 1500 bp (Gaut and Long 2003). Arabidopsis as an inbreeding species LD can vary from 1 to 50cM (millions of bp) or even more (Nordborg et al. 2002).

For a successful association mapping the candidate gene needs to have a measurable effect on a phenotypic trait with the candidate markers being either within or directly up- or downstream of this gene. In association mapping, markers associated with the phenotype are more broad-based rather than cross-specific

which makes association mapping more powerful for detection of common alleles within populations than linkage mapping (Carlson et al. 2001).

1.6 Objectives of this study and experimental design

Objectives of the study

Downy mildew caused by *Pseudoperonospora humuli* generates economically important losses in hop. Thus, disease resistances for a sustainable farming in the future are among the main goals in breeding at present. The primary objectives of this research were to identify genes, SNP markers and secondary metabolites associated with and predictive for the resistance to downy mildew, in order to (1) increase the knowledge in disease resistance (2) facilitate breeding of resistant genotypes and (3) find novel bioactive compounds applicable as bio-icides for sustainable hop production. An F1 mapping population was produced by a bi-parental mating among characterized single plant varieties contrasting in disease resistance, to obtain a full-sibling population with large variation in downy mildew symptom development. Quantitative disease resistance assessment after controlled inoculation with spores, followed by metabolite profiling at a discrete developmental stage was applied to identify metabolites with a putative role in resistance. The whole association panel (family) was genotyped-by-sequencing towards identifying putative genes associated with the resistance to downy mildew and with the metabolites associated with this phenomenon. While functional gene studies were beyond the scope of this dissertation, identified metabolites with tentative protective activity were tested functionally.

Experimental design

The goal of this study was the integration of metabolomic, phenotypic and genetic information to understand pathogen response on a biochemical molecular level. The isolation of molecular selection markers and chemical correlates of resistance was accomplished within the following objectives.

Step 1: Phenotyping of downy mildew resistance

- Development of an F1 bi-parental mapping population consisting of 192 full-siblings under controlled *ex situ* conditions.
- Scoring of downy mildew resistance (DMR) of all individuals of the family by monitoring secondary infection on leaves.

Step 2: Untargeted metabolomics

- Developing a LC-MS method for the untargeted metabolomics suitable for high-throughput-screening.
- Applying untargeted metabolomics to quantitate differences in total secondary metabolite content profiles determined by LC-MS in a mapping population, for both infected and mock treated complete progeny sets.
- Identifying metabolites enhanced in response to inoculation with *Pseudoperonospora humuli* using ANOVA.
- Identifying disease-protecting metabolites using Pearson correlation.

Step 3: Genotyping-by-sequencing and genome-wide association study

- Discovering GBS SNPs in the mapping population.
- Performing GWAS with disease incidence and metabolite profiles of infected and mock-infected plants (general linear model).
- Discovering genetic markers for DMR and control of secondary metabolites (general linear model).
- Characterizing genetic markers for control of secondary metabolites correlated to DMR (trait dissection).

The principle of the correlation and association analysis is shown below in Figure 3.

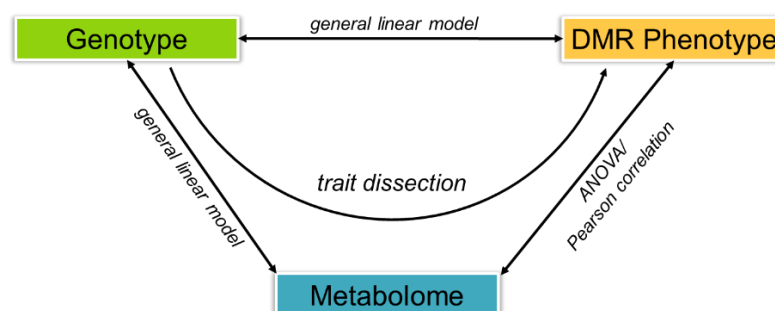


Figure 3: Correlation and association analysis of genetic, metabolic and phenotypic data.

2 Material and methods

2.1 Mapping population

Optimization experiment

Vigorous, healthy and synchronous plant growth was necessary for the infection, sampling and disease scoring. The control of confounding effects was most important in order not to stress the plants which might have correlated to environmental factors rather than the disease attack. Therefore, plants were grown under continuous conditions not to distort the metabolic readout.

A method describing growth conditions of seedlings in an incubator for hop metabolomics has not been proven before, so a proof-of-concept experiment was essential to learn more about the handling of seedlings in an incubator. Due to the limited quantity of seeds the mapping population ('Yeoman' x '21588m') an alternative cross from the existing Hopsteiner seed collection was selected. For this reason a downy mildew resistance segregating cross originated from the resistant USDA female 'Teamaker' (Henning et al. 2008) and the susceptible Hopsteiner male '#242' (Hopsteiner 2014) was germinated and 142 F1-plants were established for the optimization experiment.

Mapping population

The mapping population for the study with variation in downy mildew resistance was produced by crossing the resistant line 'Yeoman' (female) (Neve 1991) with the susceptible line '21588m' (male) (USDA 2018). The crossing partners were grown for 150 days in an experimental nursery in Yakima, WA, USA, until flowering occurred, and pollination was conducted by cross pollination. After 60 days flowers were harvested, and seeds were collected by sieving the pollinated cones.

Due to costs of GBS sequencing and metabolomic analysis the number of offsprings were set to 192, which reflects the number of two deep well plates used for sequencing format (2x96). This seemed to be an appropriate size in terms of costs, feasibility and statistical power for such a genetic and metabolic study compared to former published studies (Morreel et al. 2006; Heuberger et al. 2014; van den Oever et al. 2016).

Since downy mildew is a systemic infection it was necessary to start with asymptomatic material, therefore, seeds without any infection were used. Additionally, to minimize environmental influences plants were grown in an incubator which guaranteed homogeneous growth and infection conditions.

Unfortunately, the parents, which were only available from field and greenhouse at that time, could not be grown and tested within this experiment. Due to safety and quarantine rules it was not allowed to include plants grown outside the S1 area at the Leibniz-Institute for Plant Biochemistry (IPB). The risk to bring in pest and pathogens from field or greenhouse was too high and chemical applications prior the experiment would have distorted their reaction against the pathogen.

Seed germination

Seeds were placed in a plastic container on paper towel and misted with pure H₂O. The container of seeds was stored in a refrigerator set between 3-4°C for six weeks. After seed stratification dormancy was broken and the seeds could be germinated in moist Jiffy pots (Jiffy, 44mm) on June 15th, 2015 and grown in an incubator (CLF PERCIVAL, DR-66VL) (Figure 4). 192 random selected genotypes (males and females, undetermined) were used to perform the study. Plants were watered once a week to keep the Jiffy pots moist.



Figure 4: Mapping population grown in the incubator, week 9 after germination. Lower-level infected plant set n=192, upper level mock plant set n=192.

Growth conditions in the incubator

Optimization of growth conditions in the incubator brought the desired effect of shorter internodes and more compact plants within the 192 test genotypes. Light conditions were reduced from 250 $\mu\text{mol}/\text{m}^2/\text{s}$ to 130 $\mu\text{mol}/\text{m}^2/\text{s}$ and temperatures were also lowered at day and night (day: from 20°C to 18°C; night from 18°C to 16°C) and relative humidity was set to 75%. These conditions provided the best environment for homogeneous growth.

Cloning and fertilization of seedlings

The seedlings were cloned seven weeks after germination. Sterile softwood wedges (Oasis, 102 cell counts per tray) were used for propagation into two identical sets, one for infection and one for mock treatment (Figure 5). After four weeks, cuttings were repotted into 5x5 cm pots using sterilized and steamed potting soil. To stimulate axillary meristem growth and root development apical growth tips were pinched after two sets of leaves were developed. Plants were fertilized applying 500 ml “Kamasol brilliant blau”, N/P/K- ratio of 8/8/6 in a 0.2 % concentration directly into each tray 20 and 35 days after cloning.

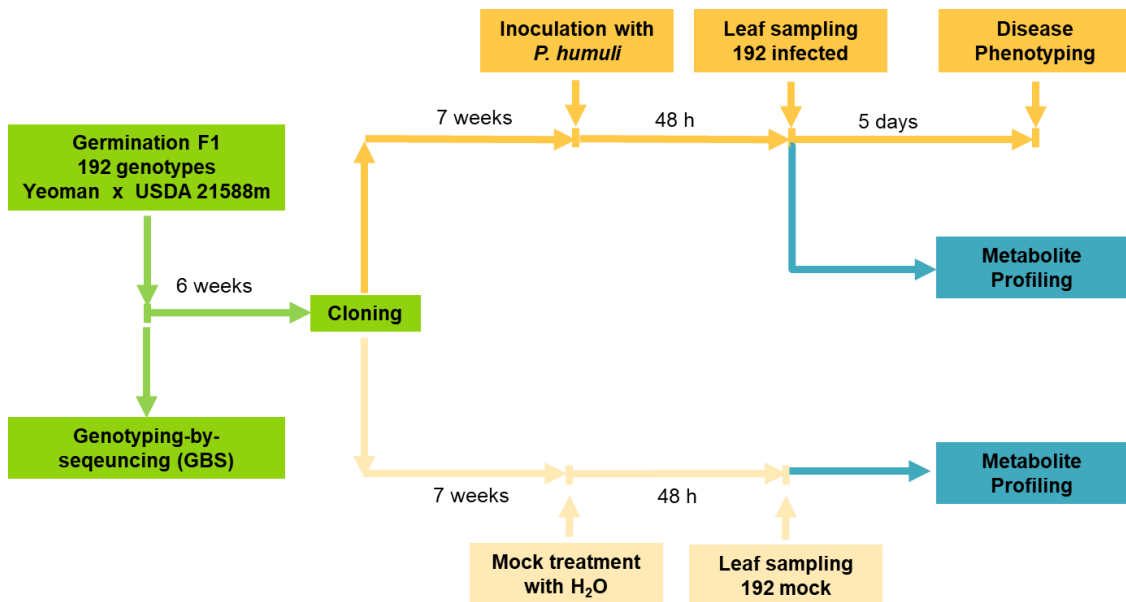


Figure 5: Timeline of preparation of the mapping population, inoculation with *P. humuli* and leaf sampling.

A detailed explanation for the timing of all executed treatments will be given in the following sections.

2.2 Inoculation with *Pseudoperonospora humuli*

To elicit the downy mildew infection phenotype and study resistance and the effect on the metabolome, the fungus *P. humuli* was cultivated and later inoculated on the hop plants of the mapping population.

2.2.1 Maintenance of the *Pseudoperonospora humuli* sporangia

Since *P. humuli* is an obligate biotrophic fungus, it does not grow on artificial media so the German susceptible cultivar 'Hallertauer Mittelfrüh' (Biendl et al. 2014) was used as propagation host. The plants were grown and infected in the greenhouse at Hopsteiner Mainburg using the identical conditions and inoculation method described below.

The original intention was to use a German field isolate for this study. However, the crop year 2015 was exceptionally dry and hot and spores were not available. Instead, an aggressive isolate from Wye Hops, Ltd, U.K. was utilized to infect the maintenance plants in order to have viable and fresh spores for the experiment. The goal of the study was to get a better understanding about the resistance mechanism independent from the source of spores while the switch to the U.K. isolate did not play a significant role. Another advantage was, that the resistance of 'Yeoman', used as the resistance source genetic donor in this study, is rated according to U.K. phenotyping results and has a resistance to this specific isolate.

2.2.2 Inoculation

Seven weeks after cloning the majority of plants were in the BBCH 19 stage of growth (Rossbauer 1995) and the inoculation with downy mildew was performed (Figure 5). Incubator conditions were set to 16°C day and 15°C night temperature during the infection with 99% relative humidity to guarantee perfect infection conditions (Royle and Thomas 1973; Neve 1991; Mitchell 2010). The sporangia were washed off from infected leaves with 4°C cold deionized H₂O. The abaxial leaf area was inoculated with a suspension of *P. humuli* (1×10^5 sporangia/ml adjusted with Neubauer hemocytometer) using a hand-held atomizer (CAMAG, reagent sprayer) until the whole leaf was covered with fine droplets. After inoculation, plants in trays were covered for 24 hours in darkness with lids to keep humidity as high as possible to ensure optimum infection conditions (Royle and

Thomas 1971, 1973; Cohen and Eyal 1980; Johnson and Skotland 1985; Mitchell 2010).

Five days post-infection the conditions were set back to day 18°C/night 16°C and plants were covered with lids again applying high humidity to improve sporulation on the infected leaves. Seven days post infection leaves were visually evaluated based on the occurrence of sporulation. The mock plant set was sprayed only with deionized H₂O but was otherwise treated identical as compared to the infected set. To prevent any cross-contamination with *P. humuli* from drips from the upper set, mock-infected plants were grown on upper level (Figure 4) in the incubator and each procedure was always started with the mock set.

2.3 Phenotyping of downy mildew resistance

Disease scoring

The infection of downy mildew on the abaxial side of the leaf is complicated to screen. An automated phenotyping method has not been developed yet and the infection had to be scored visually. To assess the infection phenotype, a visual disease scoring of the infected phenotypes was performed seven days post inoculation. In each of the two independent experiments all genotypes were scored three times in random order. Five categories denoting increasing susceptibility (Table 1) were used to assess the downy mildew infection based on the leaf area showing sporulation, chlorosis and necrosis, which is a common method used in plant phenotyping (Bundessortenamt 2000).

Table 1: Rating of sporulation on diseased leaves.

Rating	Diseased leaf area
1 = resistant	no sporulation
3 = tolerant	1-20 % of leaf area infected
5 = medium	21-50 % leaf area infected
7 = susceptible	51-80 % leaf area infected
9 = highly susceptible	81-100 % leaf area infected

To prove the reliability of the inoculation assay, the experiment including the scoring was performed twice. For each experiment the downy mildew resistance phenotype was calculated as the mean of all three phenotypic assessments.

The t-test was used for statistical comparison of reliability and repeatability of both phenotyping set across average disease indices. For the combined phenotype-chemotype analysis, phenotypic mean values of the first experiment were used only because both data domains were collected from a single experiment.

Broad-sense heritability

The broad-sense heritability defined as $h^2 = V_G/V_P$ (Allard 1960) was calculated with the R package '*lme4*' (Bates et al. 2015) while V_G stands for variation in genotype and V_P for variation in phenotype. The calculation was used to capture the proportion of phenotypic downy mildew resistance variation due to the genetic background. Input data for the calculation of h^2 were the disease scores of both phenotyping experiments taking three replicated phenotyping scores in each of two phenotyping events as variance in phenotype into account.

2.4 Untargeted metabolomics of secondary metabolites

2.4.1 Sample preparation for LC-MS measurements

Leaf sampling

All plant material (mock/infected) was harvested at the middle of the light period within two hours. Harvesting of three of in average ten fully developed leaves per individual was executed 48 hours after inoculation. The timing was chosen according comparable downy mildew studies in grapevine where metabolic changes could be observed (Bollina et al. 2010; Toffolatti et al. 2012; Chitarrini et al. 2017). The harvest happened within the S1 incubator room as quick as possible without disturbing the plants or transferring them to a location of uncontrolled conditions. Shading, cooling or mechanical quenching while harvesting was reduced to the minimum.

Approximately 200 mg of fresh material was cut off, folded and transferred to the 20 ml scintillation vial. The uncapped vial was immediately dipped completely into liquid nitrogen to terminate any further biochemical reaction. The procedure from

cutting the leaf until shock-freezing in liquid nitrogen did not take longer than 10 seconds. The opened scintillation vial was placed on dry ice for ten minutes to allow for the evaporation of liquid nitrogen before closing the vial with a screwcap. The samples were stored until further usage at -80°C .

Extraction of secondary metabolites

Deep frozen sample material was re-randomized and homogenized applying two stainless steel beads to each scintillation vial and using a robotic cryogrinder (30Hz, five minutes). Additionally, a pool sample was generated containing 10mg \pm 2 mg of each homogenized individual sample. The ground and homogenized material of each individual sample was balanced regarding genotype and treatment and 150 mg \pm 10 mg fresh weight was extracted with 1.5 ml pure methanol by shaking for 15 minutes followed by 15 minutes ultrasonification at 4°C . After centrifugation for 15 minutes at 14000 rpm at 4°C , 300 μl of the supernatant were aliquoted into LC-MS vials and dried for 3 hours at 10 mbar in a speedvac. The dried vials were filled with argon, crimped and stored in sealed bags with silica gel at -80°C until LC-MS analysis. All used reagents and equipment for the extraction of polar compounds are listed in Table 2.

Table 2: Used reagents and equipment for the extraction of polar compounds.

Reagent/equipment	Supplier
Polyvials® V – Natural HDPE	Zinsser Analytic, GmbH, Frankfurt/Main, DE
-86°C ULT Freezer, DW-86L578J	Haier Deutschland GmbH, Bad Homburg, DE
Methanol absolute ULC/MS	Biosolve B.V., Valkenschwaard, NL
2ml extraction vial	Sarstedt AG & Co, Nümbrecht, DE
Vortex Genie 2	Scientific Industries, Inc, Bohemia, USA
Eppendorf Centrifuge 5417R	Eppendorf AG, Hamburg, DE
1.0 ml conical vials	CTZ Klaus Trott, Kriftel, DE
Magnetic steel panel caps	CTZ Klaus Trott, Kriftel, DE

Speedvac RVC 2-33	Martin Christ GmbH, Osterode am Harz, DE
Argon	Air LIQUIDE Deutschland GmbH, Düsseldorf, DE
Cryo Grinder	Labman Automation Ltd., North Yorkshire, UK
Stainless steel beads, 8mm	Wälzkörper Edelstahl, INTEC Industrie- und Werkstattbedarf GmbH, Quedlinburg, DE

2.4.2 Analysis of secondary metabolites using mass spectrometry

Following the study design, sample collection and preparation, LC-MS analysis collecting MS data was performed. The data was then preprocessed, including peak picking and filtering, prior to uni- or multivariate statistical analysis. Metabolites were then identified by accurate mass and retention time, combined with MS/MS fragmentation spectra for structural elucidation, to be placed in a biological context. Additionally, reference compounds were used to validate the annotation procedure.

LC-MS analysis

Randomized and balanced samples were re-solubilized in 500 µl 100% methanol by 5 minutes ultrasonification, centrifuged for 15 minutes at 6200 g and stored in an autosampler at 4°C prior analysis (max. 24 hours before injection). 3 µl extract were injected into a 1.2 µl loop of an ultra-high-pressure injector and analytes were separated by UHPLC using a C18-column at 50°C (50 mm length × 1 mm i.d., 1.8 µm particle o.d.) and the mobile phases 0.1% formic acid in water (A) and 0.1% formic acid in acetonitrile (B). The gradient was 0.5 min: 1% B, 1.75 min: 30% B, 2.25 min: 60% B, 3.75 min: 90% B, 4 min: 99% B, 4.5 min: 99%B, 4.75 min: 1%B, 5 min: 1% B. The flow rate was 800 µl/min. MS spectra were recorded at a frequency of 5 Hz from 100 to 1500 m/z, dry temperature: 250°C, capillary voltage: 4500/-3000 (positive/negative mode), nebulizer pressure: 4 bar, dry gas: 12 L/min, dry temperature: 250°C. Data was externally and internally calibrated and exported as net.CDF file as described previously (Riewe et al. 2017) MS/MS spectra were collected from a pooled sample in auto-MS/MS mode using a scheduled precursor list with target information and identical settings as for the

MS analysis. All used reagents and equipment for the LC-MS measurements of polar compounds are listed in Table 3.

Table 3: Used reagents and equipment for the LC-MS analysis.

Reagent/equipment	Supplier
Agilent 1290 Infinity Binary LC Systems	Agilent Technologies, Santa Clara, USA
ACQUITY UPLC BEH C-18 Column	Waters, Cooperation, Milford, USA
<u>Buffer A</u>	
Water ULC/MS	Biosolve B.V., Valkenschwaard, NL
0.1% Formic acid	Biosolve B.V., Valkenschwaard, NL
<u>Buffer B</u>	
Acetonitrile	Biosolve B.V., Valkenschwaard, NL
0.1 Formic acid	Biosolve B.V., Valkenschwaard, NL
Bruker Maxis II QTOF	Bruker Corporation, Billerica, USA
MPS2 MultiPurposeSampler for LC/MS	GERSTEL GmbH & Co. KG, Mühlheim, DE
Ultra-high-pressure injector	Vici AG International, Schenk, CH

Raw data processing

LC-MS chromatograms in net.CDF format were processed using ‘*xcms*’ (Smith 2010; Kuhl et al. 2012) and ‘*CAMERA*’ as described previously by Riewe et al. (2017). The initial peaktables had 37386/20899 (positive/negative mode) peaks. Peaks eluting before 4 s or after 270 s and peaks found in more than two blank extracts with a median higher than half of the sample median (background) were discarded. *m/z* were modelled using annotation errors as described before to increase mass accuracy. Peak areas were normalized to fresh weight and median value per metabolite for each of the four extraction batches. Metabolite profiles often contain extreme single outliers or even true values, thus, the median is rather used than mean normalization (Lisec et al. 2006). MS/MS spectra were processed exactly as described before.

Peak annotation

All m/z were queried against the Kyoto Encyclopedia of Genes and Genomes (KEGG) database (Release 86.0, Kanehisa and Goto 2000) as $[M+H]^+$, and adducts including $[M+Na]^+$, $[M+CH_3OH+H]^+$ (positive mode), $[M-H]^-$, $[M-H_2O-H]^-$ or $[M+FA-H]^-$ (negative mode) using KEGGREST (Tenenbaum 2018). Sum formulae, KEGG-IDs, names, reactions, pathways and BRITE annotations were retrieved for each identified m/z .

For validation of the peak annotation process, 45 reference compounds known to be present in hops were used as authentic standard (Table 13 supplementary data). Additionally, MS/MS spectra of reference compounds and all detected metabolites in the pool sample were considered for the validation of the peak annotation. Recorded MS/MS spectra in positive and negative mode were uploaded at Global Natural Products Social Molecular Networking (GNPS) for database query.

All annotations belonging to the KEGG BRITE classes two hierarchy levels downstream “phytochemical compounds” were tested regarding overrepresentation using a Chi²-test. The sum of correlated basepeaks (FDR < 0.1) determined in infected and mock set divided by the total number of basepeaks was used as probability.

2.4.3 Pathogen-metabolite and metabolite-resistance statistical analysis

Variance of *P. humuli* induced metabolic changes

Metabolite data was log₁₀-transformed for ANOVA testing using R (R Core Team 2014). False discovery rate (FDR) corrections were applied as described Benjamini and Hochberg (1995). Metabolite variances with FDR corrected $p \leq 0.05$ were considered as significant.

Correlation between metabolites and downy mildew resistance

Metabolite data was log₁₀-transformed and Box-Cox-transformed (Box and Cox 1964) for Pearson correlation testing between metabolite abundance and DMR using R (R Core Team 2014). False discovery rate (FDR) corrections were applied as described by Benjamini and Hochberg (1995). DMR correlations with an FDR corrected $p \leq 0.05$ were considered as significant.

2.5 Downy mildew protection assay

The correlation analysis (see section 3.2) showed that certain phenylpropanoids are significantly involved in the resistance against downy mildew. Moreover, especially these compounds are pre-established prior infection and have a putative protective activity. After the noticeable correlation analysis, it was intended to test their protective activity *in planta*.

Ten downy mildew susceptible genotypes (27, 31, 34, 43, 45, 46, 101, 148, 156, 168, see sample list in supplementary data) were cloned and cultivated as described in 2.1 in order to produce asymptomatic test plants. Selected phenylpropanoids were separately dissolved in H₂O and added to final concentration of 1 mM (protection), a concentration expected to show no osmotic effect but potential protection. Pure H₂O was used as control (mock). *P. humuli* suspension was prepared as described in 2.2 (infection) and again H₂O was used as control (mock). 50 days after propagation, three replicates of each genotype were sprayed with either protection or mock solution and two hours later additionally infection or mock (Table 4) in 2 x 2 factorial design. Seven days later, the plants were disease phenotyped as described in 2.3.

Table 4: Treatments in the bioassay for activity testing of selected phenylpropanoids.

Treatment	Phenylpropanoid protection	Infection
A	Protection	Infection <i>P. humuli</i>
B	Mock (H ₂ O)	Infection <i>P. humuli</i>
C	Protection	Mock (H ₂ O)
D	Mock (H ₂ O)	Mock (H ₂ O)

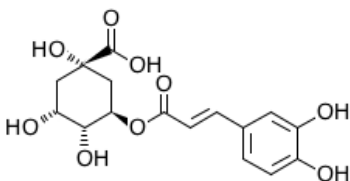
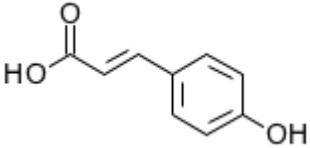
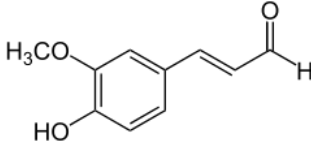
Treatment A was sprayed with the „protection-mix“ of phenylpropanoids and infected two hours later according to the inoculation experiment in section 2.2. Treatment B was mock-sprayed with deionized H₂O and infected with *P. humuli* to show the effect without „protection“. In treatment C the effect of the mix on the plant, e.g. toxic or growth-related effects, could be evaluated, while treatment D was assigned as a control (unaffected growth) with the application of H₂O only.

The statistical evaluation was made using the t-test between treatment A and B checking the significance of the effect on disease control.

Tested phenylpropanoids

Chlorogenic acid, *p*-coumaric acid and coniferyl aldehyde (all from Sigma Aldrich, Table 5) were sprayed on the lower side of the leaves two hours prior infection (same procedure as described in chapter 2.2). Each compound was dissolved by ultrasonification in deionized water at a concentration of 1mM and mixed equally together for application.

Table 5: Selected phenylpropanoids tested in bioassay (Kanehisa and Goto 2000).

Chlorogenic acid	<i>p</i> -coumaric acid	Coniferyl aldehyde
CAS: 202650-88-2 KEGG ID C00852 Molecular formula: C ₁₆ H ₁₈ O ₉ Molecular weight: 354,31 g/mol	CAS: 501-98-4 KEGG ID C00811 Molecular formula: C ₉ H ₈ O ₃ Molecular weight: 164,16 g/mol	CAS: 458-36-6 KEGG ID C02666 Molecular formula: C ₁₀ H ₁₀ O ₃ Molecular weight: 178,18 g/mol
		

2.6 Genotyping and genetic mapping

The objective of the genome-wide mapping in this study was to display the marker-trait association of downy mildew resistance and the genetic conditions of secondary metabolites correlated to resistance. The question was, if these traits of interest overlap on a molecular marker level and if they are regulated by the same loci on a genetic map. Molecular marker systems including nonreferenced genotyping-by-sequencing (GBS) markers (Matthews et al. 2013) and genome-wide association study (Henning et al. 2015; Hill et al. 2016) have been developed and used for genetic mapping of disease resistance in hops before. In this study the GBS approach outlined in Elshire et al. was applied (Elshire et al. 2011).

2.6.1 Isolation of genomic DNA and sequencing

DNA extraction

For DNA extraction and sequencing, 50 +/- 5 mg of fresh leaf material was sampled into 96-deep-well plates, lyophilized to absolute dryness and sent to LGC Genomics (Berlin, Germany). Additionally, 50 +/-5 mg of fresh leaf material of both parents, grown in the greenhouse at Hopsteiner Mainburg, were taken, lyophilized to absolute dryness and sent to LGC Genomics, too. Total genomic DNA for library construction and sequencing, as applied in Maghuly et al. (2018), was isolated from the leaf material using the high throughput DNA extraction method published by Xin and Chen (2012) with additional enzyme treatment in a subsequent normalization step. The subsequent workflow was executed for the 192 offsprings and two parents according to the following protocol wrote and provided by LGC Genomics, Berlin.

Restriction digest

100-200 ng of genomic DNA were digested with 2 Unit MspI (NEB) in 1 times NEB4 buffer in 20µl volume for 2 hours at 37°C. The restriction enzyme was heat inactivated by incubation at 80°C for 20 min.

Preparing indexed Illumina libraries

a) Ligation reaction and final repair

15 μ l were transferred to a new 96well PCR plate, mixed on ice first with 3 μ l of one of the 192 L2 Ligation Adaptors and then with 12 μ l Mastermix (combined of 4.6 μ l D1 water/ 6 μ l L1 Ligation Buffer Mix/ 1.5 μ l L3 Ligation Enzyme Mix). Ligation reaction were incubated at 25°C for 15 min and heat inactivated at 65°C for 10 min. 20 μ l Final Repair Master Mix were added to each tube and the reaction was incubated at 72°C for 3 min.

b) Library purification, amplification and pooling

Reactions were diluted with 50 μ l TE 10/50 (10mM Tris/HCl, 50mM EDTA, pH:8.0) and mixed with 80 μ l Agencourt XP beads, incubated for 10 min at RT and placed for 5 min on a magnet to collect the beads. The supernatant was discarded and the beads were washed two times with 200 μ l 80% ethanol. Beads were air dried for 10 minutes and libraries were eluted in 20 μ l Tris Buffer (5 mM Tris/HCl pH 9).

10 μ l of the 192 Libraries were separately amplified in 20 μ l PCR reactions using MyTaq (Bioline) and standard Illumina TrueSeq amplification primers. Cycle number was limited to 14 cycles.

5 μ l from each of the 192 amplified libraries were pooled. 10 μ l from each of the parent`s amplified libraries were pooled to achieve a higher coverage in the later sequencing. PCR primer and small amplicons were removed by Agencourt XP bead purification using 1 volume of beads. The PCR enzyme was removed by an additional purification on Qiagen MinElute Columns. The pooled Library was eluted in a final volume of 20 μ l Tris Buffer (5 mM Tris/HCl pH:9).

Normalization, reamplification, size selection and sequencing

Normalization was done using Trimmer Kit (Evrogen). 1 μ g pooled GBS library in 12 μ l water was mixed with 4 μ l 4x hybridization buffer, denatured for 3 min at 98°C and incubated for 5 hours at 68°C to allow reassociation of DNA fragments. 20 μ l of 2x DSN master buffer was added and the samples was incubated for 10 min at 68°C. One Unit of DSN enzyme (1U/ μ l) was added and the reaction was incubated for another 30 min. Reaction was terminated by the addition of 20 μ l

DSN Stop Solution, purified on a Qiagen MinElute Column and eluted in 10µl Tris Buffer (5 mM Tris/HCl pH:9).

The normalized library pool was amplified in 100µl PCR reactions using MyTaq (Bioline) and standard Illumina TrueSeq amplification primers. Cycle number was limited to 14 Cycles. The nGBS library was finally size selected on a LMP-Agarose gel, removing fragments smaller than 300 bp and those larger than 400 bp. Sequencing was done on an Illumina NextSeq 500 using V2 Chemistry (300 cycles).

2.6.2 Single nucleotide polymorphism calling

The TASSEL (Trait Analysis by Association Evolution and Linkage) software was used for SNP calling in both parents and all 192 offsprings of the F1 mapping family in this study (Bradbury et al. 2007; Glaubitz et al. 2014). The first step involved the quality check and trimming of adapters using Fastq-mcf. Fastq-mcf detects and removes primer and sequencing adapters from the raw sequencing data. Additionally, it removes the poor-quality reads (the reads that contain N's) and discard sequences that are too short (less than 50 bp).

The draft genome of 'Shinshu Wase' (Natsume et al. 2015) was used for the SNP calling. This reference genome with its total size of 2.05 GB covers approximately 80% of the estimated genome size of hop (2.57 Gb) and contains about 130,000 scaffolds. Tassel 5 GBS v2 Pipeline (Glaubitz et al. 2014) was applied to identify tags with at least 10x total coverage and BWA aligner was used to map the resulted tags sequences to the reference genome (H. Li and Durbin 2009). Sources of erroneous SNP calling are ambiguous, and misalignments are caused by gene duplication, the incomplete reference genome as well as low-complexity regions. SNPs with an excessive coverage can be false positives. Once coverage per sample exceeds 120 counts per tag, heterozygosity rates and minor allele frequency are significantly increased, and such SNPs were removed from the analysis. The working steps followed in this study are outlined below in Figure 6.

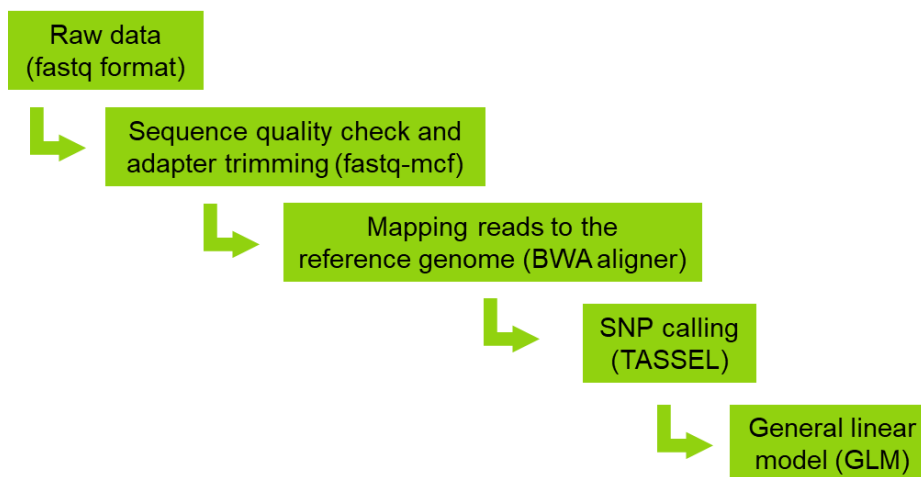


Figure 6: Analysis of the GBS sequencing data using the TASSEL pipeline.

After the SNP calling, individuals were additionally checked for site coverage and discarded if not meeting a coverage of >60%. The association studies with the observed phenotypic traits were performed using the general linear model calculation in TASSEL which is described in more detail in section 2.6.5.

2.6.3 Relatedness of offsprings

In order to identify mislabeling or sources of contamination such as pollen impurity each offspring of the mapping family was considered for quality control. The relatedness of each genotype against each parent was calculated using VCFtools and visualized using R (R Core Team 2014) according to Hyma et al. (2015). Progeny that failed to cluster with most other progeny was flagged for removal.

2.6.4 Linkage mapping of single nucleotide polymorphisms

Linkage maps

A linkage map represents the relative location of genetic markers on the chromosomes of an organism determined by recombination frequency between them after passing from parents to children through meiosis. The recombination frequencies between pairs of marker are estimated within structured mapping populations and are converted to genetic distances (B. Singh and Singh 2015). Software solutions like JoinMap® (Van Ooijen 2011) are able to calculate genetic maps based on the genotyping data. The likelihood of a separation or a linkage is tested against a certain cut off, the Logarithm of Odds (LOD). In this study a

linkage analysis with in the mapping population using JoinMap® 4.0 (Van Ooijen 2011) was conducted, applying the “2-way pseudo-testcross” strategy outlined by Grattapaglia and Sederoff (Grattapaglia and Sederoff 1994) as in other linkage analysis of hop (Seefeldler et al. 2000; Koie et al. 2005; Cerenak et al. 2006; Henning et al. 2015). As hop typically shows a high level of heterozygosity (Neve 1991), and being dioecious, this approach is expected to be an appropriate alternative to a backcross strategy. The constructed, statistical linkage map served as the frame of ordered SNPs for the subsequent association analysis results. The marker ordering and the correlated linkage into groups of markers, gave additional, positional information about associations with observed traits. The additional information from the grouping offered potential to understand the genetic phenomena of the underlying DMR correlated metabolites. For example, a larger number of trait-associated SNPs near each other, can indicate a genetic locus with multiple DNA variations affecting the degree of a trait, and thus, intercorroborate and strengthen confidence in the individual SNP associations.

SNP filtering for linkage mapping

In former linkage mapping studies, a filtering process was necessary to eliminate markers which do not follow certain Mendelian segregation patterns prior to calculation of linkage and order. Also, quality criteria of SNP calling and coverage of the population were also applied as filtering. SNP presence across both parents and occurring within >95% offspring resulted in high-confidence markers (Matthews et al. 2013). Furthermore, SNPs based on parental genotype with distorted segregation patterns were filtered using Rqtl (Broman et al. 2003) for the calculation. For the analysis in the present study, markers were grouped in three segregation types. In segregation type I (nn x np) were exclusively markers which were expected to pass from the mother in 1:1 ratio to the offsprings of the F1 population. The mother is heterozygous (np), the father homozygous (nn). Segregation type II (lm x ll) is exactly the opposite in that the father is heterozygous (lm) and the mother is homozygous (ll). Segregation type III (hk x hk), where both father and mother are heterozygous, contains markers from both father and mother segregating in a 1:2:1 ratio. Markers containing single alleles with unpredicted allele states across less than 5% of individuals were nevertheless kept in the study but the allele was set to missing data. All markers were additionally

filtered for their Mendelian segregation pattern in JoinMap® using the Chi² test of the software. Ad hoc tolerances for segregation distortion were set. Individuals with high levels of missing data ($\geq 5\%$) were also eliminated from the analysis.

Linkage mapping using JoinMap®

This procedure consisted of a “2-way pseudo-testcross” where two separate maps, one maternal (type I) and paternal (type II) linkage map, were constructed with the mapping population using the ‘BC1’ option in JoinMap®. The markers which could be mapped were used in a second step to create a map for type I and type III and for type II and type III as intermediate steps for the later consensus map. The combined male and female map was developed using the cross-pollinated coding scheme ‘CP’ option including type III segregating markers (present in both male and female maps) to develop the final consensus map. Markers were placed into linkage groups (LG) using default settings in JoinMap® v4.0 and a cut-off of recombination frequency of 0.4 and a LOD value higher than 4.0. The theoretical basis for the selection of LOD scores is discussed by Freeman et al. (Freeman et al. 2006). The LOD was selected to maintain as many markers in the analysis as possible.

Gametic phase was determined based on recombination frequency internally by the software. The optimal marker order was determined by using jump threshold of 5.0 and the ripple value of 1.0. To convert recombination data to map distances the Kosambi mapping function (Kosambi 1943) was used. The regression mapping with default settings over several stages calculated the marker placement and distance along linkage groups. The first step was the establishment of a framework map with a reliable marker order. In the second step markers were removed from the analysis until maps could have been constructed within two mapping rounds. These iterative mapping approaches of adding markers to a framework map are commonly employed (Vision et al. 2000; Cheema and Dicks 2009; Ma et al. 2012).

2.6.5 Marker-trait association through genome-wide association mapping

Genome-wide association mapping seeks to identify specific functional genetic variants linked to phenotypic differences in a specific trait. The aim of the GWA in this study was to provide marker-trait association for downy mildew resistance

and metabolite abundance. The resulting association p-values were then mapped on the developed linkage maps giving a better understanding of the genetic structure of the putative DMR control factors.

Traits of interest for the association analysis in this study were

- 1) downy mildew resistance based on DMR phenotype and
- 2) all non-redundant metabolites (basepeaks) of negative and positive ion mode within the infected and mock-infected set.

To investigate the marker-trait association the general linear model (GLM) in TASSEL (Bradbury et al. 2007) was applied. For DMR GWAS the minor allele frequency was set to >1% accepting all individuals while the GWAS for the metabolite data was set to minor allele frequency >1% accepting only individuals with minimum sample count >90%. The reason for the different settings was to get as much information out of the DMR GWAS and to reduce the computational work in the metabolite GWAS calculating thousands of metabolic traits simultaneously.

Subsequently, GLM results were checked for inconsistency by displaying quantile-quantile (Q-Q) plots of estimated $-\log_{10}(P)$ and the expected $-\log_{10}(P)$ (Pearson and Manolio 2008). The Q-Q plot helps to assess the number and magnitude of obtained associations between genotyped SNPs and the observed trait, compared to the association statistics expected under the null hypothesis of no association (The Wellcome Trust Case Control Consortium 2007). A distinct deviation of observed and expected association may be an indicator for false positive or artefacts which needs to be reviewed.

The most common way to reduce the false-positive rate is by applying the Bonferroni correction. The conventional p-value (usually $p=0.05$) is divided by the number of performed tests (number of SNPs) and used as significance cut off in the following analysis (Hochberg 1988). This method has been criticized as far too conservative because the correction assumes independent associations of each SNP with the observed trait but individual SNPs are known to be correlated to some degree due to linkage disequilibrium (Pearson and Manolio 2008).

Nevertheless, Bonferroni (Hochberg 1988) correction has generally been the most commonly used correction for multiple comparisons in GWAS and was also

used in this study. Manhattan plots were used to display the positional associations to DMR and the association overlap with significantly DMR correlated compounds on the established genetic linkage maps.

2.6.6 Sequence analysis using BLAST

In order to identify possible candidate genes on the assembled pieces of the hop genome, scaffolds of 'Shinshu Wase' reference genome (Natsume et al. 2015) used in building the SNP marker system in our study were investigated. SNPs significantly associated to DMR and additional association SNPs which are in linkage disequilibrium with $r^2 > 0.5$ to these DMR markers were used in the BLAST search. Basically, markers in strong linkage disequilibrium can be considered as linked because their observed frequencies of particular combinations of alleles at two loci is higher than expected for random association. This became an important concept in genetic studies to identify and localize genes related traits of interest (Slatkin 2008; Sved and Hill 2018). Therefore, entire scaffolds containing these association SNPs were BLAST (Basic Local Alignment Search Tool) aligned to the plant unigene database (Altschul et al. 1990) at NCBI (NCBI 2018). Scanning the scaffolds for homologies with known plant gene sequence suggested putative genes with a homology match. Sequences of candidates were further considered among knowledge of biosynthetic pathways for plant secondary metabolites and resistance function using 'The Arabidopsis Information Resource' (TAIR, release version 10, Lamesch et al. 2012).

3 Results

3.1 Phenotyping of downy mildew infection displays large variation

3.1.1 Optimization and mapping population for inoculation experiments

Optimization experiment

At the beginning of the experiments an optimization of the phenotyping assay was necessary to establish strong and homogeneous plant material. Additionally, necessary training and practice of logistics for the propagation, the inoculation with *P. humuli* and the leaf sampling within a short period of time was accomplished, in order to systematically influence the metabolic readout as less as possible. Temperature and light modifications as well as inoculation training resulted in successfully grown, infected and phenotyped plants.

Mapping population

192 genotypes were germinated and grown to fully developed plants using the experience out of the optimization experiment (Figure 7). The plant development beginning with the germinated seed growing to an advanced hop plant was comparable with expected greenhouse performance. The different plant stages of germination and propagation described in section 2.1 are shown in Figure 7.

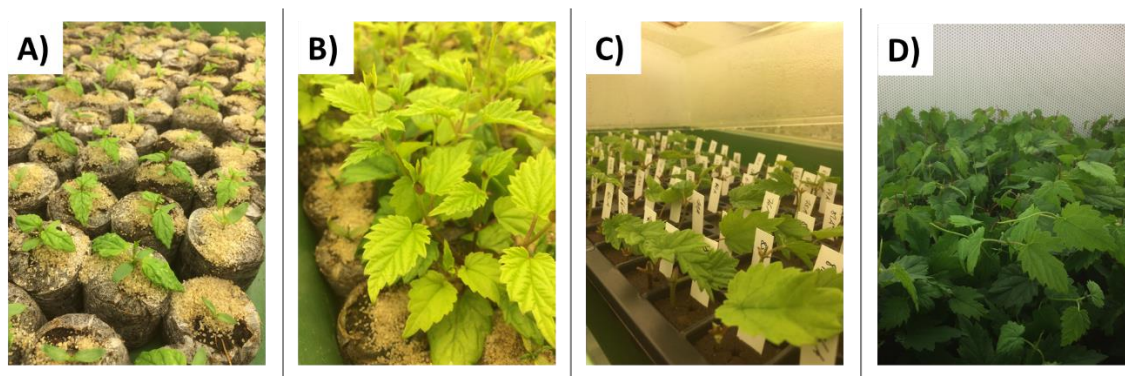


Figure 7: A) Germinated seedlings in Jiffy pots, week 2, B) seedlings week 6, just before cloning, C) cloned genotypes in Oasis wedges, week 6, D) fully developed plants, week 13, just before inoculation.

3.1.2 Phenotyping of the disease

Disease scoring

To receive reliable data for the genome-wide association study and correlation analysis of DMR, phenotyping after inoculation of the mapping population was performed in two temporally independent experiments with three replicate technical phenotyping for each experiment.

Ideal conditions for infection with the fungus on the abaxial side of the leaf are relative humidity above 90% RT and temperatures between 15-21 °C where a clear sporulation can be detected (Royle 1970; Royle and Thomas 1973; Royle and Kremheller 1981). Seven days after inoculation the symptoms of an infection were visible and fully developed for which nearly ideal conditions were present. Additionally, the appearance of all scoring values including the lowest and highest category of 1 and 9, respectively, demonstrated that the infection was fully developed in the most susceptible individuals of the population and the scoring seven days after infection was scheduled at the correct developmental stage. The mock treated plants showed no infection at all, not even at 14 days after inoculation, indicating no contamination happened between the different treatments. Figure 8 illustrates the different levels of infection from A) resistant to E) highly susceptible.

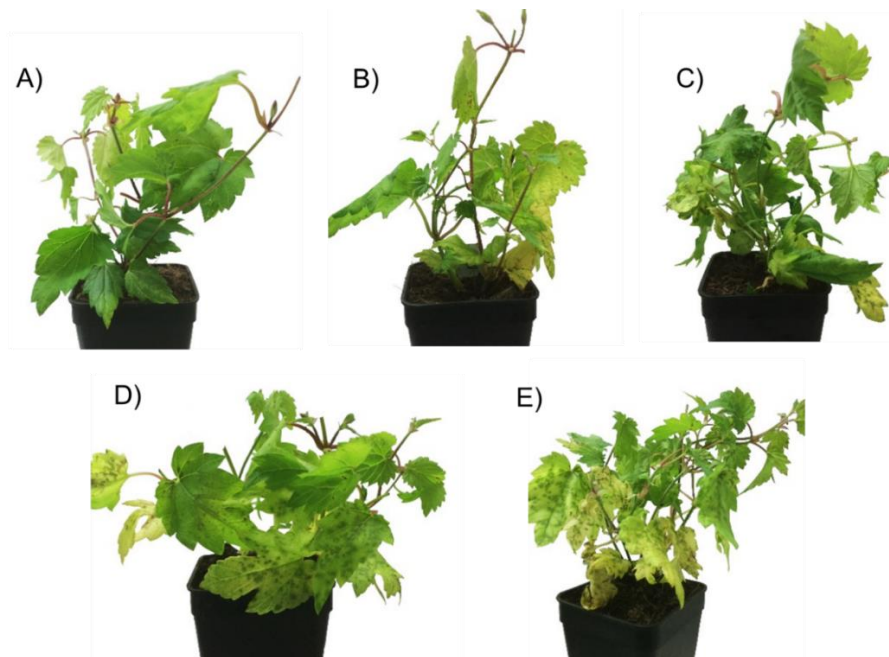


Figure 8: Different levels of downy mildew infection seven days after inoculation across the mapping population. A) resistant=1, B) tolerant =3, C) medium=5, D) susceptible=7, E) highly susceptible=9. Pot size=5 x 5 cm.

Disease scoring of optimization experiment

The optimization achievements resulted in a consistent infection within the test population of 142 individuals. The distribution of the disease scores from 1 to 9 showed that the inoculation was applied correctly and the infection with *P. humuli* could be evaluated. In Figure 9 the frequencies of all disease scores are shown.

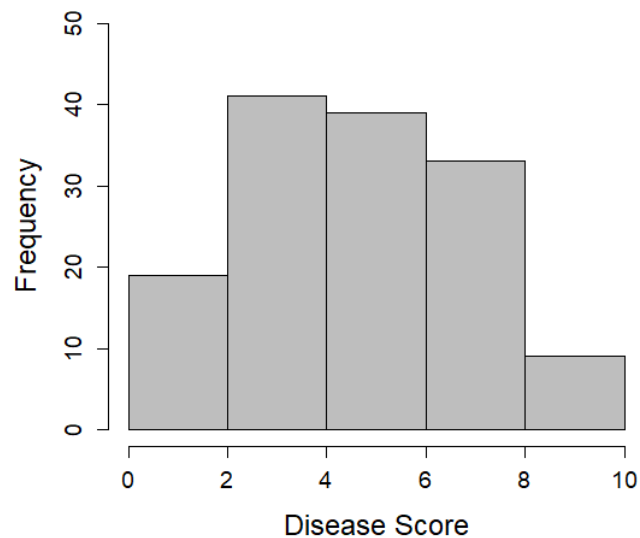


Figure 9: Frequency of mean values of disease scores of n=142 disease phenotyped hop individuals used for the optimization of the phenotyping experiment.

Disease scoring of the mapping population

The downy mildew scoring along the mapping family showed a normal distribution in both independent inoculation tests (Figure 10). Because there were no significant differences between replicated phenotyping scores, data was averaged across the scorings for further correlation analysis. The first experiment showed a slightly higher median (Phenotyping I; M=5.57) in comparison to the second experiment (Phenotyping II; M=5.39) without any significant difference between the groups ($t(382) = -1.0934$, $p=0.2749$), therefore the downy mildew phenotyping assay could be described as consistent and the trait as quantitative (Figure 11).

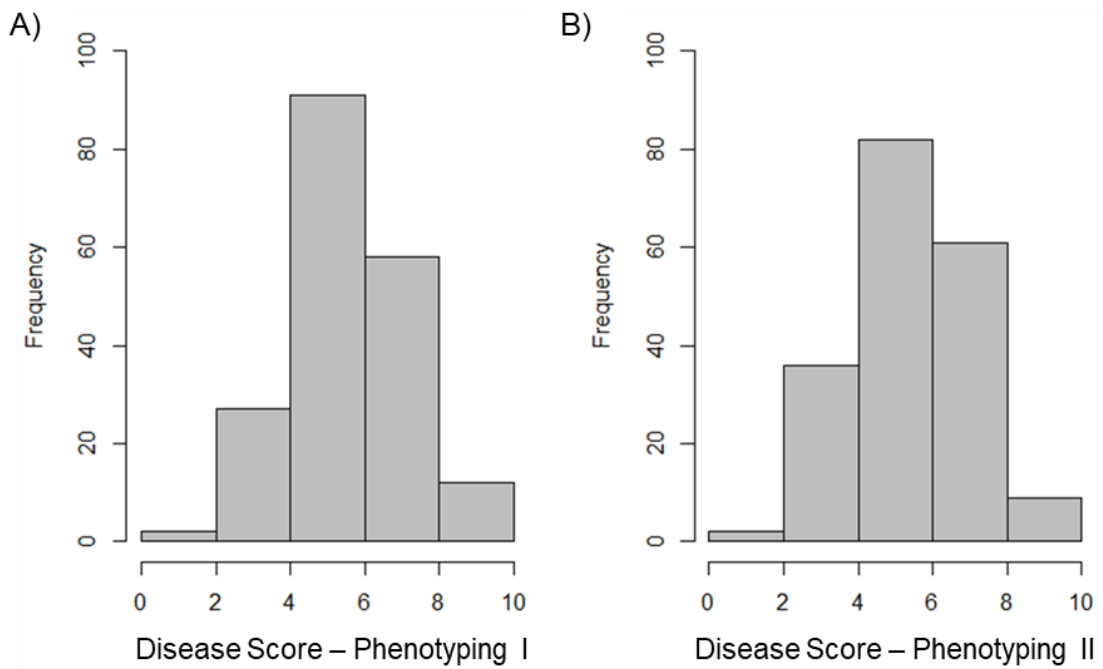


Figure 10: Frequency of mean values of disease scores of n=192 disease phenotyped hop individuals. A) Inoculation experiment 1 and B) inoculation experiment 2.

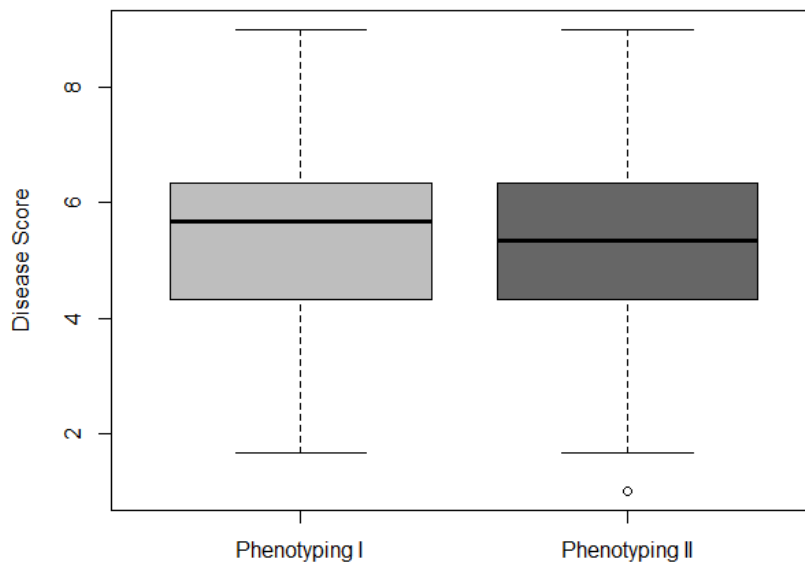


Figure 11: Distribution of disease scores in both independent inoculation experiments (n=192). Lines are medians, boxes are interquartiles and whiskers 1.5x the interquartile range.

Broad-sense heritability

The calculated heritability for the trait “downy mildew resistance” in this mapping family was $h^2 = 0.81$. The high broad-sense heritability value for these conditions and population suggests that the DMR trait variation is genetically determined in the population in this study. Therefore, efforts to limit environmental and systematic influence on trait variation were successful, thus, genetic effects on the trait are accurately measurable and amenable to association with markers. Furthermore, the high heritability in a controlled family makes the prospect of translational application into feasible genetic selection tools for use in other families and environments in a breeding program tenable.

3.2 Pre-formed metabolites are correlated with downy mildew resistance

3.2.1 Untargeted profiling and annotation of specialized metabolites

Untargeted profiling

Polar metabolites from all 384 samples were extracted and analyzed using high-resolution liquid chromatography-mass spectrometry (LC-MS) in both positive and negative ion mode. Per extract, 27324 positive mode and 16256 negative mode redundant chromatographic m/z features were recorded (Table 6) and left after background subtraction, forming 10781 (positive) and 7361 (negative) non-redundant pseudospectra with basepeaks likely representing individual metabolites (Kuhl, Tautenhahn et al. 2012). All m/z were queried against compounds in the KEGG database (Kanehisa and Goto 2000) with an error tolerance of 0.5 ppm, but only annotations of monoisotopic basepeaks with an isotope pattern fit of <60 mSigma (Thiele, McLeod et al. 2011) were considered.

Table 6: Summary of positive and negative peak tables, basepeak annotations and MS/MS spectra of pool sample and authentic standards.

Feature characteristic	Positive mode	Negative mode	Total
<i>m/z</i> features after background subtraction	27324	16256	43580
Pseudospectra/basepeaks (non-redundant analytes)	10781	7361	18142
Identified sum formulae	3312	4047	7359
Unique LC-MS IDs	12567	17896	30463
<i>m/z</i> features with annotation(s)	2567	2287	4854
Pseudospectra/basepeaks with annotation(s)	1774	1942	3716
MS/MS spectra of pseudospectra/basepeaks	4327	1948	6275
MS/MS spectra of authentic standards	15	11	26

The high abundant and over-represented acids in hops, lupulon and colupulon were both at saturation limit. It was assumed that these compounds might have no influence on the downy mildew resistance in hops. Therefore, the dilution of the leaf extract and the measurement of metabolites were optimized in the way that the majority of compounds was in the linear detection area and also minor components could be detected with the limitation in neglecting the activity role of lupulon and colupulon. The injection volume was set to the lowest possible volume of 1.2 μL in order to maximize the chromatographic separation. In Figure 12 the total ion (TIC) and basepeak chromatogram of the pool sample in positive and negative ion mode are shown.

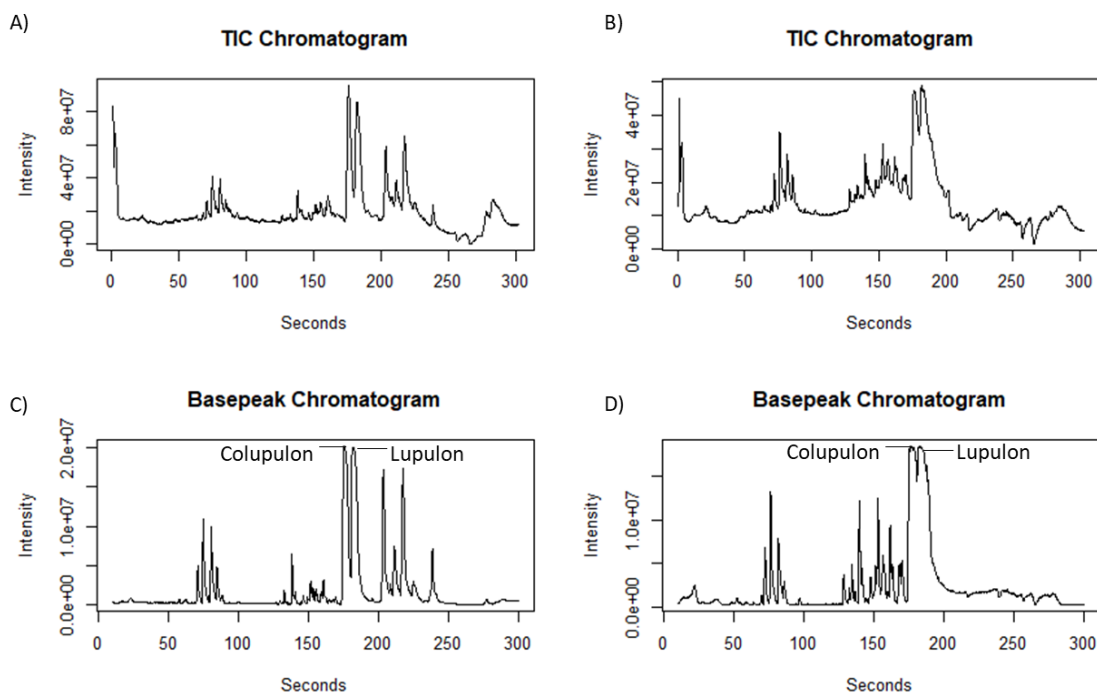


Figure 12: Total ion chromatogram of the pool sample in A) positive ion mode and B) negative ion mode. Basepeak chromatogram of the pool sample in C) positive ion mode and D) negative ion mode.

Authentic standards were used to validate the putative peak annotation in KEGG. Therefore, well known hop compounds were included in the study and measured along with all leaf samples in the MS and MS/MS analysis. The following example shows the validation of the compound putatively annotated as rutin. This metabolite could be validated because of its perfect match in accurate mass, isotope pattern ($m\sigma < 60$), retention time and MS/MS spectrum. In Figure 13 the extracted ion chromatogram (EIC) and MS/MS spectra of rutin in the pool sample and authentic standard is shown.

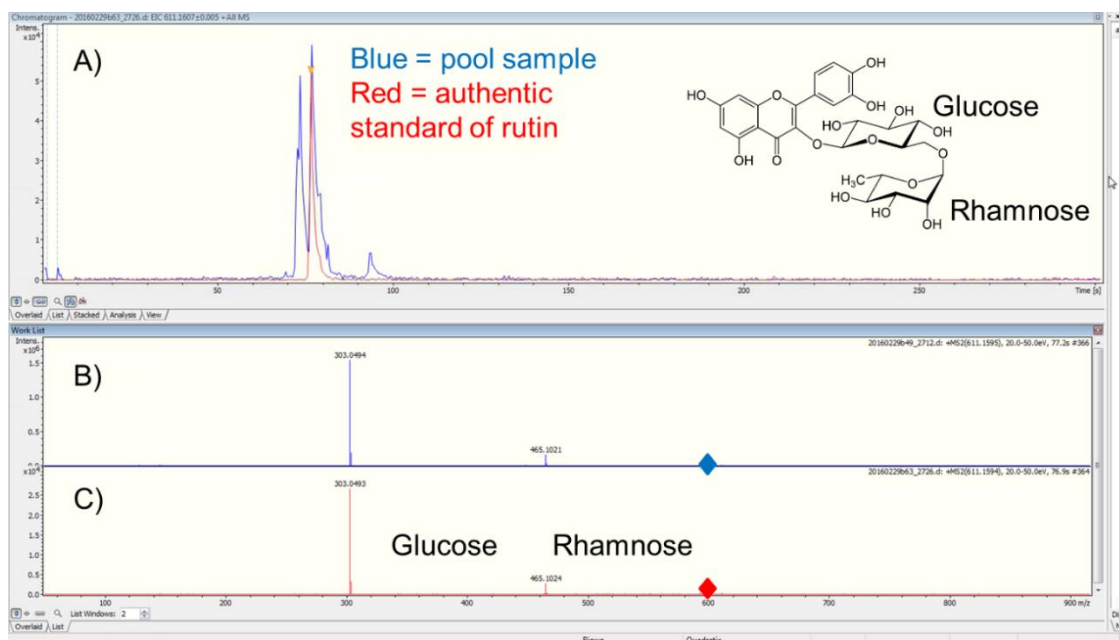


Figure 13: Validation of rutin in a pool sample with authentic standard in positive mode. A) Extracted ion chromatogram of $m/z = 611.1607 \pm 0.005$ Da of pool sample (blue) and rutin (red). B) MS/MS spectrum of pool sample with precursor $m/z = 611.1595$, $rt = 77.2$, 20.0-50.0 eV and C) MS/MS spectrum of pure rutin standard with precursor $m/z = 611.1594$, $rt = 76.9$, 20.0-50.0 eV.

Annotation of specialized metabolites

One or more KEGG sum formulae/structures were assigned to 512 (positive) and 666 (negative) basepeak m/z , and 259 (positive) and 395 (negative) of these basepeaks had a “phytochemical compound” annotation. Table 7 lists the number of “phytochemical compounds” tentatively detected two levels down the KEGG BRITE compound specific hierarchical relationships. While the number of detected alkaloids, fatty acids and amino acids related compounds was low in both modes (<15 per class), the number of flavonoids, phenylpropanoids, and terpenoids was relatively high (> 60). In general, there was consistency in the number of detected metabolites per class between positive and negative mode.

Table 7: Features/annotations up- or down-regulated 24 hours after inoculation with *Pseuoperonospora humuli* and correlated to disease score seven days after inoculation.

Feature type/annotation	Positive mode up/down/total	Negative mode up/down/total
m/z (after background subtraction)	8971/1330/27324***	4165/505/16256***
Pseudospectra/base peaks	2825/533/10781***	1853/256/7361***
Base peaks with KEGG annotations	265/20/512***	286/11/666***
KEGG BRITE phytochemical annotations	143/8/259***	179/6/395***
Alkaloids	4/2/12	4/1/5
derived from ornithine	0/0/1	0
derived from lysine	0/0/2	0/1/1
derived from nicotinic acid	0	1/0/1
derived from tyrosine	3/0/3	2/0/2
derived from tryptophan and anthranilic acid	3/2/8	3/1/4
derived from histidine	0	0
derived by amination reactions	0	0
Others	0	0
Flavonoids	42/0/75***	44/0/103***
Flavonoids	34/0/63***	34/0/82***
Isoflavonoids	16/0/23**	26/0/45***
Complex flavonoids	6/0/10	3/0/12
Phenylpropanoids	30/1/61***	37/1/91***
Monolignols	4/1/18	9/0/37*
Lignans	17/0/21**	24/0/40***
Coumarins	10/0/27*	19/1/38**
Shikimate/acetate-malonate derived	16/0/22**	8/0/16*
Stilbenoids	12/0/17*	4/0/12
Others	4/0/5	4/0/4
Terpenoids	81/5/132***	127/4/255***
Hemiterpenoids (C5)	0	0
Monoterpenoids (C10)	13/1/19*	22/0/54***
Sesquiterpenoids (C15)	29/0/43***	57/0/108***
Diterpenoids (C20)	42/0/58***	65/0/106***
Sesterpenoids (C25)	0	0
Triterpenoids (C30)	15/0/28**	50/1/79***
Steroids	6/0/8	23/1/39***
Carotenoids and apocarotenoids	6/4/20	2/2/10
Others	0	0
Polyketides	22/1/37**	36/1/69***
Anthraquinones	8/0/11*	5/0/12
Pyrones	4/0/15	11/1/25*
Others	10/1/12*	21/0/34***
Fatty acids related compounds	0/0/4	5/0/11
Fatty acids	0/0/4	5/0/11
Amino acid related compounds	1/0/3	1/0/2
Betalains	0/0/1	0
Cyanogenic glucosides	1/0/1	0
Glucosinolates	0	0
Others	0/0/1	1/0/2
Others	3/0/5	4/0/8
Naphthoquinones	0/0/2	1/0/2
Tannins and galloyl derivatives	0	0
Others	3/0/3	3/0/6
	correlated/total	correlated/total
Pseudospectra/base peaks	177/10781	118/7361
Phenylpropanoids	4/61*	8/91***
Coumarins	3/27*	6/38***
Monolignols	3/18**	6/37***

*FDR-P <0.05, **FDR-P <0.005, ***FDR-P <0.0005

3.2.2 Downy mildew infection triggers massive mobilization of specialized metabolites

To test if a biochemical defense response 48 hours after infection is in effect, the levels of salicylic acid were compared (validated by an authentic standard) between the infected and the mock set. In average, the 192 infected plants contained 2.1x more salicylic acid than their 192 mock controls (FDR = 5.8E-34). From this relative high degree of induction of phytochemicals (see Figure 14) it is concluded that early molecular defense processes are ongoing and detectable a few hours after infection.

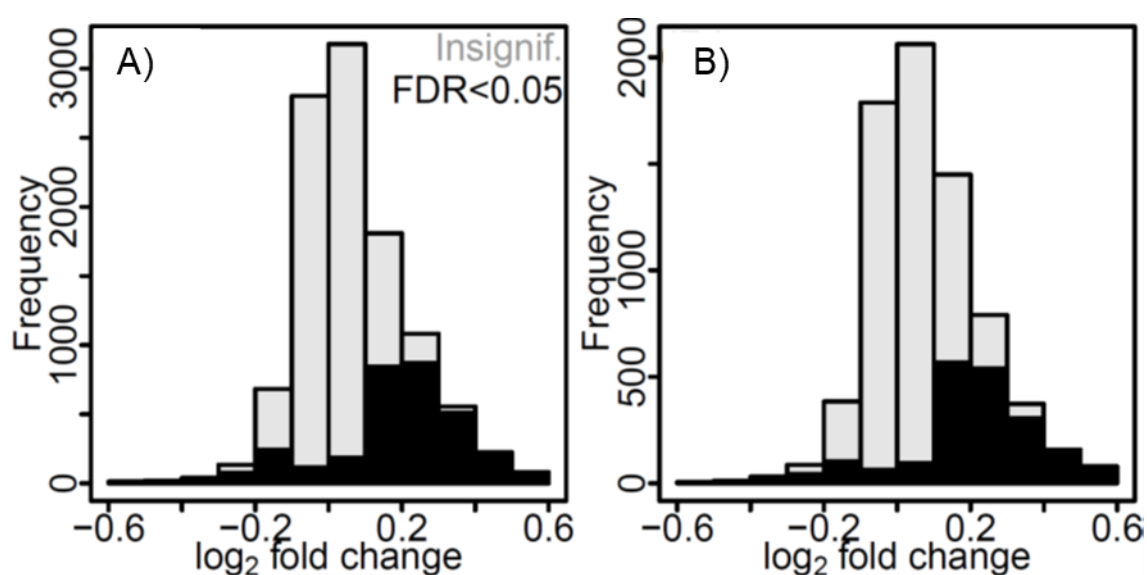


Figure 14: *Pseudoperonospora humuli*-induced phytochemical response in the hop leaf. Log₂-fold changes of all basepeaks recorded in A) positive and B) negative ion mode 48 hours after infection. In grey the insignificant responses and in black the significant FDR < 0.05 corrected inductions after infection are shown.

All non-redundant features for differential abundance were tested using ANOVA. It was found that the levels of 3358 out of 10781 (31%, positive) and 2109 out of 7361 (29%, negative) basepeaks were significantly altered between the infection and mock set (Table 7 and Figure 14). Of these significantly altered basepeaks, 2825 (84%, positive) and 1853 (88%, negative) were up-regulated. This clear trend towards up-regulation is even more evident for the basepeaks with phytochemical annotation. 151 (58%, positive) and 185 (46%, negative) of these metabolites were elevated (Table 7 and Figure 15) and out of these, 143 (95%, both modes) and 179 (97%, negative) were up-regulated.

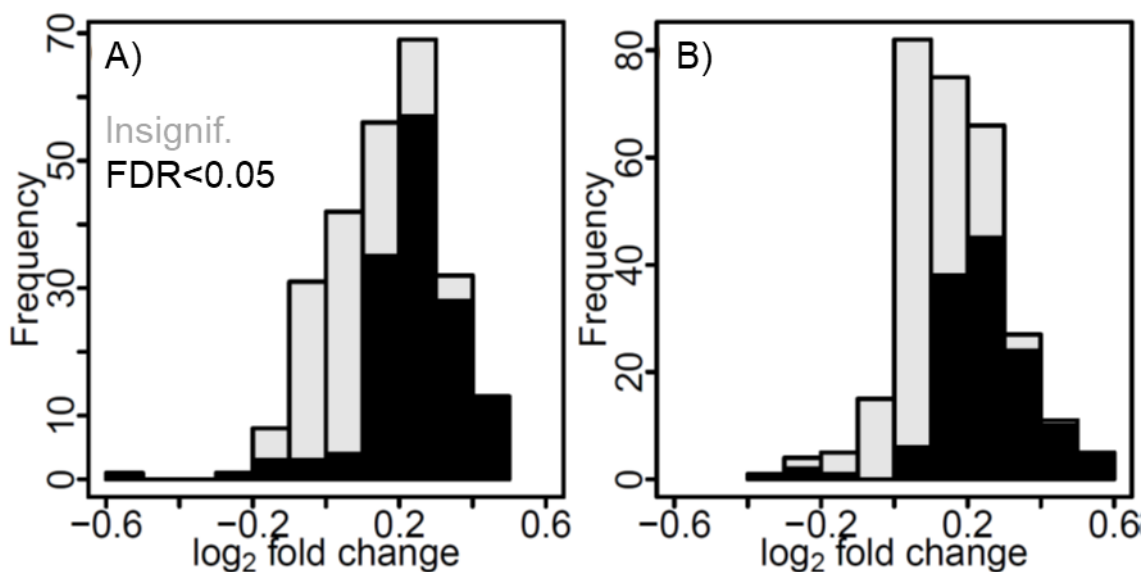


Figure 15: Log₂-fold changes of basepeaks with phytochemical annotation in A) positive and B) negative mode. In grey the insignificant responses and in black the significant FDR < 0.05 corrected inductions after infection are shown.

This trend was also significant for all compound classes which could be reasonably tested using an FDR-corrected binomial test (>7 up- or down-regulations). Roughly one third of all compound classes, typically the more abundant classes mentioned above, showed significantly more metabolite inductions than reductions in both detection modes. With the exception of the 20/10 (positive/negative) carotenoids and apocarotenoids, of which 4/2 were found to be reduced upon infection, there was not a single phytochemical class with significantly more down-regulated than up-regulated compounds in the KEGG BRITE system. Besides this hierarchical annotation system also six compounds with KEGG annotation were found as either coumaroylputrescine or feruloylputrescine exclusively among the 25 most reduced basepeaks in positive ion mode. These compounds are amides of phenylpropanoids and the polyamine putrescine. Although they are known plant metabolites, these substances do not have a KEGG BRITE annotation, yet. While the fraction of significantly elevated phytochemical compounds is relatively high, the magnitude of their accumulation is moderate. With very few exceptions, the increase in abundance in up-regulated phytochemicals was between 5% and 60% in both modes and reductions were of lower extent. In conclusion, infection by *P. humuli* elicits a broad, but unspecific production of specialized metabolites in the hop leaf within 48 hours.

3.2.3 Downy mildew resistance is correlated to a small set of metabolites with putative protective function

Direct induction of biochemistry is unlikely to be the case for all the polar metabolites found up- or down-regulated in this untargeted study, as described in 3.2.2. Thus, a search for metabolites protective against downy mildew in a dose-dependent manner by calculating Pearson correlations between DMR-scores seven days after inoculation with *P. humuli* and each metabolite level in this set, recorded five days earlier, 48 hours after inoculation was conducted. To account for the differences in sampling time, data domains and categorical data for DMR scores, the FDR threshold was raised to 0.1. However, only 166 out of 10781 (positive) and 55 out of 7361 (negative) metabolites displayed significant correlations ($FDR < 0.1$) to DMR within the infected set, with r ranging between -0.38 to 0.33 and a normal distribution between the extremes apexing around 0 (Figure 16). Figure 17 shows the second strongest out of 10781 correlations between a basepeak ($r = 0.34$, ID = pos6197) from the infected sample set to the DMR score. The disease score is lower when the metabolite is more abundant, providing evidence for a putative protective function of this metabolite against DM. 134 (positive) and 12 (negative) basepeaks were negatively correlated to the disease score. These correlations are in strong support that the resistance of hop against downy mildew is, at least in parts, executed by small molecules with putative protective properties.

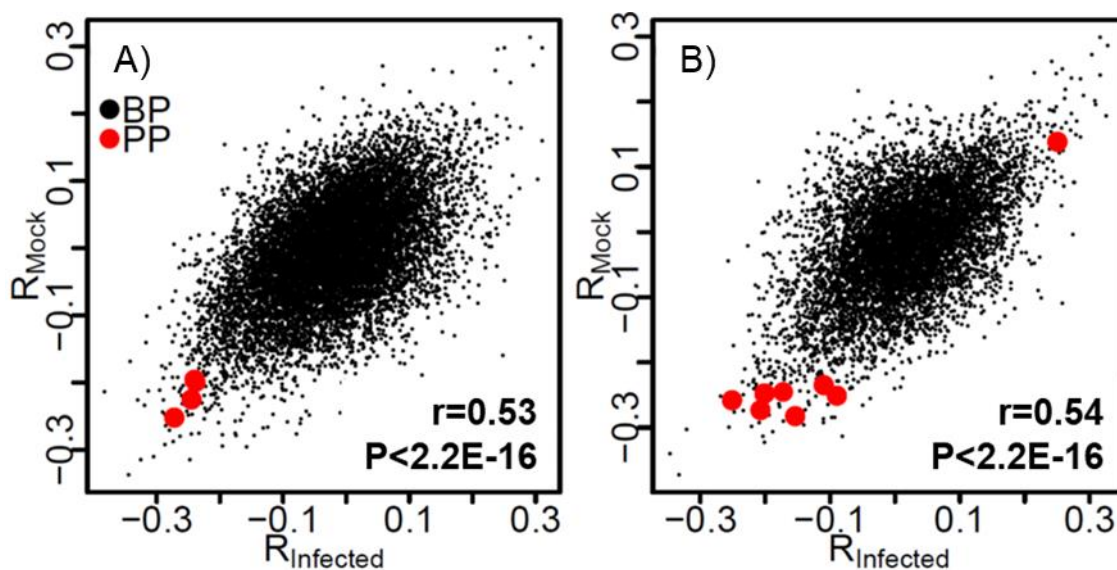


Figure 16: Correlation between the DMR-to-metabolite correlation coefficients from the infected plant set (R_{Infected}) and the DMR-to-metabolite correlation coefficients from the mock treated plant set (R_{Mock}) in A) positive and B) negative mode. BP=basepeaks, PP=phenylpropanoid annotations.

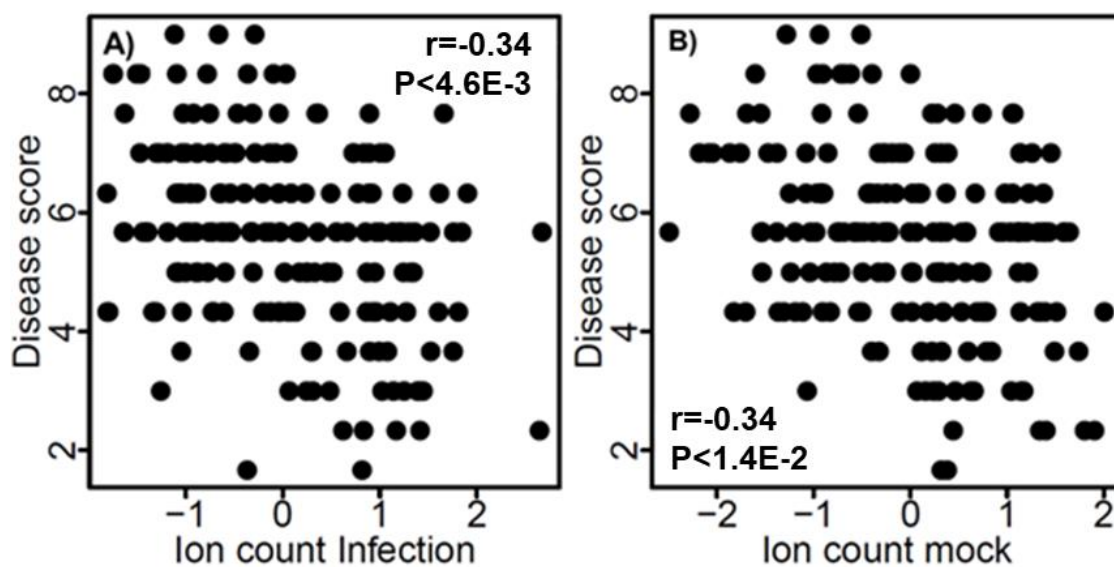


Figure 17: Correlation between DMR seven days after infection and the power-transformed, scaled and centered ion count of basepeak ID pos6197 quantified in leaves 48 hours after infection. A) infected plant set and the B) mock treated plant set.

DMR is predictable from uninfected control samples

Analogous to the correlations calculated above within the infected set, the correlations between DMR of the infected plant set was determined seven days after pathogen inoculation to the metabolite levels of the mock plant set 48 hours after mock-infection. Unexpectedly, a comparable number of metabolites correlated to DMR (28 positive, 82 negative, FDR < 0.1) were identified and the range of r was similar to the infected set (-0.37 to 0.31, Figure 16).

Figure 17 shows the correlation between ID pos6197 to DMR in the infected (A) and mock sample set (B) which was determined as the highest correlated metabolite out of 7361 in the mock set. But in both treatments the same degree of correlation of $r = -0.34$ appeared. It can be excluded that these correlations were caused by a response of the control plants to contamination with *P. humuli* because they showed no signs of DMR seven days after mock-infection. These results provide evidence that DMR is dependent on the heritable metabolic status in the hop leaf before or when the pathogen attacks.

DMR is pre-established in hop

Motivated by the finding that pos6197 exhibited the second highest out of 10781 correlations to DMR when measured in the infected set and the highest when measured in the mock set, a search for such co-occurrence systematically was conducted across the data set. By correlating the correlation coefficients of the infected (R_{Infected}) to the mock set (R_{Mock}), an overall relationship between the putative protective metabolites detected by correlation analysis from the infected set and those found to be predictive from the analysis of the mock set was found. As described above for pos6197, many other basepeaks found to be predictive were also protective at a comparable level. There was a highly significant correlation between R_{Infected} and R_{Mock} independently whether it was tested in data collected in positive ($r = 0.53$, $P < 2.2E-16$) or negative mode ($r = 0.54$, $P < 2.2E-16$, Figure 16). It can be concluded that, to a large degree, protective metabolites are formed before *P. humuli* attacks the plant. And this applies in particular to the metabolites with high potential protective activity.

Phenylpropanoids have highest DM-protective potential

ANOVA led to no conclusive results with respect to compound classes involved in DMR, because metabolites of almost all phytochemical classes were induced 48 hours after infection. Therefore, a search for compound classes significantly enriched in metabolite content correlated to DMR was conducted. According to dose-response relationships, such metabolites could also possess direct biological activity against the pathogen. All annotations belonging to the KEGG BRITE classes two hierarchy levels downstream “Phytochemical compounds” were tested regarding overrepresentation using a Chi²-test. The sum of correlated basepeaks (FDR < 0.1) determined in infected and mock set divided by the total number of basepeaks was used as probability. Remarkably, only phenylpropanoids and the subclasses coumarins and monolignols are significantly more often correlated to DMR as would be expected (Table 7).

As shown in Figure 16 and in support of their putative beneficial role in DMR, these phenylpropanoid contents were almost exclusively negatively correlated to the DM disease score. The availability or even direct biological activity of phenylpropanoids plays a more relevant role in DMR than other phytochemical compounds within the KEGG BRITE system.

Table 8: Correlation of phenylpropanoids extracted from either infected (R_{Infected}) or control (R_{Mock}) plants 48 hours after treatment to DMR in plants seven days after infection (FDR < 0.1).

ID ¹	rt ²	m/z	R_{Infected}	R_{Mock}	Formula	KEGG structure	MS/MS scan ³	MS/MS validation
pos11841	10.6	371.0971	-0.24	-0.20	C ₁₆ H ₁₈ O ₁₀	Fraxin	n.a.	no
neg4563	21.5	353.0876	-0.15	-0.28	C ₁₆ H ₁₈ O ₉	Chlorogenic/Neochlorogenic acid ⁴	509	yes
pos10896	22.6	355.1023	-0.25	-0.23	C ₁₆ H ₁₈ O ₉	Chlorogenic/Neochlorogenic acid ⁴	1314	yes
neg4566	42.1	353.0878	-0.25	-0.26	C ₁₆ H ₁₈ O ₉	Chlorogenic/Neochlorogenic acid	n.a.	no
pos10893	47.7	355.1023	-0.27	-0.25	C ₁₆ H ₁₈ O ₉	Chlorogenic/Neochlorogenic acid ⁵	1312	yes
neg4564	48.1	353.0877	-0.21	-0.27	C ₁₆ H ₁₈ O ₉	Chlorogenic/Neochlorogenic acid ⁵	510	yes
neg3624	48.5	325.0928	0.25	0.14	C ₁₅ H ₁₈ O ₈	<i>cis-/trans-</i> -β-D-Glucosyl-2-hydroxycinnamic acid	359	no
neg4500	52.0	351.0721	-0.11	-0.23	C ₁₆ H ₁₈ O ₁₀	Fraxin	498	no
neg5122	80.2	369.0827	-0.17	-0.24	C ₁₆ H ₁₈ O ₁₀	Fraxin	n.a.	no
neg1121	96.8	195.0662	-0.20	-0.25	C ₉ H ₁₀ O ₂	4-Coumaryl alcohol	85	no
					C ₁₀ H ₁₂ O ₄	5-Hydroxyconiferyl alcohol	85	no
neg4072	98.2	339.0721	-0.09	-0.25	C ₁₅ H ₁₆ O ₉	Sinapoyl malate/Cichoriin/Esculin	426	no
pos3313	109.3	211.0965	-0.24	-0.20	C ₁₀ H ₁₀ O ₃	Coniferyl aldehyde	406	no
					C ₁₁ H ₁₄ O ₄	Sinapyl alcohol	406	no

¹pos = positive mode, neg = negative mode. ²retention time in seconds

³Scan No. corresponds to page in PDF of all recorded MS/MS spectra, supplementary data; n.a. = no MS/MS spectrum recorded.

^{4,5}The putative Chlorogenic/Neochlorogenic acids eluting at ⁴rt=21-23 sec and ⁵rt=47-49 sec in both modes are likely identical

Reference compounds of well-known hop metabolites were included in the MS and MS/MS study. Unfortunately, these were not the compounds which were correlated to downy mildew resistance. Therefore, only MS/MS spectra were used to query against the database at Global Natural Products Social Molecular Networks (GNPS) to validate the annotation of correlated compounds. Figure 18 to Figure 21 show the MS/MS match of chlorogenic acid (neg4563/4564 and pos10896/10893) of the database query (black spectra) against the GNPS library (green spectra). The cosine value between 0.94 up to 0.98 gives more evidence that the detected and putatively annotated compound is chlorogenic acid. Recorded MS/MS spectra of all other annotated and DMR correlated phenylpropanoids listed in Table 8 are attached in the supplementary data.

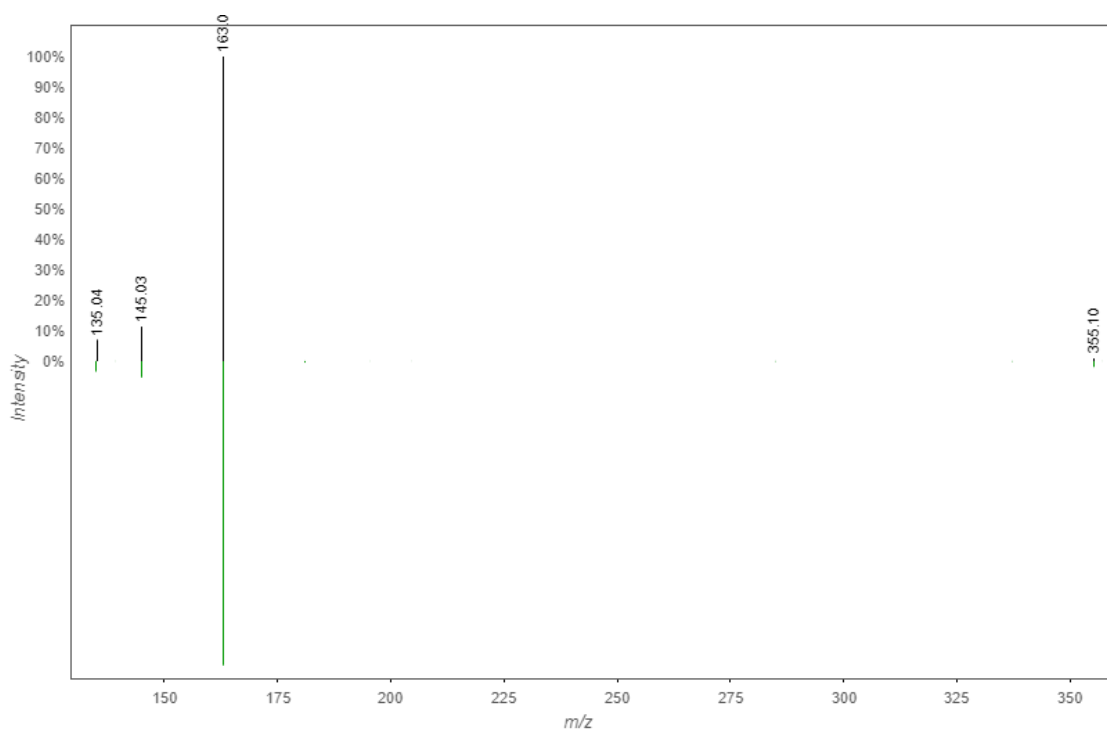


Figure 18: MS/MS scan 1314, MS/MS spectrum of $[M-H]^+$ ion of m/z 355.10 at $rt=22.6$ sec, cosine=0.98, shared peaks=3.

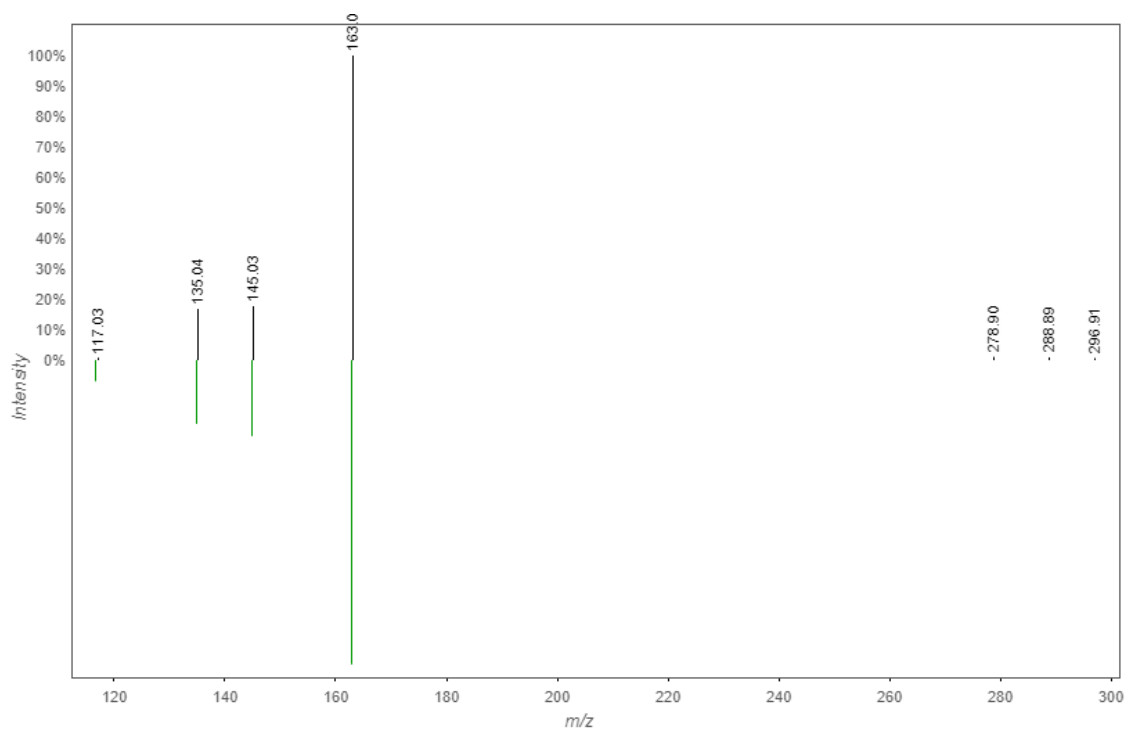


Figure 19: MS/MS scan 1312, MS/MS spectrum of $[M-H]^+$ ion of m/z 355.10 at $rt=47.7$ sec, cosine=0.98, shared peaks=4.

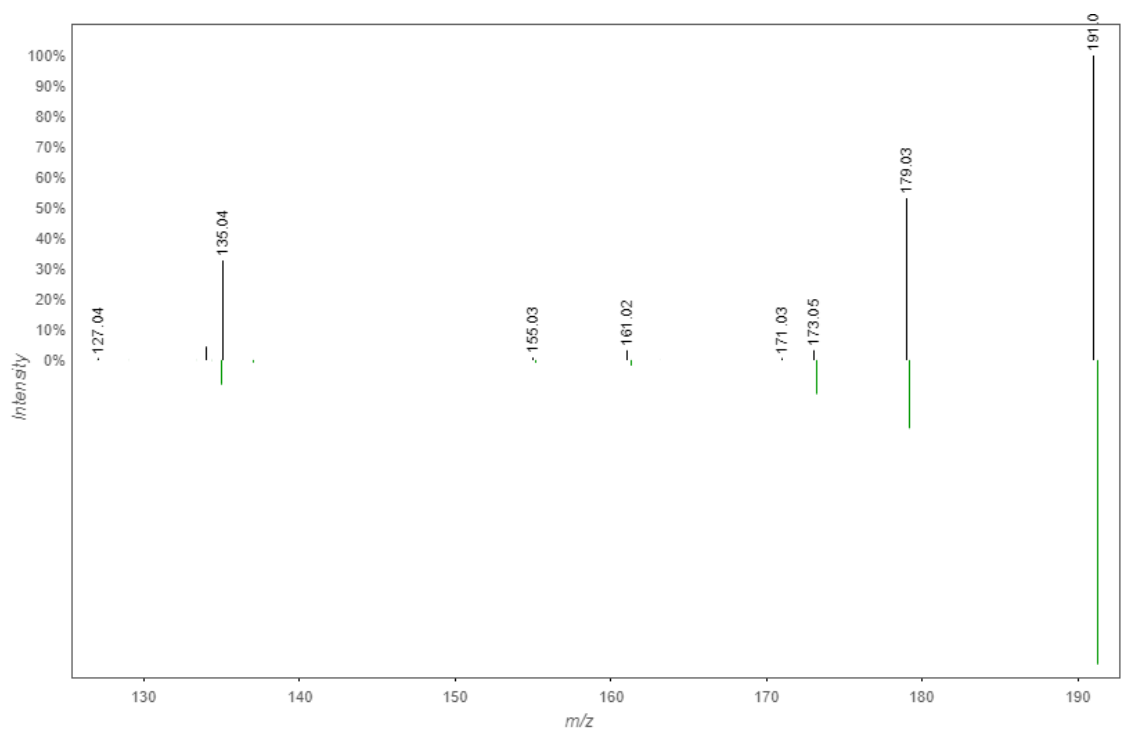


Figure 20: MS/MS scan 509, MS/MS spectrum of $[M-H]^-$ ion of m/z 353.09 at $rt=21.5$ sec, cosine=0.94, shared peaks=5.

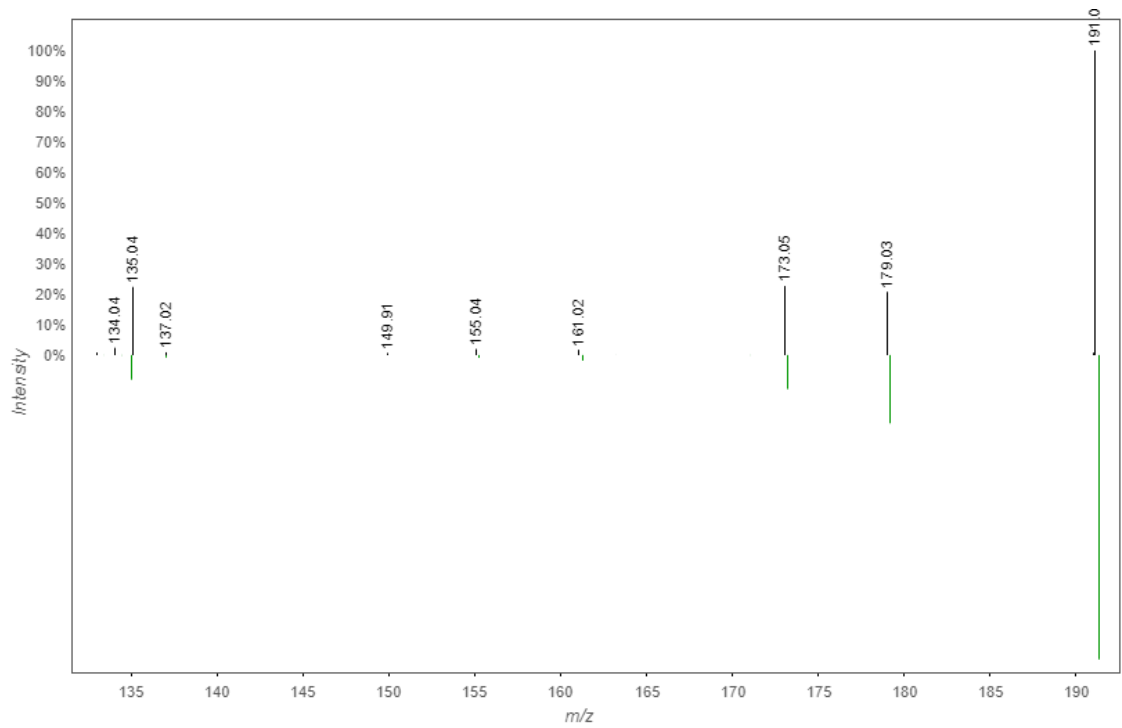


Figure 21: MS/MS scan 510, MS/MS spectrum of $[M-H]^-$ ion of m/z 353.09 at $rt=48.1$ sec, cosine=0.96, shared peaks=5.

3.3 Application of phenylpropanoids mix protects from downy mildew

Due to the strong correlation of phenylpropanoids to downy mildew resistance, two of those most highly correlated compounds in this pathway (see Table 8) were tested for their protective activity against downy mildew. Chlorogenic acid (positive mode: pos10896, pos10893; negative mode: neg4563, neg4564) and coniferyl aldehyde (positive mode: pos3313) were the chosen candidates and inoculated alongside with *P. humuli*. Additionally, *p*-coumaric acid was chosen as a third candidate as it also strongly correlated (peaktable, supplementary data) with the resistance and was easily available. Only three compounds were selected for the testing to keep the complexity of the mixture as low as possible for further potential investigations.

The infection and phenotyping of downy mildew infection was assessed with the same procedure as outlined in 2.2, 2.3 and 2.5 using categories (from 1=resistant to 9= highly susceptible). Figure 22 demonstrates the effect of the different treatments on one genotype (here: genotype 168). No toxic activity of the phenylpropanoid mix on the plants (treatment C) was noted in all monitored genotypes. However, the phenylpropanoid treated plants had a noticeable healthier appearance.

This external application of putative prophylactic compounds led to a reduced leaf infection in treatment A versus treatment B, thus validating their protective activity of some of the identified metabolites. The t-test showed a significant difference between the phenylpropanoid-mix protected group and the mock-control ($t(17.112) = -4.2604$, $p = 0.00052$). The results are shown in the boxplot in Figure 23.

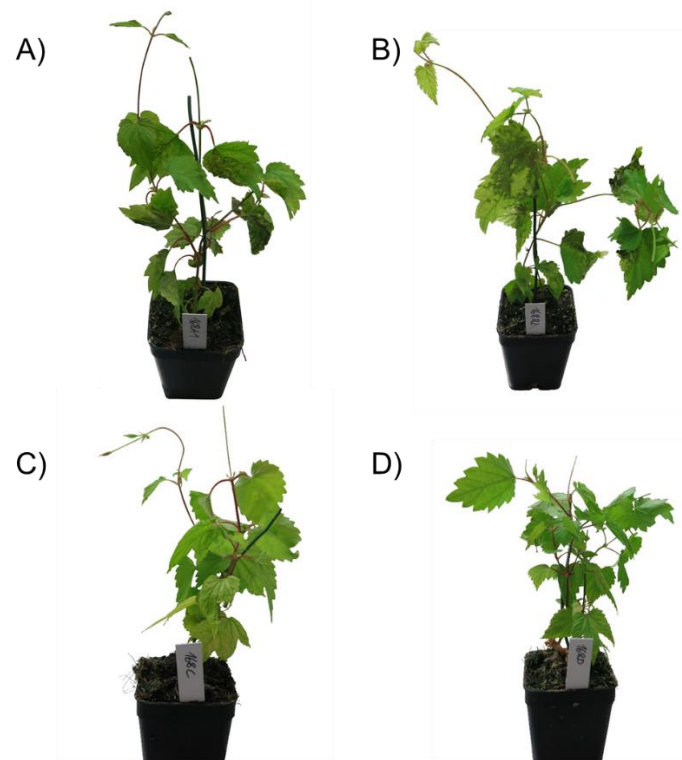


Figure 22: Phenotypic effects of the four conditions in the DM protection assay on genotype 168. (A) Protection/Infection. (B) Mock/Infection. (C) Protection/Mock. (D) Mock/Mock. Pot size= 5x5 cm.

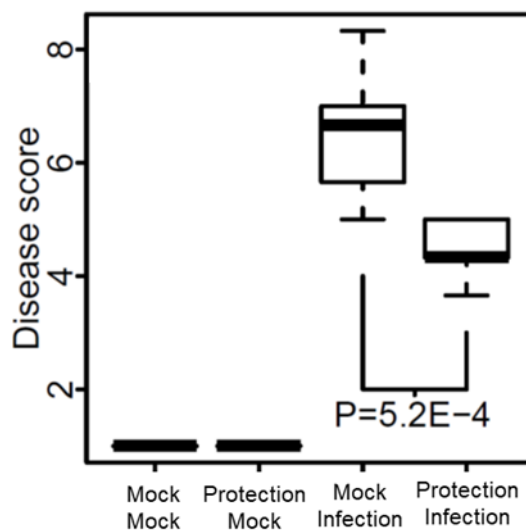


Figure 23: Boxplots of candidate metabolites protection assay, mock control for either protection or infection solution/suspension. Protection solution with 1mM mix of candidate metabolites, infection suspension with *P. humuli*. n=10.

3.4 Genetic mapping displays the overlay of specialized metabolites and downy mildew resistance

3.4.1 Quality filtering of single nucleotide polymorphism markers

To check the data set of the SNP calling in TASSEL described in section 2.6.2 for any outliers, a relatedness analysis of all offspring was performed. During pollination it can happen that an undesired pollen enters the pollination bag and contaminates the developed mapping population. The analysis of relatedness showed no contamination within the filtered data set since no outliers could have been detected in Figure 24.

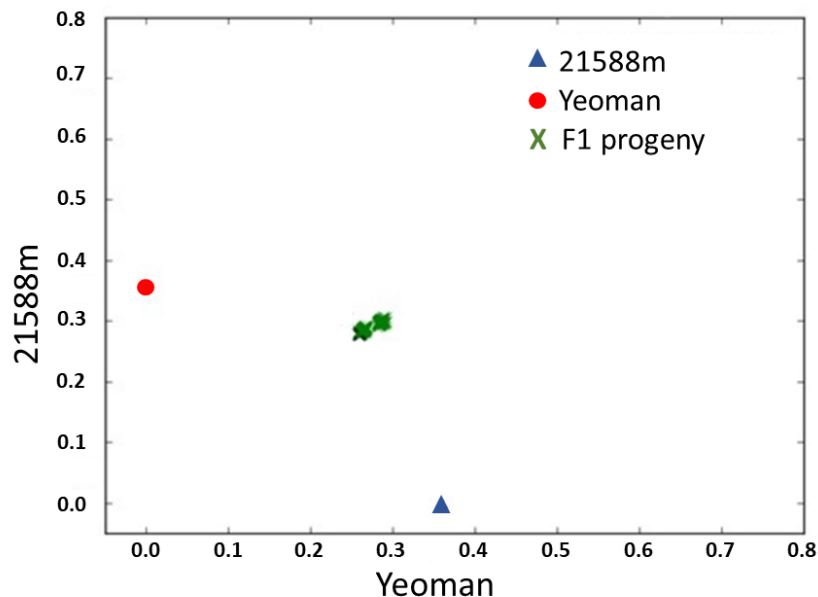


Figure 24: Relatedness of 192 individuals of F1 mapping population against parents 'Yeoman' x '21588m'.

The relatedness plot shows the offsprings as descendent from the cross made of 'Yeoman' x '21588m' cluster with approximately 30% difference to them. All individuals are clustering together indicating that no outliers are included. Therefore, all individuals of the mapping family were kept for further analysis.

A high proportion of SNPs exhibit minor allele frequencies (MAF) not matching Mendelian expectations in the full-sibling family derived from a cross of heterozygous parents (Figure 25).

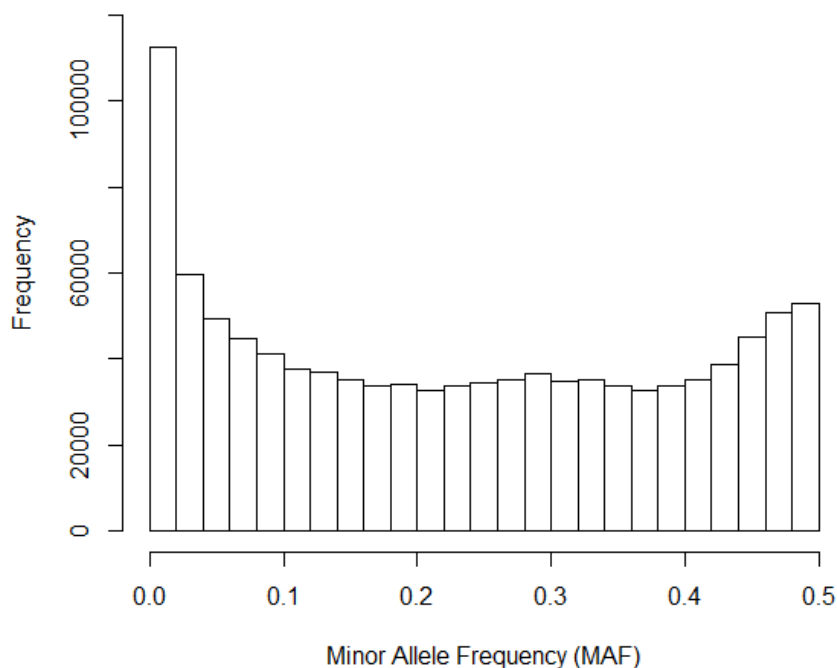


Figure 25: Minor allele frequency of 1,049,502 SNPs within the 192 F1 genotypes of the mapping population.

The expected distribution of MAF should contain optima at segregation frequencies of 0.25 and 0.5 (Matthews et al. 2013). According to Zhang et al. (2017) a major proportion of the hop genome is in translocation during meiosis, while many SNPs show a distorted segregation pattern. The large number of SNP markers with $MAF < 0.1$ are likely to represent systematic errors from DNA sequencing, calling errors for genotypes due to coverage, lack of resolution of predicted phase, and a large and unresolved, highly repetitive and duplicated genome. Additionally, markers with low MAF are likely to exhibit distribution and frequency assumption used in GLM and generate many spurious associations. But as these markers can still be trait associated (Zhang et al. 2017), markers with minor allele frequency $\geq 1\%$ were kept for the subsequent marker-trait analysis.

3.4.2 Linkage mapping of single nucleotide polymorphism

A major goal of this study was to identify the genetic factors related to downy mildew resistance and chemical contents correlated with resistance. For this purpose, a genetic map using SNP markers was created using JoinMap® v4.0. Prior the calculation, SNP marker filtering as described in 2.6 was necessary to eliminate markers with distorted segregation and non-Mendelian segregation. Starting with 950,479 SNP marker after GBS builds in TASSEL and using the pseudo-testcross approach outlined in 2.6.4 and the Chi² test ($p=0.05$) for expected segregation in JoinMap®, only 676 non-redundant markers were left for grouping and ordering within the segregation types (Table 9). After data treatment and filtering of SNPs, the linkage mapping was calculated. The first step was to use marker of type I and type II as detailed in 2.6.4 to create a maternal and paternal map.

Maternal and paternal maps

The first data set contained 201 female markers of type I (nn x np). In the second data set 262 male markers of type II (lm x ll) were collected. Both datasets were calculated separately and resulted in female and male linkage groups. The assignment of linkage groups within all three mapping types came along with the chronological order of group calculation in JoinMap®.

On the maternal map, 161 markers could be grouped and ordered within 9 linkage groups and a total distance of 513.5 cM with 40 markers not included due to insufficient linkage. The paternal map contained 259 markers with 8 linkage groups and total distance of 392.1 cM and only 3 markers could not be allocated to the map. Both the paternal and maternal maps are shown in Figure 26.

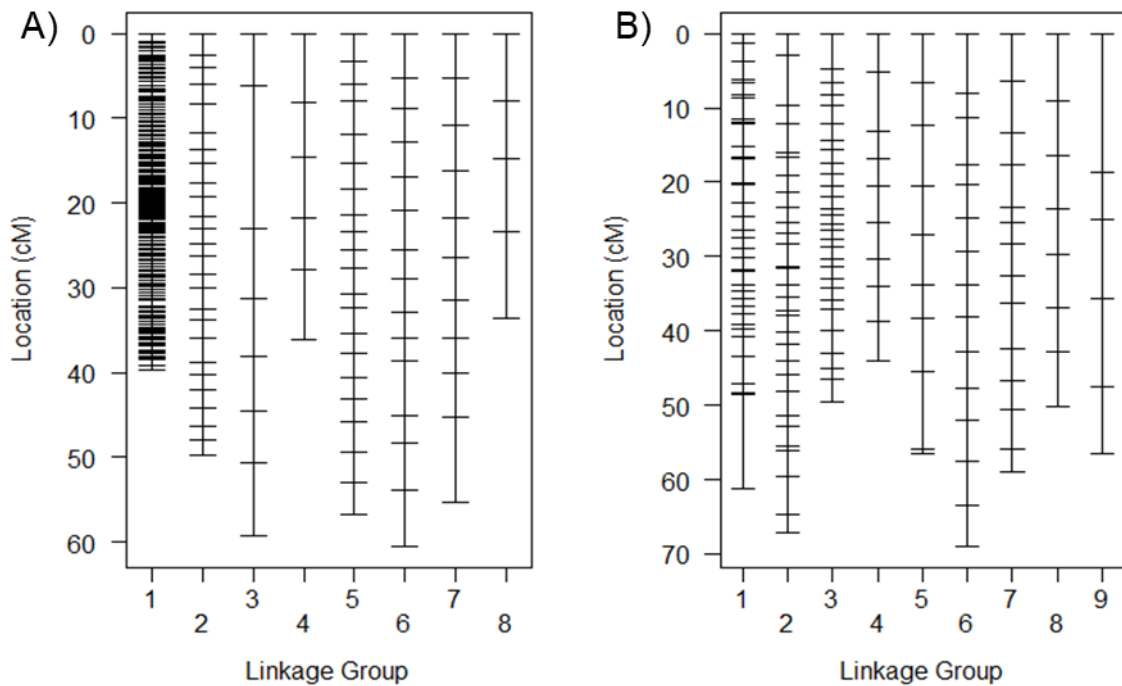


Figure 26: Genetic maps. A) paternal map of 259 SNPs ('21588m'), segregation type II and B) maternal map of 161 SNPs ('Yeoman'), segregation type I.

The distribution of markers across linkage groups especially in the paternal map was quite unbalanced. The number of markers in the paternal map varied from a high number of 167 in linkage group 1 to 5 markers in linkage group 8 with distances from 60.53 cM (LG 6) to 33.65 cM (LG 8). The maternal map was a little bit more equally distributed with 40 markers on linkage group 1 and 6 on linkage group 9 ranging from 69.0 cM (LG 6) to 44.13 cM (LG 4).

Consensus map

The third data set contained all mapped markers from the paternal and maternal map as well as the markers from segregation type III (hk x hk). These markers were used due to their presence in both parents and are utilized as link between both maps to calculate the consensus map displayed in Figure 27.

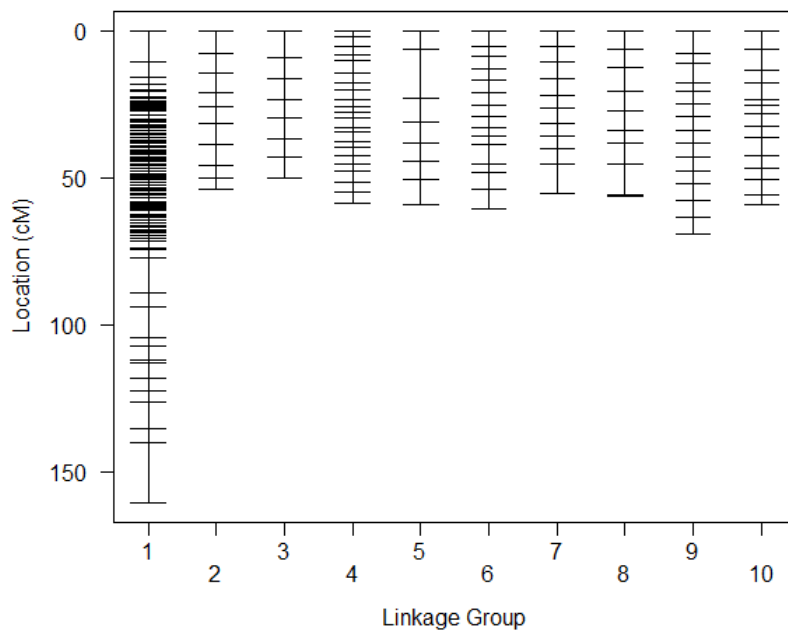


Figure 27: Consensus map of maternal and paternal markers, segregation types I, II and III, containing 210 SNP markers.

371 markers were put in the calculation and 210 markers were left to calculate the consensus map with 10 linkage groups and a total distance of 683.3 cM. The segregation type III made it possible to produce 10 linkage groups representing the 10 chromosomes of *Humulus lupulus* L. Also in this map the uneven distribution was observed especially in linkage group 1 with 97 markers and a distance of 160.58 cM where the other groups contain between 22 and 8 markers ranging from 69.0 cM to 50.27 cM.

The summary of marker filtering starting from over one million SNPs down to 210 finally mapped is presented in Table 9.

Table 9: Identified and mapped SNPs of mapping family on consensus map.

Characteristics of SNP markers	No. of markers
Initially identified in 192 offsprings	1,049,502
Identified with MAF \geq 1%	950,479
Present in > 95% of individuals and MAF >10%	140,465
Present in both parents	10,182
Included markers of segregation type I, II and III	676
Mapped on consensus map	210
Number of linkage groups	10
Total distance mapped (cM)	683.3

3.4.3 Genome-wide association of downy mildew resistance

A total of 950,479 with MAF \geq 1% were retained and the general linear model (GLM) according to section 2.6.5 was used to assess genotype–phenotype association. The Bonferroni method was used to adjust the significance cutoff for an overall probability of 0.05 for type I error (Bonferroni: $0.05/950,479 = 5e-08$).

The genome-wide associations between SNP markers and all individuals were assessed. Only three markers were identified showing a significant association to downy mildew resistance what is shown in the QQ-plot in Figure 28.

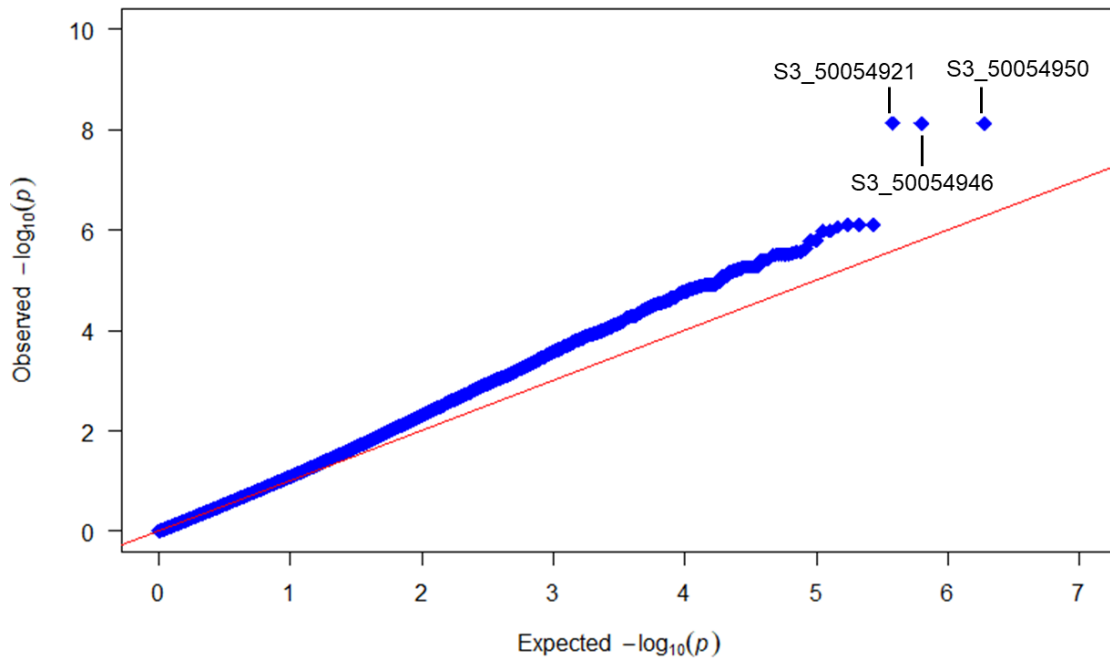


Figure 28: Log quantile-quantile (QQ) plot of 950,479 association tests (SNPs) for downy mildew resistance in the mapping family. Significant markers after Bonferroni correction were S3_50054921, S3_50054946 and S3_50054950.

Deviations from the diagonal identity line in a QQ-plot suggest that either the assumed distribution is incorrect or that the sample contains values arising in some other way as by a true association. Since the observed p-values do not differ substantially and stay along the expected diagonal with only three markers have significant DMR association above the Bonferroni cut-off, phenotype-genotype association is plausible for the three markers.

Further analysis supplied evidence that these three SNPs S3_50054921, S3_50054946 and S3_50054950 are all located on the same scaffold on the 'Shinshu Wase' genome (Natsume et al. 2015) and are therefore expected to originate from the same genetic region (Table 10). Their flanking markers on the scaffold do not have significant association to DMR because their allele states in the mapping family do not correlate with the phenotype at all. Unfortunately, due to distorted segregation these three markers are not included in the genetic maps created in section 3.4.2.

Table 10: Flanking markers on the DMR significant scaffold LD153786 on the ‘Shinshu Wase’ reference genome (Natsume et al. 2015). Significant DMR association markers are marked in bold.

SNP marker	DMR p-value	Position on scaffold (bp)
S3_50046430	0.80741	3749
S3_50046443	0.80741	3762
S3_50046565	NA	3884
S3_50046595	NA	3914
S3_50053270	NA	10589
S3_50054921	1.9878e-08	12240
S3_50054946	1.9878e-08	12265
S3_50054950	1.9878e-08	12269
S3_50055759	0.4388	13078
S3_50055764	0.00070026	13083
S3_50055892	0.00322	13211
S3_50055914	0.00322	13233
S3_50057392	0.30902	14711
S3_50057415	0.30902	14734
S3_50057436	0.30902	14755
S3_50057505	0.03708	14824
S3_50058404	0.01567	15723
S3_50060329	0.02662	17648
S3_50060451	0.0586	17770
S3_50060566	0.0084	17885
S3_50064348	0.60914	21667

3.4.4 Downy mildew resistance and phenylpropanoid levels are regulated by overlapping locus

Association of DMR and phenylpropanoids on maternal and paternal maps

For each marker on the maternal and paternal linkage maps associations to DMR and metabolite contents were determined by GLM. To show the genetic overlap of DMR and the significantly DMR correlated phenylpropanoids, DMR association p-values of SNPs were plotted using their grouping and ordering information out of the genetic maps. SNP markers with significant association (Bonferroni corrected) to annotated phenylpropanoids out of Table 8 were additionally highlighted. The positional association of DMR markers and their phenylpropanoid association (positive and negative ion mode) of either maternal or paternal segregating markers are shown in the Manhattan plots in Figure 29.

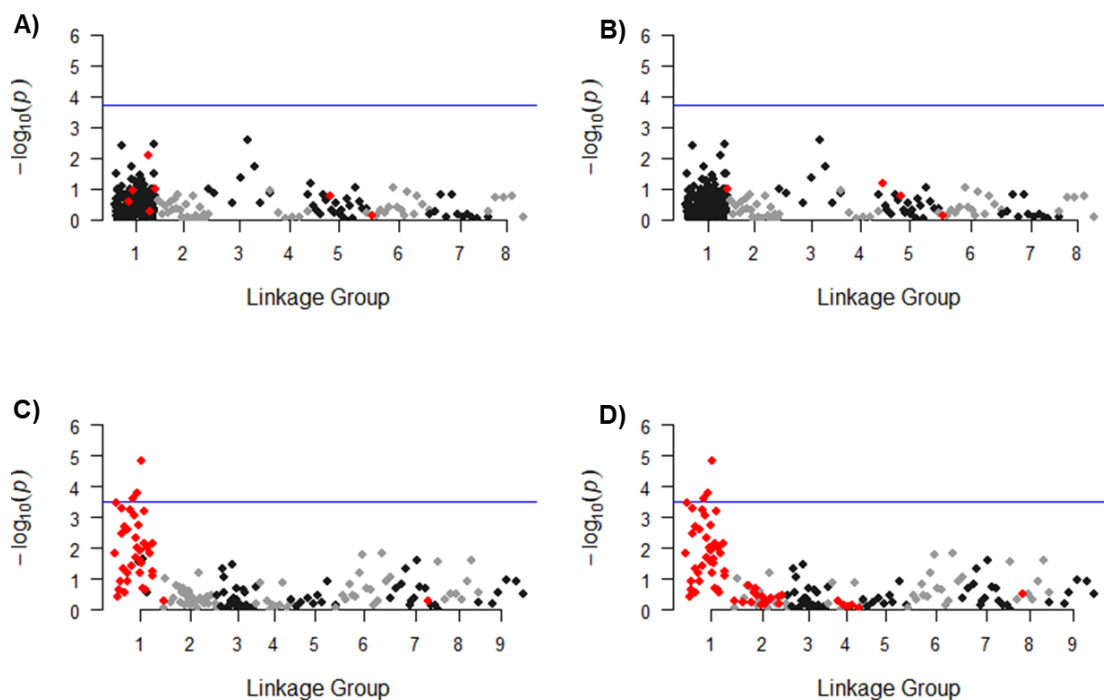


Figure 29: Linkage group-based (black and grey) Manhattan plots of DMR markers. Significant phenylpropanoid associations are highlighted in red (positive ion mode A),C); negative ion mode B), D)). A, B) 259 paternal ('21588m') segregating DMR markers (Bonferroni $p=0.05/259=1.9e-04$, blue line). C, D) 161 maternal ('Yeoman') segregating DMR markers (Bonferroni $p=0.05/161=3.1e-04$, blue line)

The Bonferroni cut off was calculated using the $p\text{-value}=0.05$ divided by the containing markers in each map. The Manhattan plots of paternal and maternal markers show that DMR is only associated with maternal segregating markers. As proposed at the beginning of the study, the resistant 'Yeoman' genotype should have been the source of resistance in the mapping population.

It was also observed that the downy mildew resistance associated SNP markers overlay with the significantly correlated phenylpropanoid associations (positive and negative ion mode) using their grouping and position information of the genetic maps. In positive MS mode only LG 1 in the maternal map shows significant association to both the DMR and phenylpropanoid content. Additionally, LG2 and LG4 in negative MS mode contain significant phenylpropanoid association but without any DMR significance. Significant associations to phenylpropanoid contents across whole linkage groups on the maternal map, the quality of ordering and grouping of the genetic maps is discussed in section 4.1 and 4.2. On the paternal map in both MS modes no clear association to phenylpropanoids within the eight linkage groups could have been detected, suggesting that the DMR correlated phenylpropanoid levels are passed by the resistant mother 'Yeoman'.

Association of DMR and phenylpropanoids on consensus map

The identical procedure as used for maternal and paternal markers was applied to plot the association of downy mildew resistance and phenylpropanoid content on the consensus map and is shown in Figure 30. Also here, the remarkable and significant overlay of correlated compounds and DMR in LG 1 could have been noticed in both MS modes (positive and negative).

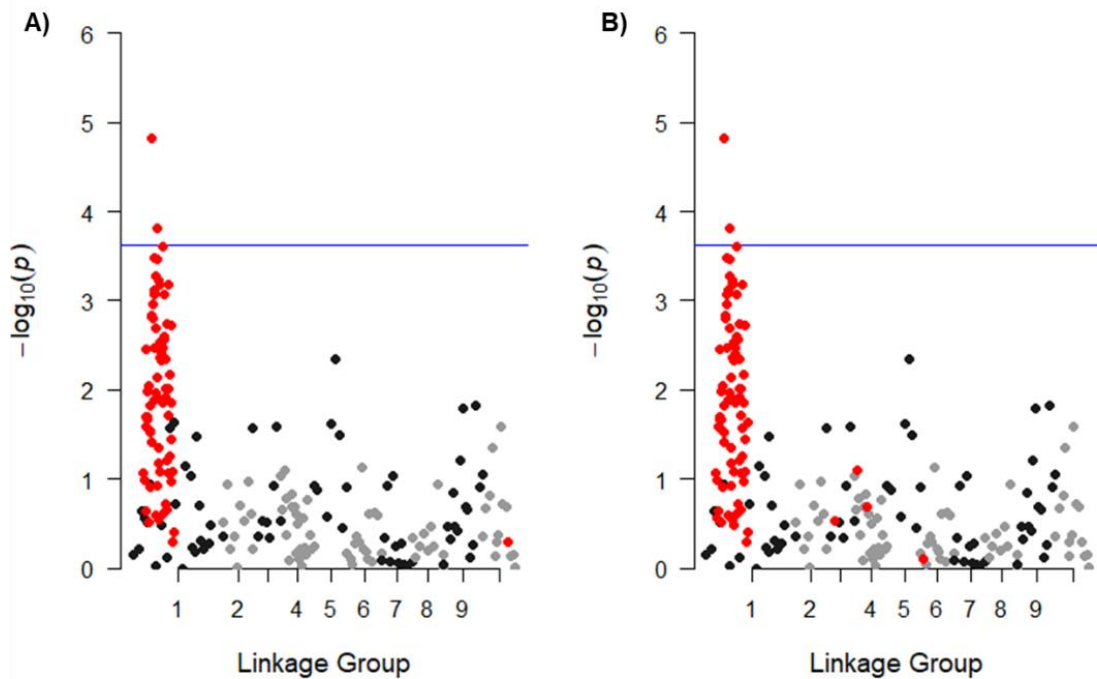


Figure 30: Linkage group-based (black and grey) Manhattan plots of 210 DMR markers (Bonferroni $p=0.05/210=2.4e-04$, blue line) on consensus map of 10 linkage groups. Significant phenylpropanoid associations of positive ion mode A) and negative ion mode B) are highlighted in red.

3.4.5 Sequence BLAST of downy mildew resistance association markers

The three significant DMR association markers (S3_50054921, S3_50054946, S3_50054950) and 323 additional association SNPs which are in linkage disequilibrium with $r^2 > 0.5$ to these DMR markers were blasted were BLAST aligned to the plant unigene database (Altschul et al. 1990) at NCBI (NCBI 2018). Fifty-five associated SNPs were found to be located on scaffolds that contained presumptive genes (Table 15 supplementary data). The remaining SNPs resided on scaffolds with no known gene homology.

The molecular function of the homologue genes of all these genes were manually inspected in the source organism, in most cases *Arabidopsis thaliana*, to assess the candidate's potential involvement in phenylpropanoid metabolism or resistance to pathogens. Six interesting SNP containing scaffolds and their annotation information are shown in Table 11.

Table 11: Candidate genes on 'Shinshu Wase' scaffolds containing SNPs in LD with DMR Markers S3_50054921, S3_50054946, S3_50054950 in target organism *Arabidopsis thaliana* (Lamesch et al. 2012). The complete list of genes and scaffolds is shown in the supplementary data.

Scaffold	SNP	bp	Gene start	Gene stop	DMR p-value	E value	BLAST Match	target sequence ID	Protein	Involved in
LD140310	S1_656189702	21429	1470	2795	5.18E-06	3E-79	99%	gi 25453190 sp O23044.1 PER3_ARATH	Peroxidase 3	Removal of H ₂ O ₂ , oxidation of toxic reductants, biosynthesis and degradation of lignin, suberization, auxin catabolism, response to environmental stresses such as wounding, pathogen attack and oxidative stress
LD150129	S2_365162646	29886	8009	8329	2.61E-05	7E-38	22%	gi 75249447 sp Q93Z00.1 TCP14_ARATH	Transcription factor TCP14	Cell proliferation, inflorescence development, regulation of defense response, regulation of seed germination, regulation of transcription, DNA-templated, response to abscisic acid, response to cytokinin, response to gibberellin
LD137981	S1_506116632	37940	12387	13879	7.24E-05	0	90%	gi 5921932 sp Q42600.1 C84A1_ARATH	Ferulate-5-hydroxylase	Lignin biosynthetic process, oxidation-reduction process, phenylpropanoid biosynthetic process, response to UV-B
LD180108	S5_157986106	2781	9467	10016	7.89E-05	3E-28	43%	gi 75338958 sp Q9ZSA8.1 DLO1_ARATH	Protein DMR6-like oxygenase 1	Defense response to oomycetes, leaf senescence, oxidation-reduction process, response to bacterium, response to fungus, response to oomycetes, response to salicylic acid, salicylic acid catabolic process, secondary metabolic process
LD153337	S3_33002210	3751	20927	22204	8.66E-05	8E-138	94%	gi 75273965 sp Q9LSF1.1 OXI1_ARATH	Serine/threonine-protein kinase OXI1	Defense response, protein phosphorylation, response to oxidative stress, response to wounding
LD149073	S2_320518853	1819	12065	13504	8.79E-05	2E-105	98%	gi 75215431 sp Q9XGN4.1 GOLS1_AJURE	Galactinol synthase 1	Major galactinol synthase mainly involved in the biosynthesis of storage raffinose family oligosaccharides (RFOs) that function as osmoprotectants. May promote plant stress tolerance

4 Discussion

The primary objective of this work was to identify metabolites and genes with a role in DMR at a population level. For this purpose, a mapping population was created, genotyped, phenotyped and chemotyped after infection with *P. humuli* or mock-infection. The resulting three data domains were interrelated to find associations between genotype-chemotype, genotype-phenotype and chemotype-phenotype. The results provide evidence for an important metabolic DMR component regulated by the genetic control of phenylpropanoid levels.

4.1 Phenotyping and genetic regulation of downy mildew resistance

In diverse previous studies, researcher have shown that artificial infection with the obligate biotrophic fungus *Pseudoperonospora humuli* is a critical process (Royle and Kremheller 1981; Mitchell 2010; Forster et al. 2014). The reproducible inoculation and development of the downy mildew infection within the mapping population was one of the most critical steps in this study. Optimizations in temperature and light conditions as well as fertilizer and irrigation management led to positive, uniform plant development and made a homogeneous infection feasible. All experiments including the repeat were successful and the results were highly reproducible and, therefore, reliable. Additionally, *P. humuli* is an obligate biotrophic fungus and can not be propagated and cultivated under *in vitro* culture conditions. Therefore, the spores were maintained, propagated and transferred from living plants. Controlled growth conditions were an advantage in the incubator: The fungus *P. humuli* need a certain temperature and humidity for ideal infection on the leaves.

Furthermore, broad-sense heritability, which is usually employed to find the genetic proportion of trait heritability in populations across variable climates, was applied in this study to measure the experimental, systematic and the environmental component of DMR variation in the mapping population. The high value of broad-sense heritability $h^2 = 0.81$ within the observed family demonstrates that DMR was minimally influenced by environmental and systematic effects and the

genetic component of variation was effectively transmitted to the progeny in this study. Henning et al. 2015 published heritabilities across three environments varying from $h^2=0.38$ under greenhouse conditions to $h^2=0.57$ under field conditions (Henning et al. 2015). The comparable high heritability in this study might be influenced by the single environment and controlled conditions in the incubator but demonstrate that the inoculation protocol was applied correctly. Both studies of DMR heritability, including the extension in a controlled, single environmental treatment, support the notion that DMR has an inherited genetic component, which is amenable to plant selection and breeding programs.

Unfortunately, an automated phenotyping assay for downy mildew screening on hop leaves has not been developed before. Detached leaf assays could not be considered because the wounding of leaves would have affected the metabolic readout or the infection by *P. humuli* (Liu et al. 2007). Therefore, the disease level was scored on living plants using five categories judging the infection severity. To minimize the errors and to detect outliers, the inoculation with *P. humuli* was done twice with three scorings in different order per experiment. Since no obvious difference across both phenotyping events were detected, the scoring results were accepted and the potential for subjective phenotyping errors considered in the multiple-testing correction of phenotype-chemotype interaction.

A major objective was to develop a genetic map using SNP markers and to identify loci linked to resistance. After practical filtering steps, necessary for the current status of molecular marker systems and partial whole genome assemblies (Natsume et al. 2015) in hop genomics, 210 markers were left to calculate the consensus map with 10 linkage groups and total distance of 683.3 cM representing the 10 chromosomes of *H. lupulus*. The distance and distribution of markers among linkage groups is also comparable to already published genetic maps, where SNP markers were used to create genetic marker maps (Henning et al. 2015; Henning, Gent, et al. 2017; Henning, Hill, et al. 2017). With the obtained linkage map it was possible to map the downy mildew resistance association to putative “chromosomes” and one DMR locus on LG1 was detected. Applying the Bonferroni correction only two SNP markers of the filtered marker set were left being significantly associated with the phenotypic trait. However, the heavy filtering of SNP markers, the distorted distribution of markers among linkage groups,

the and the disputable ordering of markers within linkage groups increases the demand for new mapping strategies in hops. Furthermore, many discovered, GLM associated markers were not mapped to any linkage groups in this study due to unusual segregation ratios. However, even if they are not contained on the current genetic map, the significantly associated markers and SNPs in linkage disequilibrium with the associated SNPs could be used in a BLAST search to find homologous proteins and candidate genes.

4.2 Segregation distortion requires new mapping tools

The development of the genetic map in this study followed certain and approved methods. However, for the future is not suggested to order markers in linkage groups, until a complete whole genome chromosome assembly is available for hops. All existing software solutions used in genetic mapping were designed for inbred lines (e.g. Arabidopsis) and adjustable but not particularly suitable for hops, because of its heterozygous and otherwise, very complex nature of the hop genome. Nevertheless, a combination of resources using NGS coupled to GWAS, a partial whole genome reference assembly, haplotype mapping (LD mapping) and genomic DNA scaffold examination could replace most of the QTL mapping studies. In particular, QTLs remain important for independent confirmation studies of selection markers, but the importance of mapping families, large sets of siblings that need to be carried for years, has greatly diminished. Association panels, which are a large number of collected plants, where the genetic relations are known or assessed by marker-based genetic distance measurements, can replace mapping families for training genetic selection models as already shown in other crops (Chakradhar et al. 2017; Bazakos et al. 2017; Manivannan et al. 2018).

Recent studies by Zhang et al. (2017) and Easterling et al. (2018) give evidence that genomic regions are duplicated across the genome by translocation in hop and “super-linkage groups” are prevalent and observed across several full-sibling families showing diverse correlation between different linkage groups. Common translocation occurs in the parents of families carried differentially on into its progeny, so each offspring may have unique genomic structures and, thus map discrepancies. Miss-ordering of markers within linkage groups using recombination

frequency as genetic distance between markers is problematic in general in hops. GBS markers (Matthews et al. 2013) and GWAS (Henning et al. 2015; Hill et al. 2016) have been developed and deployed for genetic mapping in disease resistance or sex determination. Nevertheless, the understanding of genetic inheritance patterns in hop remains a major challenge. Significant distortion from Mendelian segregation expectations in diverse mapping populations has been repeatedly reported in the past (Seefelder et al. 2000; McAdam et al. 2013). Additionally, female-biased sex ratios have been observed in most families, but was not well-understood (Neve 1991; Jakse et al. 2008). The segregation phenomena in hops are similar to segregation distortion systems that are well described in other species known to exhibit chromosomal rearrangements (Snow 1960; Wiens and Barlow 1975; Carr and Carr 1983; Rauwolf et al. 2008; Golczyk et al. 2014). Another problem in the genetic resolution in hops, recombination suppression leads to very strong linkage disequilibrium across the genome because large, complete blocks of genome may be barred from participation in recombination due to pairing incompetence caused by translocation structures. Nevertheless, as demonstrated in this study, progress in selection markers production and biochemical genetic understanding of disease mechanisms can be accomplished.

4.3 Downy mildew resistance is a metabolic phenomenon

4.3.1 Downy mildew resistance is largely prophylactic

Metabolites induced or repressed upon stress have specific roles in the responses and metabolite abundance may directly affect tolerance to a particular stress (Dixon and Paiva 1995; Dixon 2001; Chong et al. 2009; Bollina et al. 2010; Malacarne et al. 2011; Chitarrini et al. 2017). Unfortunately, ANOVA led to no conclusive observation of covariance of disease state with respect to compound classes involved in DMR, because metabolites of almost all phytochemical classes were induced 48 hours after infection. Since approximately every third compound was upregulated in both MS modes, a search for compound classes significantly enriched in metabolites correlated to the disease score was necessary. Only about 1% of all metabolites content variations in positive MS as well as in negative MS mode displayed significant correlations to DMR within the infected

set, with R ranging between -0.38 to 0.33. Most of these basepeaks were negatively correlated to the disease score indicating that the infection was lower when the metabolite was more abundant. The same effect was investigated in the mock treated plant set which indicates that the resistance of hop against downy mildew is constitutively conditioned by metabolites with protective properties. A major, important finding in this study is that hop DMR correlated metabolites are pre-established prior contact with the fungi and are not induced after the infection and deserves careful consideration in disease management and breeding strategies in the future.

4.3.2 Phenylpropanoids are the protective compounds

A systematical analysis provided more evidence that some metabolites possess a significant high DMR correlation in both the infected and mock experimental sets. Connecting two different data domains, especially the visual downy mildew infection rate, by setting FDR corrected p-values below 0.1, was justified as useful in this specific correlation analysis.

Only phenylpropanoids and the subclasses coumarins and monolignols are significantly more often correlated to DMR as would be expected by the statistical model. Specific compounds were almost exclusively negatively correlated to the DM disease score. The availability or even direct biological activity of phenylpropanoids plays a highly relevant role in DMR than other phytochemical compounds within the KEGG BRITE annotation system. Almost all candidates show a negative correlation to the downy mildew infection, which means the higher the abundance the lower the infection. Only *cis/trans*- β -D-glucosyl-2-hydroxycinnamic acid is characterized with a positive correlation. Noteworthy, this single positively correlated phenylpropanoid differs to the other negatively correlated ones by being glycosylated and it is located in a different branch of the phenylpropanoid pathway than the candidates with a positive DMR function (Figure 31).

This effect might indicate once this specific path is promoted the protecting compounds are less likely produced and resistance against downy mildew is reduced. That glycosylated phenylpropanoids provide a source for biologically active non-glycosylated compounds has been shown in other studies (Pezet et al. 2004; Roy et al. 2016). Also in *A. thaliana* glycosylation may play a role in maintaining a

specific pool of pathogen-specific molecules in the phenylpropanoid pathway (Langenbach et al. 2013). Glycosylation is a typical modification used for inactivation, storage or mobilization. Thus, it reduces the pool of active (free) phenylpropanoids but may act as a control or mobilization tool. Nevertheless, direct study of metabolites as storage or metabolic precursors, such as carotenoids and sugar-bound cinnamates, to norcarotenoids and lignols, is noted, but beyond the scope of the current dissertation.

Due to the observed strong correlation of phenylpropanoids to downy mildew resistance, three compounds of this pathway were tested for their protective activity against downy mildew. Chlorogenic acid, coniferyl aldehyde and *p*-coumaric acid were chosen and inoculated alongside with *P. humuli*. The phenylpropanoid-mix was applied two hours prior infection on the underside of the leaf. This external application of putative prophylactic compounds led to a reduced leaf infection on ten highly susceptible genotypes thus validating their protective activity.

The accumulation of these phenolic compounds at the site of pathogen inoculation has been reported before. These metabolites are also the precursors of lignin, which acts as a general barrier for pathogen progression in the cell wall (Bily et al. 2003; Z. Chen et al. 2006; Boutigny et al. 2008). A number of studies (Mabry and Ulubelen 1980; Bourgaud et al. 2006; Tiago et al. 2017) have shown that phenylpropanoid derivatives are able to protect plants against several biotic infection by viruses, bacteria or fungi. Also abiotic stress for example low or high temperatures or wounding is correlated with a change of metabolite levels belonging to this pathway (Dixon and Paiva 1995).

Monolignols are essential for cell wall reinforcement (Whetten and Sederoff 1995) and proanthocyanidin accumulation, which are also phenylpropanoid-derived and are toxic to some pathogens (Dixon et al. 2005; Mellway et al. 2009). Also the resistance to oomycete *Plasmopara viticola* in grapevine was found to coincide with stilbenoid accumulation which belong to the phenylpropanoids (Malacarne et al. 2011; Figueiredo et al. 2015). Improved stilbene production in hops could also be achieved by gene transfer (Schwekendiek et al. 2007), as well as increased flavonoid production by transcription factor changes in hop (Gatica-Arias et al. 2012). Noteworthy, findings in this study also provide leads for crop engineering, but which are beyond the scope of the current dissertation

4.4 The major downy mildew resistance locus likely confers resistance by regulating the phenylpropanoid biosynthetic pathway

The genetic map provided evidence for the overlap of DMR associated markers and correlated metabolites. On the consensus map one major locus on LG1 was found to be significantly involved in both resistance and a candidate genetic function for accumulation of specific phenylpropanoids.

SNPs significantly associated with DMR and additionally associated markers, which are in linkage disequilibrium with these DMR SNPs were BLAST aligned to the plant unigene database. Six interesting SNPs were found with an annotation to known resistance genes or genes with a function in the phenylpropanoid biosynthesis. LD140310 is an interesting scaffold containing the homologous protein peroxidase 3 involved in the biosynthesis and degradation of lignin and response to environmental stresses such as wounding or pathogen attack (Chittoor et al. 1997; Passardi et al. 2005). Peroxidases prevent cellular diffusion of pathogens by production of reactive oxygen or nitrogen species (ROS and RNS, resp.), creating a highly toxic environment for the pathogen or by supporting the development of structural barriers. The transcription factor TCP14 is localized on scaffold LD150129 which is also involved in the regulation of defense responses in other plants (M. Li et al. 2018). Nevertheless, the low E-value and BLAST match indicate that it might be a different homologue in hops and might have a different function in target organism *H. lupulus*.

The most promising candidate gene is localized on scaffold LD137981. The homologous protein ferulate-5-hydroxylase can be aligned with the lignin and phenylpropanoid biosynthetic process which showed a correlative function in protecting hops against *P. humuli* in this study.

All annotated DMR correlated compounds in positive and negative ion mode (Table 8) were mapped to the phenylpropanoid biosynthesis pathway on the following KEGG map (Kanehisa and Goto 2000) (Figure 31).

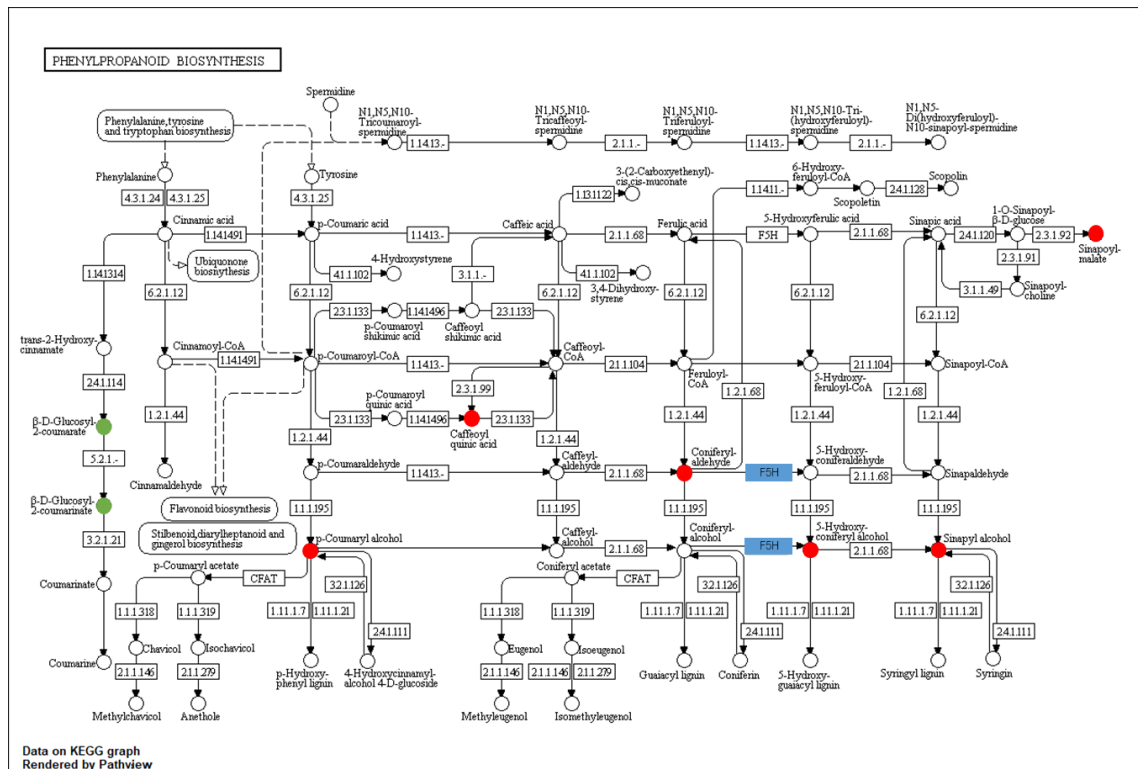


Figure 31: Phenylpropanoid biosynthesis pathway on KEGG map. DMR correlated metabolites with negative correlation are marked in red, positive correlated compounds are marked in green. Ferulate-5-hydroxylase (F5H) as a DMR associated candidate is marked in blue.

Almost all candidates show a negative correlation (red) to the downy mildew infection which means the higher the abundance the lower the infection. Only *cis-/trans*- β -D-Glucosyl-2-hydroxycinnamic acid is characterized with a positive correlation (green) with its role being discussed in 4.3.2. Ferulate-5-hydroxylase (blue) is directly involved in the conversion of two DMR correlated phenylpropanoids, coniferyl aldehyde and 5-hydroxy-coniferyl alcohol.

The role of lignification and enzymes involved in the phenylpropanoid biosynthesis providing resistance has been investigated in other research previously (Matros and Mock 2004; Langenbach et al. 2013; König et al. 2014). Therefore, these results give evidence for the interdependences of specified metabolites and downy mildew resistance. Further transcriptome and expression analysis between susceptible and resistant genotypes in the presented mapping population could provide an insight into the regulation of resistance on gene level.

Nevertheless, the coincidental finding of putative genetic factors for biosynthesis of DMR correlated accumulation pathway intermediates suggests the need for

further studies in the leaf tissues of hops in relation to constitutive and induced expression of metabolic defense compounds. Infection studies to assess whether the resistance symptomology and life cycle stage is consistent with phenylpropanoid prevalence could corroborate the findings. Furthermore, localization studies of the indicted phenylpropanoids in resistant and non-resistant plants and analyte determination after treatment could provide an even better understanding of the underlying resistance mechanism. Additionally, functional studies with enzyme inhibitors, antibodies against certain phenylpropanoids or other inactivation strategies could further elucidate the downy mildew resistance mechanism in hops.

4.5 Application in breeding and development of bio-fungicides

Molecular markers for DMR greatly increase the efficiency of breeding, especially for growing hops in areas suffering heavily from infection with *P. humuli*. The understanding of the chemical nature of DMR allows carefully planned breeding strategies resulting in technologically advanced selections. Through targeted breeding the constitutive amount of specialized phenylpropanoids present in a genotype could be increased to develop higher levels of resistance. Thus, these strategies could result in a real and progressively increasing genetic gain. An analogous achievement was the significant increase in alpha-acid content in hops which is seen as one of the greatest successes of hop breeding (Darby 2006).

These selection markers for DMR increase breeding efficiency and makes it possible to efficiently introgress downy mildew resistance genetic factors with other desirable traits such as other DMR genetics, powdery mildew or wilt resistance genetic factors (stacked resistance), and other quality traits in hops. Furthermore, the understanding of complex traits such as DMR allows quality assurance to brewers and makes varieties more attractive for farmers in the future. Through the increase in efficiency of hop breeding, field time as well as costs can be minimized and gives potential for smaller progeny screens and removes the need for specialized facilities such as for disease screening.

Endogenous bioactive small molecules, investigated in this study, may also be utilized to develop “organic” fungicides. Previously shown chlorogenic acid has

the ability to inhibit germination and growth as well as membrane permeabilization of pathogenic fungi which causes its cell death (Martínez et al. 2017). *In vitro* studies with *p*-coumaric acid indicated that already a concentration of 10ppm inhibited the growth of *Phytium* sp. and *Corticium rolfsii* (Tawata et al. 1996).

Keen and Littlefield showed that coniferyl aldehyde may be a part of a mechanism for restriction of *Melampsora lini* on flax leaved and may represent an effective phytoalexins for controlling fungi pathogens in the future (Keen and Littlefield 1979).

These phenylpropanoids also tested in this study or derivatives of them could be applied in organic plant protection. The decreasing acceptance for conventional plant protection products in the public and their potential risks, but also the damages caused by Cu-application in “organic” production urge the need for new innovative products like plant-derived fungicides. These phenylpropanoids could also trigger solutions for new product developments in the fight against oomycetes in grapes, tomatoes and potatoes. Resistance breeding in hops is not always a straight option because the market relies on specific cultivars known and popular for their flavor characteristics. Some of these varieties are not resistant to major pathogens and need to be protected by chemicals in the medium-term, potentially by a mix of phenylpropanoids. The mode of action, concentrations, synergistic and additive effects and combination of single compounds is still unclear and will require future investigation. However, the potential application in organic plant protection is promising and there is a clear demand by society to move from conventional to more ecological and sustainable plant protection systems.

5 Summary

Downy mildew in hops is caused by *Pseudoperonospora humuli* and generates significant losses in cone quality and yield as well as rootstock death. To identify the molecular processes conferring natural downy mildew resistance (DMR) and to determine genetic and metabolic markers for breeding, a metabolome-genome-wide association study was carried out.

An F1 hop population consisting of 192 individuals from parents contrasting in DMR was germinated and grown under *ex situ* conditions. Inoculation of the population of full-siblings with the fungus *P. humuli* led to both variation in specialized metabolites and downy mildew resistance phenotypes. ANOVA between infected and control plants showed that metabolites of almost all phytochemical classes were induced 48 hours after induction, providing evidence for a general and massive allocation of carbon into pathways with function in pathogen defense, but this approach did not lead to the identification of metabolites with direct activity against the pathogen. Using Pearson correlation analysis, a small number of metabolites with potential protective function against downy mildew were identified and mapped to the phenylpropanoid biosynthetic pathway. These metabolites were even correlated to DMR of the infected set when determined from the mock-infected plant set, suggesting that DMR is established prior contact with the pathogen. Genome-wide association study and genetic mapping detected a colocalization of the major downy mildew resistance locus and the phenylpropanoid pathway metabolite markers, indicating that the major contribution to resistance is mediated by these metabolites, in a heritable way.

In an independent validation experiment, a mix of three putative prophylactic phenylpropanoids was co-inoculated alongside with *P. humuli* on downy mildew susceptible genotypes. This external application led to a reduced leaf infection, thus confirming the phenylpropanoid's protective activity either directly or as precursors of active compounds.

These novel metabolic and genetic markers provide a better basis for the precise selection of crossing partners and progeny in hop breeding strategies in the future and may facilitate the development of bio-based fungicides for secured and sustainable cultivation of hop and other plant species affected by downy mildew.

6 Deutsche Zusammenfassung

Falscher Mehltau im Hopfen wird durch *Pseudoperonospora humuli* verursacht und führt zu erheblichen Ernteeinbußen und verminderter Doldenqualität - auch ein Absterben der Wurzelstöcke ist möglich. Um die molekularen Prozesse einer natürlichen Resistenz gegen den Falschen Mehltau (DMR) sowie genetische und metabolische Marker für die Hopfenzucht zu identifizieren, wurde eine Metabolom-Genomweite Assoziationsstudie durchgeführt.

Unter dem Ansatz des "Untargeted Metabolomics" wurde eine F1-Kartierpopulation aus 192 Individuen unter *ex-situ* Bedingungen gekeimt und aufgezogen. Deren Inokulation mit *P. humuli* führte sowohl zu Veränderungen im Gehalt von Sekundärmetaboliten als auch zu unterschiedlichen Resistenzausprägungen in Bezug auf den Falschen Mehltau. Die ANOVA zwischen infizierten und scheininfizierten Pflanzen lieferte keine spezifizierbaren Ergebnisse, da 48 Stunden nach Infektion Metaboliten aus nahezu allen phytochemischen Klassen induziert wurden. Durch Anwendung der Korrelationsanalyse nach Pearson konnte jedoch eine geringe Anzahl von Metaboliten mit potenzieller Schutzfunktion gegen den Falschen Mehltau identifiziert und dem Phenylpropanoid-Biosyntheseweg zugeordnet werden. Gleichzeitig korrelierten diese Metaboliten auch im scheinbehandelten Pflanzensatz mit der Resistenzausprägung der infizierten Pflanzen, was darauf schließen lässt, dass die Krankheitsresistenz vor dem Kontakt mit dem Erreger hergestellt wird. Die genomweite Assoziationsstudie und die genetische Kartierung zeigten, dass der Resistenzloкус mit den Phenylpropanoid-Stoffwechselmarkern kolokalisiert. Dies verdeutlicht, dass diese Metaboliten auf vererbare Weise den Hauptbeitrag für Resistenz liefern.

In einem unabhängigen Validierungsexperiment wurde eine Mischung aus drei mutmaßlich prophylaktischen Phenylpropanoiden zusammen mit *P. humuli* auf anfällige Genotypen aufgetragen. Die äußerliche Anwendung dieser Substanzen, welche in resistenten Genotypen überrepräsentiert sind, führte zu einer verringerten Blattinfektion. Dadurch wurde ihre Schutzaktivität entweder direkt oder als Vorläufer von aktiven Verbindungen bestätigt.

Die durch diese Studie gewonnenen metabolischen und genetischen Marker liefern ein besseres Verständnis über die zugrundeliegende Resistenz gegenüber dem

Falschen Mehltau. Zukünftig kann dadurch eine präzisere Selektion von Kreuzungspartnern und -nachkommen in der Hopfenzüchtung erfolgen. Darüber hinaus können die vorliegenden Ergebnisse dazu beitragen, bio-basierte Fungizide für die sichere und nachhaltige Kultivierung von Hopfen, und anderen von Falschem Mehltau betroffenen Pflanzenarten, zu entwickeln.

7 References

- Allard, R. 1960. *Principle of Plant Breeding*. New York.: John Wiley and Sons, Inc.
- Altschul, S., W. Gish, W. Miller, E. Myers, and D. Lipman. 1990. "Basic Local Alignment Search Tool." *Journal of Molecular Biology* 215 (3). England:403–10. [https://doi.org/10.1016/S0022-2836\(05\)80360-2](https://doi.org/10.1016/S0022-2836(05)80360-2).
- Bakel, H. van, J. Stout, A. Cote, C. Tallon, A. Sharpe, T. Hughes, and J. Page. 2011. "The Draft Genome and Transcriptome of Cannabis Sativa." *Genome Biology* 12 (October):1–17. <https://doi.org/10.1186/gb-2011-12-10-r102>.
- Barrie, F. 2011. "Report of the General Committee: 11." *Taxon* 60 (4). International Association for Plant Taxonomy (IAPT):1211–14. <http://www.jstor.org/stable/41317343>.
- Bates, D., M. Mächler, B. Bolker, and S. Walker. 2015. "Fitting Linear Mixed-Effects Models Using {lme4}." *Journal of Statistical Software* 67 (1):1–48. <https://doi.org/10.18637/jss.v067.i01>.
- Bazakos, C., M. Hanemian, C. Trontin, J. Jimenez-Gomez, and O. Loudet. 2017. "New Strategies and Tools in Quantitative Genetics: How to Go from the Phenotype to the Genotype." *Annual Review of Plant Biology* 68 (April). United States:435–55. <https://doi.org/10.1146/annurev-arplant-042916-040820>.
- Benjamini, Y., and Y. Hochberg. 1995. "Controlling the False Discovery Rate: A Practical and Powerful Approach to Multiple Testing." *Journal of the Royal Statistical Society B*. <https://doi.org/10.2307/2346101>.
- Biendl, M., B. Englhard, A. Forster, A. Gahr, A. Lutz, W. Mitter, R. Schmidt, and C. Schönberger. 2014. *Hops - Their Cultivation, Composition and Usage*. Nürnberg, Germany: Fachverlag Hans Carl GmbH.
- Bily, A., L. Reid, J. Taylor, D. Johnston, C. Malouin, A. Burt, B. Bakan, et al. 2003. "Dehydrodimers of Ferulic Acid in Maize Grain Pericarp and Aleurone: Resistance Factors to Fusarium Graminearum." *Phytopathology* 93 (6). United States:712–19. <https://doi.org/10.1094/PHYTO.2003.93.6.712>.

- Bollina, V., G. Kumaraswamy, A. Kushalappa, T. Choo, Y. Dion, S. Rioux, D. Faubert, and H. Hamzehzarghani. 2010. "Mass Spectrometry-Based Metabolomics Application to Identify Quantitative Resistance-Related Metabolites in Barley against Fusarium Head Blight." *Molecular Plant Pathology* 11 (6). England:769–82. <https://doi.org/10.1111/j.1364-3703.2010.00643.x>.
- Bourgaud, F., A. Hehn, R. Larbat, S. Doerper, E. Gontier, S. Kellner, and U. Matern. 2006. "Biosynthesis of Coumarins in Plants: A Major Pathway Still to Be Unravelling for Cytochrome P450 Enzymes." *Phytochemistry Reviews* 5 (2–3):293–308. <https://doi.org/10.1007/s11101-006-9040-2>.
- Boutigny, A., F. Richard-Forget, and C. Barreau. 2008. Natural Mechanisms for Cereal Resistance to Fusarium Mycotoxins Accumulation. *European Journal of Plant Pathology*. Vol. 121. <https://doi.org/10.1007/s10658-007-9266-x>.
- Box, G., and D. Cox. 1964. "An Analysis of Transformations." *Journal of the Royal Statistical Society. Series B (Methodological)* 26 (2). [Royal Statistical Society, Wiley]:211–52. <http://www.jstor.org/stable/2984418>.
- Bradbury, P., Z. Zhang, D. Kroon, T. Casstevens, Y. Ramdoss, and E. Buckler. 2007. "TASSEL: Software for Association Mapping of Complex Traits in Diverse Samples." *Bioinformatics* 23 (19):2633–35. <https://doi.org/10.1093/bioinformatics/btm308>.
- Broman, K., H. Wu, S. Sen, and G. Churchill. 2003. "R/qtl: QTL Mapping in Experimental Crosses." *Bioinformatics* 19 (7):889–90. <https://doi.org/10.1093/bioinformatics/btg112>.
- Bundessortenamt. 2000. Richtlinien Für Die Durchführung von Landwirtschaftlichen Wertprüfungen Und Sortenversuchen. Hannover: Landbuch Verlag mbH.
- Camera, S. La, G. Gouzerh, S. Dhondt, L. Hoffmann, B. Fritig, M. Legrand, and T. Heitz. 2004. "Metabolic Reprogramming in Plant Innate Immunity: The Contributions of Phenylpropanoid and Oxylin Pathways." *Immunological Reviews* 198 (April). England:267–84.
- Carlson, C., M. Eberle, L. Kruglyak, and D. Nickerson. 2004. "Mapping Complex Disease Loci in Whole-Genome Association Studies." *Nature* 429 (6990). England:446–52. <https://doi.org/10.1038/nature02623>.
- Carlson, C., T. Newman, and D. Nickerson. 2001. "SNPing in the Human Genome." *Current Opinion in Chemical Biology* 5 (1). England:78–85.

- Carr, R., and G. Carr. 1983. "Chromosome Races and Structural Heterozygosity in *Calycadenia Ciliosa* Greene (*Asteraceae*)." *American Journal of Botany* 70 (5). Wiley-Blackwell:744–55. <https://doi.org/10.1002/j.1537-2197.1983.tb12454.x>.
- Carreno-Quintero, N., H. Bouwmeester, and J. Keurentjes. 2013. "Genetic Analysis of Metabolome-Phenotype Interactions: From Model to Crop Species." *Trends in Genetics* 29 (1):41–50. <https://doi.org/10.1016/j.tig.2012.09.006>.
- Cerenak, A., D. Kralj, and B. Javornik. 2009. "Compounds of Essential Oils as Markers of Hop Resistance (*Humulus Lupulus*) to Powdery Mildew (*Podosphaera Macularis*)." *Acta Agriculturae Slovenica* 93 (3):267–73. <https://doi.org/10.2478/v10014-009-0015-z>.
- Cerenak, A., Z. Satovic, and B. Javornik. 2006. "Genetic Mapping of Hop (*Humulus Lupulus* L.) Applied to the Detection of QTLs for Alpha-Acid Content." *Genome / National Research Council Canada = Genome / Conseil National de Recherches Canada* 49 (5):485–94. <https://doi.org/10.1139/G06-007>.
- Chakradhar, T., V. Hindu, and P. Reddy. 2017. "Genomic-Based-Breeding Tools for Tropical Maize Improvement." *Genetica* 145 (6). Netherlands:525–39. <https://doi.org/10.1007/s10709-017-9981-y>.
- Cheema, J., and J. Dicks. 2009. "Computational Approaches and Software Tools for Genetic Linkage Map Estimation in Plants." *Briefings in Bioinformatics* 10 (6). England:595–608. <https://doi.org/10.1093/bib/bbp045>.
- Chen, J., S. Chang, and A. Anyia. 2011. "Gene Discovery in Cereals through Quantitative Trait Loci and Expression Analysis in Water-Use Efficiency Measured by Carbon Isotope Discrimination." *Plant, Cell & Environment* 34 (12). Wiley/Blackwell (10.1111):2009–23. <https://doi.org/10.1111/j.1365-3040.2011.02397.x>.
- Chen, W., Y. Gao, W. Xie, L. Gong, K. Lu, W. Wang, Y. Li, et al. 2014. "Genome-Wide Association Analyses Provide Genetic and Biochemical Insights into Natural Variation in Rice Metabolism." *Nature Genetics* 46 (June). Nature Publishing Group, a division of Macmillan Publishers Limited. All Rights Reserved.:714. <https://doi.org/10.1038/ng.3007>.
- Chen, Z., R. Brown, K. Rajasekaran, K. Damann, and T. Cleveland. 2006. "Identification of a Maize Kernel Pathogenesis-Related Protein and Evidence for Its Involvement in Resistance to *Aspergillus Flavus* Infection and Aflatoxin Production." *Phytopathology* 96 (1). United States:87–95. <https://doi.org/10.1094/PHYTO-96-0087>.

- Chitarrini, G., E. Soini, S. Riccadonna, P. Franceschi, L. Zulini, D. Masuero, A. Vecchione, et al. 2017. "Identification of Biomarkers for Defense Response to *Plasmopara Viticola* in a Resistant Grape Variety." *Frontiers in Plant Science* 8 (September):1–11. <https://doi.org/10.3389/fpls.2017.01524>.
- Chittoor, J., J. Leach, and F. White. 1997. "Differential Induction of a Peroxidase Gene Family during Infection of Rice by *Xanthomonas Oryzae* P.v. *Oryzae*." *Molecular Plant-Microbe Interactions: MPMI* 10 (7). United States:861–71. <https://doi.org/10.1094/MPMI.1997.10.7.861>.
- Chong, J., A. Poutaraud, and P. Huguene. 2009. "Metabolism and Roles of Stilbenes in Plants." *Plant Science* 177 (3):143–55. <https://doi.org/10.1016/j.plantsci.2009.05.012>.
- Cohen, Y., and H. Eyal. 1980. "Effects of Light during Infection on the Incidence of Downy Mildew (*Pseudoperonospora Cubensis*) on Cucumbers." *Physiological Plant Pathology* 17 (1):53–62. <http://www.lib.ncsu.edu.www.lib.ncsu.edu:2048/cgi-bin/proxy.pl?server=http://search.ebscohost.com/login.aspx?direct=true&db=lah&AN=19801366805&site=ehost-live&scope=site>.
- Croteau, R., T. Kutchan, and N. Lewis. 2000. "Natural Plants (Secondary Metabolites)." *Biochemistry and Molecular Biology of Plants* 24 (3):1250–1319.
- Darby, P. 2006. "The History of Hop Breeding and Development." *Journal of the Brewery History Society* 121:94–111.
- Dixon, R. 2001. "Natural Products and Plant Disease Resistance." *Nature* 411 (6839):843–47. <https://doi.org/10.1038/35081178>.
- Dixon, R., and N. Paiva. 1995. "Stress-Induced Phenylpropanoid Metabolism." *The Plant Cell* 7 (7):1085–97. <https://doi.org/10.1105/tpc.7.7.1085>.
- Dixon, R., D. Xie, and S. Sharma. 2005. "Proanthocyanidins-a Final Frontier in Flavonoid Research?" *The New Phytologist* 165 (1). England:9–28. <https://doi.org/10.1111/j.1469-8137.2004.01217.x>.
- Easterling, K., N. Pitra, R. Jones, L. Lopes, J. Aquino, D. Zhang, P. Matthews, and H. Bass. 2018. "3D Molecular Cytology of Hop (*Humulus Lupulus*) Meiotic Chromosomes Reveals Non-Disomic Pairing and Segregation, Aneuploidy, and Genomic Structural Variation." *Frontiers in Plant Science* 9 (November):1–13. <https://doi.org/10.3389/fpls.2018.01501>.

- Ellis, D., W. Dunn, J. Griffin, J. Allwood, and R. Goodacre. 2007. "Metabolic Fingerprinting as a Diagnostic Tool." *Pharmacogenomics* 8 (9). England:1243–66. <https://doi.org/10.2217/14622416.8.9.1243>.
- Elshire, R., J. Glaubitz, Q. Sun, J. Poland, K. Kawamoto, E. Buckler, and S. Mitchell. 2011. "A Robust, Simple Genotyping-by-Sequencing (GBS) Approach for High Diversity Species." *PLoS ONE* 6 (5):1–10. <https://doi.org/10.1371/journal.pone.0019379>.
- Eyck, L., and D. Gehring. 2015. *The Hop Grower's Handbook: The Essential Guide for Sustainable, Small-Scale Production for Home and Market*. 1sted. Chelsea Green Publishing.
- Frag, M., E. Mahrous, T. Lübken, A. Porzel, and L. Wessjohann. 2014. "Classification of Commercial Cultivars of *Humulus Lupulus* L. (Hop) by Chemometric Pixel Analysis of Two Dimensional Nuclear Magnetic Resonance Spectra." *Metabolomics* 10 (1):21–32. <https://doi.org/10.1007/s11306-013-0547-4>.
- Frag, M., A. Porzel, J. Schmidt, and L. Wessjohann. 2012. "Metabolite Profiling and Fingerprinting of Commercial Cultivars of *Humulus Lupulus* L. (Hop): A Comparison of MS and NMR Methods in Metabolomics." *Metabolomics* 8 (3):492–507. <https://doi.org/10.1007/s11306-011-0335-y>.
- Frag, M., A. Porzel, and L. Wessjohann. 2012. "Comparative Metabolite Profiling and Fingerprinting of Medicinal Licorice Roots Using a Multiplex Approach of GC-MS, LC-MS and 1D NMR Techniques." *Phytochemistry* 76 (April). England:60–72. <https://doi.org/10.1016/j.phytochem.2011.12.010>.
- Frag, M., M. Weigend, F. Luebert, G. Brokamp, and L. Wessjohann. 2013. "Phytochemical, Phylogenetic, and Anti-Inflammatory Evaluation of 43 *Urtica* Accessions (Stinging Nettle) Based on UPLC-Q-TOF-MS Metabolomic Profiles." *Phytochemistry* 96 (December). England:170–83. <https://doi.org/10.1016/j.phytochem.2013.09.016>.
- Fiehn, O. 2002. "Metabolomics-the Link between Genotypes and Phenotypes." *Plant Molecular Biology* 48 (1–2). Netherlands:155–71.
- Fiehn, O., J. Kopka, P. Dörmann, T. Altmann, R. Trethewey, and L. Willmitzer. 2000. "Metabolite Profiling for Plant Functional Genomics." *Nature Biotechnology* 18 (11):1157–61. <https://doi.org/10.1038/81137>.

- Figueiredo, A., J. Martins, F. Monteiro, A. Coelho, and M. Pais. 2015. "Early Events of Grapevine Resistance towards Downy Mildew by a Systems Biology Approach." *Revista de Ciências Agrárias* 38 (2):124–30.
- Forster, B., A. Lutz, and E. Seigner. 2014. "Detached Leaf Assay to Test for Downy Mildew Tolerance in Hops." *Institute for Crop Science and Plant Breeding Hop Breeding Research*, 2014.
- Freeman, J., B. Potts, M. Shepherd, and R. Vaillancourt. 2006. "Parental and Consensus Linkage Maps of *Eucalyptus Globulus* Using AFLP and Microsatellite Markers." *Silvae Genetica* 55 (4–5):202–17. <https://doi.org/10.1515/sg-2006-0028>.
- Gatica-Arias, A., M. Farag, M. Stanke, J. Matoušek, L. Wessjohann, and G. Weber. 2012. "Flavonoid Production in Transgenic Hop (*Humulus Lupulus* L.) Altered by PAP1/MYB75 from *Arabidopsis Thaliana* L." *Plant Cell Reports* 31 (1):111–19. <https://doi.org/10.1007/s00299-011-1144-5>.
- Gaut, B., and A. Long. 2003. "The Lowdown on Linkage Disequilibrium." *The Plant Cell* 15 (7):1502–6. <https://doi.org/10.1105/tpc.150730>.
- Gent, D., J. Barbour, A. Dreves, D. James, R. Parker, and D. Walsh. 2009. Field Guide for Integrated Pest Management in Hops. *Washington State University, Oregon State University, University of Idaho, and USDA Agricultural Research Service*. <https://doi.org/10.1017/CBO9781107415324.004>.
- Gent, D., Y. Cohen, and F. Runge. 2017. "Homothallism in *Pseudoperonospora Humuli*." *Plant Pathology*. <https://doi.org/10.1111/ppa.12689>.
- Glaubitz, J., T. Casstevens, F. Lu, J. Harriman, R. Elshire, Q. Sun, and E. Buckler. 2014. "TASSEL-GBS: A High Capacity Genotyping by Sequencing Analysis Pipeline." *PLoS ONE* 9 (2). <https://doi.org/10.1371/journal.pone.0090346>.
- Golczyk, H., A. Massouh, and S. Greiner. 2014. "Translocations of Chromosome End-Segments and Facultative Heterochromatin Promote Meiotic Ring Formation in Evening Primroses." *The Plant Cell* 26 (3). American Society of Plant Biologists:1280–93. <https://doi.org/10.1105/tpc.114.122655>.
- Grattapaglia, D, and R Sederoff. 1994. "Genetic Linkage Maps of *Eucalyptus Grandis* and *Eucalyptus Urophylla* Using a Pseudo-Testcross: Mapping Strategy and RAPD Markers." *Genetics* 137 (4):1121–37. <https://doi.org/10.1007/s11033-010-0612-2>.
- Gupta, P., J. Kumar, R. Mir, and A. Kumar. 2010. "Marker-Assisted Selection as a Component of Conventional Plant Breeding." *Plant Breeding Reviews*. Wiley Online Books. <https://doi.org/doi:10.1002/9780470535486.ch4>.

- He, J., X. Zhao, A. Laroche, Z. Lu, H. Liu, and Z. Li. 2014. "Genotyping-by-Sequencing (GBS), an Ultimate Marker-Assisted Selection (MAS) Tool to Accelerate Plant Breeding." *Frontiers in Plant Science* 5:484. <https://doi.org/10.3389/fpls.2014.00484>.
- Henning, J., D. Gent, M. Townsend, J. Woods, S. Hill, and D. Hendrix. 2017. "QTL Analysis of Resistance to Powdery Mildew in Hop (*Humulus Lupulus* L.)." *Euphytica* 213 (4). Springer Netherlands:98. <https://doi.org/10.1007/s10681-017-1849-9>.
- Henning, J., D. Gent, M. Twomey, M. Townsend, N. Pitra, and P. Matthews. 2015. "Precision QTL Mapping of Downy Mildew Resistance in Hop (*Humulus Lupulus* L.)." *Euphytica* 202 (3):487–98. <https://doi.org/10.1007/s10681-015-1356-9>.
- Henning, J., A. Haunold, M. Townsend, D. Gent, and T. Parker. 2008. "Registration of 'Teamaker' Hop." *Journal of Plant Registrations* 2 (1):13. <https://doi.org/10.3198/jpr2007.02.0105crc>.
- Henning, J., S. Hill, P. Darby, and D. Hendrix. 2017. "QTL Examination of a Bi-Parental Mapping Population Segregating for 'short-Stature' in Hop (*Humulus Lupulus* L.)." *Euphytica* 213 (3). Springer Netherlands:77. <https://doi.org/10.1007/s10681-017-1848-x>.
- Heuberger, A., C. Broeckling, K. Kirkpatrick, and J. Prenni. 2014. "Application of Nontargeted Metabolite Profiling to Discover Novel Markers of Quality Traits in an Advanced Population of Malting Barley." *Plant Biotechnology Journal* 12 (2). England:147–60. <https://doi.org/10.1111/pbi.12122>.
- Hill, S., J. Coggings, A. Liston, D. Hendrix, and J. Henning. 2016. "Genomics of the Hop Pseudo-Autosomal Regions." *Euphytica* 209 (1). Springer Netherlands:171–79. <https://doi.org/10.1007/s10681-016-1655-9>.
- Hochberg, Y. 1988. "A Sharper Bonferroni Procedure for Multiple Tests of Significance." *Biometrika* 75 (4):800–802. <http://dx.doi.org/10.1093/biomet/75.4.800>.
- Hollywood, K., D. Brison, and R. Goodacre. 2006. "Metabolomics: Current Technologies and Future Trends." *Proteomics* 6 (17):4716–23. <https://doi.org/10.1002/pmic.200600106>.
- Hopsteiner. 2014. "Hopsteiner Internal Breeding Records." Mainburg.
- . 2018. "Entscheidungsdaten Für Den Hopfeneinkauf." Mainburg. <https://www.hopsteiner.com/de/news/type/entscheidungsdaten-fur-den-hopfeneinkauf/>.

- Hyma, Katie E., Paola Barba, Minghui Wang, Jason P. Londo, Charlotte B. Acharya, Sharon E. Mitchell, Qi Sun, Bruce Reisch, and Lance Cadle-Davidson. 2015. "Heterozygous Mapping Strategy (HetMappS) for High Resolution Genotyping-by-Sequencing Markers: A Case Study in Grapevine." *PLoS ONE* 10 (8):1–31. <https://doi.org/10.1371/journal.pone.0134880>.
- Jakse, J., N. Stajner, P. Kozjak, A. Cerenak, and B. Javornik. 2008. "Trinucleotide Microsatellite Repeat Is Tightly Linked to Male Sex in Hop (*Humulus Lupulus* L.)." *Molecular Breeding* 21 (2):139–48. <https://doi.org/10.1007/s11032-007-9114-x>.
- Johnson, D., and C. Skotland. 1985. "Effects of Temperature and Relative-Humidity on Sporangium Production of *Pseudoperonospora-Humuli* on Hop." *Phytopathology* 75 (2):127–29.
- Kanehisa, M., and S. Goto. 2000. "KEGG: Kyoto Encyclopedia of Genes and Genomes." *Nucleic Acids Research* 27 (1):29–34. <https://doi.org/10.1093/nar/27.1.29>.
- Keen, N., and L. Littlefield. 1979. "The Possible Association of Phytoalexins with Resistance Gene Expression in Flax to *Melampsora Lini*." *Physiological Plant Pathology* 14 (3):265–80. [https://doi.org/https://doi.org/10.1016/0048-4059\(79\)90048-1](https://doi.org/https://doi.org/10.1016/0048-4059(79)90048-1).
- Knoch, D., D. Riewe, R. Meyer, A. Boudichevskaia, R. Schmidt, and T. Altmann. 2017. "Genetic Dissection of Metabolite Variation in Arabidopsis Seeds: Evidence for mQTL Hotspots and a Master Regulatory Locus of Seed Metabolism." *Journal of Experimental Botany*. <https://doi.org/10.1093/jxb/erx049>.
- Kogel, K., L. Voll, P. Schafer, C. Jansen, Y. Wu, G. Langen, J. Imani, et al. 2010. "Transcriptome and Metabolome Profiling of Field-Grown Transgenic Barley Lack Induced Differences but Show Cultivar-Specific Variances." *Proceedings of the National Academy of Sciences* 107 (14):6198–6203. <https://doi.org/10.1073/pnas.1001945107>.
- Koie, K., A. Inaba, Y. Okada, T. Kaneko, and K. Ito. 2005. "Construction of the Genetic Linkage Map and QTL Analysis on Hop (*Humulus Lupulus* L.)." *Acta Horticulturae* 668:59–66.
- Konig, S., K. Feussner, A. Kaefer, M. Landesfeind, C. Thurow, P. Karlovsky, C. Gatz, A. Polle, and I. Feussner. 2014. "Soluble Phenylpropanoids Are Involved in the Defense Response of Arabidopsis against *Verticillium Longisporum*." *The New Phytologist* 202 (3). England:823–37. <https://doi.org/10.1111/nph.12709>.

- Kosambi, D. 1943. "The Estimation of Map Distances From Recombination Values." *Annals of Eugenics* 12 (1):172–75. <https://doi.org/10.1111/j.1469-1809.1943.tb02321.x>.
- Kráľová, K., J. Jampílek, and I. Ostrovský. 2012. "Metabolomics - Useful Tool for Study of Plant Responses to Abiotic Stresses." *Ecological Chemistry and Engineering S* 19 (2):133–61. <https://doi.org/10.2478/v10216-011-0012-0>.
- Kuhl, C., R. Tautenhahn, C. Boettcher, T. Larson, and S. Neumann. 2012. "CAMERA: An Integrated Strategy for Compound Spectra Extraction and Annotation of Liquid Chromatography/mass Spectrometry Data Sets." *Analytical Chemistry* 84:283–89. <http://pubs.acs.org/doi/abs/10.1021/ac202450g>.
- Kumar, J., A. Choudhary, R. Solanki, and A. Pratap. 2011. "Towards Marker-Assisted Selection in Pulses: A Review." *Plant Breeding* 130 (3). Wiley/Blackwell (10.1111):297–313. <https://doi.org/10.1111/j.1439-0523.2011.01851.x>.
- Kutyniok, M., and C. Müller. 2012. "Crosstalk between above- and Belowground Herbivores Is Mediated by Minute Metabolic Responses of the Host *Arabidopsis Thaliana*." *Journal of Experimental Botany* 63 (17):6199–6210.
- Lamesch, P., T. Berardini, D. Li, D. Swarbreck, C. Wilks, R. Sasidharan, R. Muller, et al. 2012. "The Arabidopsis Information Resource (TAIR): Improved Gene Annotation and New Tools." *Nucleic Acids Research* 40 (D1):1202–10. <https://doi.org/10.1093/nar/gkr1090>.
- Langenbach, C., R. Campe, U. Schaffrath, K. Goellner, and U. Conrath. 2013. "UDP-Glucosyltransferase UGT84A2/BRT1 Is Required for Arabidopsis Nonhost Resistance to the Asian Soybean Rust Pathogen *Phakopsora Pachyrhizi*." *The New Phytologist* 198 (2). England:536–45. <https://doi.org/10.1111/nph.12155>.
- Laursen, L. 2015. "Botany: The Cultivation of Weed." *Nature* 525 (7570):4–5. <https://doi.org/10.1038/525S4a>.
- Lazazzara, V., C. Bueschl, A. Parich, I. Pertot, R. Schuhmacher, and M. Perazzolli. 2018. "Downy Mildew Symptoms on Grapevines Can Be Reduced by Volatile Organic Compounds of Resistant Genotypes." *Scientific Reports* 8 (1):1618. <https://doi.org/10.1038/s41598-018-19776-2>.
- Li, H., and R. Durbin. 2009. "Fast and Accurate Short Read Alignment with Burrows-Wheeler Transform." *Bioinformatics* 25 (14):1754–60. <https://doi.org/10.1093/bioinformatics/btp324>.

- Li, M., H. Chen, J. Chen, M. Chang, I. Palmer, W. Gassmann, F. Liu, and Z. Fu. 2018. "TCP Transcription Factors Interact With NPR1 and Contribute Redundantly to Systemic Acquired Resistance." *Frontiers in Plant Science* 9 (August):1–12. <https://doi.org/10.3389/fpls.2018.01153>.
- Lisec, J., N. Schauer, J. Kopka, L. Willmitzer, and A. Fernie. 2006. "Gas Chromatography Mass Spectrometry-Based Metabolite Profiling in Plants." *Nature Protocols* 1 (1):387–96. <https://doi.org/10.1038/nprot.2006.59>.
- Liu, G., R. Kennedy, D. Greenshields, G. Peng, L. Forseille, G. Selvaraj, and Y. Wei. 2007. "Detached and Attached Arabidopsis Leaf Assays Reveal Distinctive Defense Responses against *Hemibiotrophic Colletotrichum* Spp." *Molecular Plant-Microbe Interactions : MPMI* 20 (10). United States:1308–19. <https://doi.org/10.1094/MPMI-20-10-1308>.
- Lokhov, P., and A. Archakov. 2009. "Mass Spectrometry Methods in Metabolomics." *Biochemistry (Moscow) Supplement Series B: Biomedical Chemistry* 3 (1):1–9. <https://doi.org/10.1134/S1990750809010016>.
- Luo, J. 2015. "Metabolite-Based Genome-Wide Association Studies in Plants." *Current Opinion in Plant Biology* 24. Elsevier Ltd:31–38. <https://doi.org/10.1016/j.pbi.2015.01.006>.
- Ma, X., E. Jensen, N. Alexandrov, M. Troukhan, L. Zhang, S. Thomas-Jones, K. Farrar, et al. 2012. "High Resolution Genetic Mapping by Genome Sequencing Reveals Genome Duplication and Tetraploid Genetic Structure of the Diploid *Miscanthus Sinensis*." *PLoS ONE* 7 (3). <https://doi.org/10.1371/journal.pone.0033821>.
- Mabry, T., and A. Ulubelen. 1980. "Chemistry and Utilization of Phenylpropanoids Including Flavonoids, Coumarins, and Lignans." *Journal of Agricultural and Food Chemistry* 28 (2). American Chemical Society:188–96. <https://doi.org/10.1021/jf60228a024>.
- Maghuly, F., S. Pabinger, J. Krainer, and M. Laimer. 2018. "The Pattern and Distribution of Induced Mutations in *J. Curcas* Using Reduced Representation Sequencing." *Frontiers in Plant Science* 9:524. <https://doi.org/10.3389/fpls.2018.00524>.
- Malacarne, G., U. Vrhovsek, L. Zulini, A. Cestaro, M. Stefanini, F. Mattivi, M. Delledonne, R. Velasco, and C. Moser. 2011. "Resistance to *Plasmopara Viticola* in a Grapevine Segregating Population Is Associated with Stilbenoid Accumulation and with Specific Host Transcriptional Responses." *BMC Plant Biology* 11 (1). BioMed Central Ltd:114. <https://doi.org/10.1186/1471-2229-11-114>.

- Malamy, J., and D. Klessig. 1992. "Salicylic Acid and Plant Disease Resistance." *Plant Journal* 2 (5):643–54.
- Manivannan, A., J. Kim, E. Yang, Y. Ahn, E. Lee, S. Choi, and D. Kim. 2018. "Next-Generation Sequencing Approaches in Genome-Wide Discovery of Single Nucleotide Polymorphism Markers Associated with Pungency and Disease Resistance in Pepper." *BioMed Research International* 2018. Hindawi. <https://doi.org/10.1155/2018/5646213>.
- Martínez, G., M. Regente, S. Jacobi, M. Del Rio, M. Pinedo, and L. de la Canal. 2017. "Chlorogenic Acid Is a Fungicide Active against Phytopathogenic Fungi." *Pesticide Biochemistry and Physiology* 140:30–35. <https://doi.org/https://doi.org/10.1016/j.pestbp.2017.05.012>.
- Matros, A., and H. Mock. 2004. "Ectopic Expression of a UDP-Glucose:phenylpropanoid Glucosyltransferase Leads to Increased Resistance of Transgenic Tobacco Plants against Infection with Potato Virus Y." *Plant & Cell Physiology* 45 (9). Japan:1185–93. <https://doi.org/10.1093/pcp/pch140>.
- Matthews, P., M. Coles, and N. Pitra. 2013. "Next Generation Sequencing for a Plant of Great Tradition: Application of NGS to SNP Detection and Validation in Hops (*Humulus Lupulus* L.)." *BrewingScience* 66 (December):185–91.
- Mauch-Mani, B. 1996. "Production of Salicylic Acid Precursors Is a Major Function of Phenylalanine Ammonia-Lyase in the Resistance of Arabidopsis to *Peronospora Parasitica*." *The Plant Cell Online* 8 (2):203–12. <https://doi.org/10.1105/tpc.8.2.203>.
- McAdam, E., J. Freeman, S. Whittock, E. Buck, J. Jakse, A. Cerenak, B. Javornik, et al. 2013. "Quantitative Trait Loci in Hop (*Humulus Lupulus* L.) Reveal Complex Genetic Architecture Underlying Variation in Sex, Yield and Cone Chemistry." *BMC Genomics* 14:360. <https://doi.org/10.1186/1471-2164-14-360>.
- Mellway, R., L. Tran, M. Prouse, M. Campbell, and C. Constabel. 2009. "The Wound-, Pathogen-, and Ultraviolet B-Responsive MYB134 Gene Encodes an R2R3 MYB Transcription Factor That Regulates Proanthocyanidin Synthesis in Poplar." *Plant Physiology* 150 (2):924–41. <https://doi.org/10.1104/pp.109.139071>.
- Miranda, C., V. Elias, J. Hay, J. Choi, R. Reed, and J. Stevens. 2016. "Xanthohumol Improves Dysfunctional Glucose and Lipid Metabolism in Diet-Induced Obese C57BL/6J Mice." *Archives of Biochemistry and Biophysics* 599 (June). Academic Press:22–30. <https://doi.org/10.1016/j.abb.2016.03.008>.

- Mitchell, M. 2010. "Addressing the Relationship Between *Pseudoperonospora Cubensis* and *P. Humuli* Using Phylogenetic Analyses and Host Specificity Assays." Master Thesis, Oregon State University.
- Miyabe, K., and Y. Takahashi. 1906. "A New Disease of the Hop-Vine Caused by *Peronoplasmopara Humuli* N. Sp." *Trans. Sapporo Nat. Hist. Soc* 1:149–57.
- Moir, M. 2000. "Hops - A Millennium Review." *Journal of the American Society of Brewing Chemists* 58 (January):131–46.
- Morreel, K., G. Goeminne, V. Storme, L. Sterck, J. Ralph, W. Coppieters, P. Breyne, et al. 2006. "Genetical Metabolomics of Flavonoid Biosynthesis in *Populus*: A Case Study." *Plant Journal* 47 (2):224–37. <https://doi.org/10.1111/j.1365-313X.2006.02786.x>.
- Murakami, A. 2000. "Comparison of Sequence of *rbcL* and Non- Coding Regions of Chloroplast DNA and ITS2 Region of rDNA in Genus *Humulus*." *Breeding Science* 50:155–60. <https://doi.org/10.1248/cpb.37.3229>.
- Murakami, A., P. Darby, B. Javornik, M. Pais, E. Seigner, A. Lutz, and P. Svoboda. 2006. "Molecular Phylogeny of Wild Hops, *Humulus Lupulus* L." *Heredity* 97 (1):66–74. <https://doi.org/10.1038/sj.hdy.6800839>.
- Nagel, J., L. Culley, Y. Lu, E. Liu, P. Matthews, J. Stevens, and J. Page. 2008. "EST Analysis of Hop Glandular Trichomes Identifies an O-Methyltransferase That Catalyzes the Biosynthesis of Xanthohumol." *Plant Cell* 20 (1):186–200. <https://doi.org/10.1105/tpc.107.055178>.
- Natsume, S., H. Takagi, A. Shiraishi, J. Murata, H. Toyonaga, J. Patzak, M. Takagi, et al. 2015. "The Draft Genome of Hop (*Humulus Lupulus*), an Essence for Brewing." *Plant and Cell Physiology* 56 (3):428–41. <https://doi.org/10.1093/pcp/pcu169>.
- NCBI. 2018. "National Center for Biotechnology Information." 2018.
- Neve, R. 1986. "Centenary Review Hop Breeding Worldwide - Its Aims And Achievements." *J. Inst. Brew.* 92:21–24.
- . 1991. *Hops*. Dordrecht: Springer Netherlands. <https://doi.org/10.1007/978-94-011-3106-3>.
- Neve, R., and P. Darby. 1983. "Yeoman and Zenith: Two New Varieties." Nordborg.
- Nordborg, M., J. Borevitz, J. Bergelson, C. Berry, J. Chory, J. Hagenblad, M. Kreitman, et al. 2002. "The Extent of Linkage Disequilibrium in *Arabidopsis Thaliana*." *Nature Genetics* 30 (2). United States:190–93. <https://doi.org/10.1038/ng813>.

- Oever-van den Elsen, F. van den, A. Lucatti, S. van Heusden, C. Broekgaarden, R. Mumm, M. Dicke, and B. Vosman. 2016. "Quantitative Resistance against *Bemisia Tabaci* in *Solanum Pennellii*: Genetics and Metabolomics." *Journal of Integrative Plant Biology* 58 (4):397–412. <https://doi.org/10.1111/jipb.12449>.
- Ooijen, J. Van. 2011. "Multipoint Maximum Likelihood Mapping in a Full-Sib Family of an Outbreeding Species." *Genetics Research* 93 (5). Cambridge University Press:343–49. <https://doi.org/DOI:10.1017/S0016672311000279>.
- Ososki, A., and E. Kennelly. 2003. "Phytoestrogens: A Review of the Present State of Research." *Phytotherapy Research* 17 (8):845–69. <https://doi.org/10.1002/ptr.1364>.
- Paranidharan, V., Y. Abu-Nada, H. Hamzehzarghani, A. Kushalappa, O. Mamer, Y. Dion, S. Rioux, A. Comeau, and L. Choiniere. 2008. "Resistance-Related Metabolites in Wheat against *Fusarium Graminearum* and the Virulence Factor Deoxynivalenol (DON)." *Botany* 86 (10):1168–79. <https://doi.org/10.1139/B08-052>.
- Parker, T. 2007. "Investigation of Hop Downy Mildew through Association Mapping and Observations of the Oospore."
- Passardi, F., C. Cosio, C. Penel, and C. Dunand. 2005. "Peroxidases Have More Functions than a Swiss Army Knife." *Plant Cell Reports* 24 (5). Germany:255–65. <https://doi.org/10.1007/s00299-005-0972-6>.
- Patti, G., O. Yanes, and G. Siuzdak. 2012. "Innovation: Metabolomics: The Apogee of the Omics Trilogy." *Nature Publishing Group* 13 (4):263–69. <https://doi.org/10.1038/nrm3314>.
- Patzak, J. 2005. "PCR Detection of *Pseudoperonospora Humuli* and *Podosphaera Macularis*." *Plant Protect. Sci.* 41 (4):141–49.
- Pearson, T., and T. Manolio. 2008. "How to Interpret a Genome-Wide Association Study." *JAMA* 299 (11):1335. <https://doi.org/10.1001/jama.299.11.1335>.
- Pezet, R., K. Gindro, O. Viret, and J. L. Spring. 2004. "Glycosylation and Oxidative Dimerization of Resveratrol Are Respectively Associated to Sensitivity and Resistance of Grapevine Cultivars to Downy Mildew." *Physiological and Molecular Plant Pathology* 65 (6):297–303. <https://doi.org/10.1016/j.pmpp.2005.03.002>.
- Pillay, M., and S. Kenny. 1996. "Structure and Inheritance of Ribosomal DNA Variants in Cultivated and Wild Hop, *Humulus Lupulus* L." *Theoretical and Applied Genetics* 93 (3):333–40. <https://doi.org/10.1007/BF00223173>.

- Pool, R., L. Creasy, and A. Frackelton. 1981. "Resveratrol and the Viniferins, Their Application to Screening for Disease Resistance in Grape Breeding Programs." *Vitis* 145:136–45.
- R Core Team. 2014. "R: A Language and Environment for Statistical Computing." Vienna, Austria. <http://www.r-project.org/>.
- Rauwolf, U., H. Golczyk, J. Meurer, R. Herrmann, and S. Greiner. 2008. "Molecular Marker Systems for Oenothera Genetics." *Genetics* 180 (3). Genetics:1289–1306. <https://doi.org/10.1534/genetics.108.091249>.
- Reeves, P., and C. Richards. 2011. "Species Delimitation under the General Lineage Concept: An Empirical Example Using Wild North American Hops (*Cannabaceae: Humulus Lupulus*)." *Systematic Biology* 60 (1):45–59. <https://doi.org/10.1093/sysbio/syq056>.
- Riedelsheimer, C., J. Lisec, A. Czedik-eyenberg, R. Sulpice, A. Flis, C. Grieder, T. Altmann, M. Stitt, L. Willmitzer, and A. Melchinger. 2012. "Genome-Wide Association Mapping of Leaf Metabolic Profiles for Dissecting Complex Traits in Maize." *Proceedings of the National Academy of Sciences* 109 (23):8872–77. <https://doi.org/10.1073/pnas.1120813109/-/DCSupplemental.www.pnas.org/cgi/doi/10.1073/pnas.1120813109>.
- Riewe, D., J. Wiebach, and T. Altmann. 2017. "Structure Annotation and Quantification of Wheat Seed Oxidized Lipids by High Resolution LC-MS/MS." *Plant Physiology* 175 (October):600–618. <https://doi.org/10.1104/pp.17.00470>.
- Roepenack-Lahaye, E. von, T. Degenkolb, M. Zerjeski, M. Franz, U. Roth, L. Wessjohann, J. Schmidt, D. Scheel, and S. Clemens. 2004. "Profiling of Arabidopsis Secondary Metabolites by Capillary Liquid Chromatography Coupled to Electrospray Ionization Quadrupole Time-of-Flight Mass Spectrometry." *Plant Physiology* 134 (2). United States:548–59. <https://doi.org/10.1104/pp.103.032714>.
- Rossbauer, G. 1995. "BBCH-Codierung Der Phänologischen Entwicklungsstadien von Hopfen (*Humulus Lupulus* L.)." Landesanstalt für Landwirtschaft, Hopfen.
- Roy, J., B. Huss, A. Creach, S. Hawkins, and G. Neutelings. 2016. "Glycosylation Is a Major Regulator of Phenylpropanoid Availability and Biological Activity in Plants" 7 (735). <https://doi.org/10.3389/fpls.2016.00735>.
- Royle, D. 1970. "Infection Periods in Relation to the Natural Development of Hop Downy Mildew (*Pseudoperonospora Humuli*)." *Ann. Appl. Biol.*, no. 1933:2–4.

- Royle, D., and H. Kremheller. 1981. Downy Mildew of the Hop. *In: Spencer, D. M., Ed. The Downy Mildews*. New York, NY, USA: Academic Press 395-419.
- Royle, D., and G. Thomas. 1971. "The Influence of Stomatal Opening on the Infection of Hop Leaves by *Pseudoperonospora Humuli*." *Physiological Plant Pathology* 1 (3):329–43. [https://doi.org/10.1016/0048-4059\(71\)90053-1](https://doi.org/10.1016/0048-4059(71)90053-1).
- . 1973. "Factors Affecting Zoospore Responses towards Stomata in Hop Downy Mildew (*Pseudoperonospora Humuli*) Including Some Comparisons with Grapevine Downy Mildew (*Plasmopara Viticola*)." *Physiological Plant Pathology* 3 (3):405–17. [https://doi.org/10.1016/0048-4059\(73\)90013-1](https://doi.org/10.1016/0048-4059(73)90013-1).
- Schaid, D., W. Chen, and N. Larson. 2018. "From Genome-Wide Associations to Candidate Causal Variants by Statistical Fine-Mapping." *Nature Reviews. Genetics* 19 (8). England:491–504. <https://doi.org/10.1038/s41576-018-0016-z>.
- Schwekendiek, A., O. Spring, A. Heyerick, B. Pickel, N. Pitsch, F. Peschke, D. de Keukeleire, and G. Weber. 2007. "Constitutive Expression of a Grapevine Stilbene Synthase Gene in Transgenic Hop (*Humulus Lupulus* L.) Yields Resveratrol and Its Derivatives in Substantial Quantities." *Journal of Agricultural and Food Chemistry* 55 (17). United States:7002–9. <https://doi.org/10.1021/jf070509e>.
- Seefeldler, S., H. Ehrmaier, G. Schweizer, and E. Seigner. 2000. "Male and Female Genetic Linkage Map of Hops, *Humulus Lupulus*." *Plant Breeding* 119:249–55.
- Semagn, K., A. Bjornstad, and M. Ndjiondjop. 2006. "An Overview of Molecular Marker Methods for Plants." *African Journal of Biotechnology* 5 (25):2540–68. <https://doi.org/10.5897/AJB2006.000-5110>.
- Shulaev, V. 2006. "Metabolomics Technology and Bioinformatics." *Briefings in Bioinformatics* 7 (2). England:128–39. <https://doi.org/10.1093/bib/bbl012>.
- Singh, B., and A. Singh. 2015. *Marker-Assisted Plant Breeding: Principles and Practices*. Marker-Assisted Plant Breeding: Principles and Practices. <https://doi.org/10.1007/978-81-322-2316-0>.
- Singh, D., A. Kumar, A. Kumar, P. Chauhan, V. Kumar, N. Kumar, A. Singh, et al. 2011. Marker Assisted Selection and Crop Management for Salt Tolerance: A Review. *African Journal of Biotechnology*. Vol. Vol. 10. <https://doi.org/10.5897/AJB11.049>.
- Siragusa, G., G. Haas, P. Matthews, R. Smith, R. Buhr, N. Dale, and M. Wise. 2008. "Antimicrobial Activity of Lupulone against *Clostridium Perfringens* in the Chicken Intestinal Tract Jejunum and Caecum." *Journal of Antimicrobial Chemotherapy* 61 (4):853–58. <https://doi.org/10.1093/jac/dkn024>.

- Skotland, C. 1961. "Infection of Hop Crowns and Roots by *Pseudoperonospora Humuli* and Its Relation to Crown and Root Rot and Overwintering of the Pathogen. ." *Phytopathology* 51:241–44.
- Skotland, C., and R. Romanko. 1964. "Life History of the Hop Downy Mildew Fungus. Bull." *Idaho Agric. Exp. Stn.* 424.
- Slatkin, M. 2008. "Linkage Disequilibrium — Understanding the Evolutionary Past and Mapping the Medical Future." *Nature Reviews Genetics* 9 (6):477–85. <https://doi.org/10.1038/nrg2361>.Linkage.
- Small, E. 1978. "A Numerical and Nomenclatural Analysis of Morpho-Geographic Taxa of *Humulus*." *Systematic Botany* 3 (1). American Society of Plant Taxonomists:37–76. <http://www.jstor.org/stable/2418532>.
- Smith, C. 2010. "LC/MS Preprocessing and Analysis with Xcms." *Documentation of Bioconductor Xcms Package*. <http://bioconductor.org/packages/release/bioc/vignettes/xcms/inst/doc/xcmsPreprocess.pdf>.
- Snow, R. 1960. "Chromosomal Differentiation in *Clarkia Dudleyana*." *American Journal of Botany* 47 (4):302–9. <https://doi.org/10.1002/j.1537-2197.1960.tb07129.x>.
- Stevens, J., and J. Page. 2004. "Xanthohumol and Related Prenylflavonoids from Hops and Beer: To Your Good Health!" *Phytochemistry* 65 (10):1317–30. <https://doi.org/10.1016/j.phytochem.2004.04.025>.
- Sumner, L., P. Mendes, and R. Dixon. 2003. "Plant Metabolomics: Large-Scale Phytochemistry in the Functional Genomics Era." *Phytochemistry* 62 (6). England:817–36.
- Sved, J., and W. Hill. 2018. "One Hundred Years of Linkage Disequilibrium." *Genetics* 209 (3):629 LP-636. <https://doi.org/10.1534/genetics.118.300642>.
- Tawata, S., S. Taira, N. Kobamoto, J. Zhu, M. Ishihara, and S. Toyama. 1996. "Synthesis and Antifungal Activity of Cinnamic Acid Esters." *Bioscience, Biotechnology, and Biochemistry* 60 (5). England:909–10.
- Tenenbaum, Dan. 2018. "KEGGREST: Client-Side REST Access to KEGG. R Package Version 1.20.0."
- Thakur, M., and B. Sohal. 2013. "Role of Elicitors in Inducing Resistance in Plants against Pathogen Infection: A Review." *ISRN Biochemistry* 2013:1–10. <https://doi.org/10.1155/2013/762412>.

- The Wellcome Trust Case Control Consortium. 2007. "Genome-Wide Association Study of 14 000 Cases of Seven Common Diseases and 3 000 Shared Controls." *Nature* 447 (7145):661–78. <https://doi.org/10.1038/nature05911>. Genome-wide.
- Thordal-Christensen, H. 2003. "Fresh Insights into Processes of Nonhost Resistance." *Current Opinion in Plant Biology* 6 (4). England:351–57.
- Tiago, O., N. Maicon, R. Ivan, N. Diego, J. Vinícius, F. Mauricio, J. Alan, and Q. Velci. 2017. "Plant Secondary Metabolites and Its Dynamical Systems of Induction in Response to Environmental Factors: A Review." *African Journal of Agricultural Research* 12 (2):71–84. <https://doi.org/10.5897/AJAR2016.11677>.
- Toffolatti, S., G. Venturini, D. Maffi, and A. Vercesi. 2012. "Phenotypic and Histochemical Traits of the Interaction between *Plasmopara Viticola* and Resistant or Susceptible Grapevine Varieties." *BMC Plant Biology* 12 (1). BMC Plant Biology:1. <https://doi.org/10.1186/1471-2229-12-124>.
- USDA. 2018. "USDA Natural Resources Conservation Service." 2018. <https://plants.usda.gov/core/profile?symbol=hulu>.
- Vinayavekhin, N., E. Homan, and A. Saghatelian. 2010. "Exploring Disease through Metabolomics." *ACS Chemical Biology* 5 (1). United States:91–103. <https://doi.org/10.1021/cb900271r>.
- Vision, T., D. Brown, D. Shmoys, R. Durrett, and S. Tanksley. 2000. "Selective Mapping: A Strategy for Optimizing the Construction of High-Density Linkage Maps." *Genetics* 155 (1):407–20. <http://www.ncbi.nlm.nih.gov/pmc/articles/PMC1461083/>.
- Wasternack, C. 2007. "Jasmonates: An Update on Biosynthesis, Signal Transduction and Action in Plant Stress Response, Growth and Development." *Annals of Botany* 100 (4):681–97. <https://doi.org/10.1093/aob/mcm079>.
- Wen, Weiwei, Dong Li, Xiang Li, Yanqiang Gao, Wenqiang Li, Huihui Li, Jie Liu, et al. 2014. "Metabolome-Based Genome-Wide Association Study of Maize Kernel Leads to Novel Biochemical Insights." *Nature Communications* 5. Nature Publishing Group:3438. <https://doi.org/10.1038/ncomms4438>.
- Whetten, R, and R Sederoff. 1995. "Lignin Biosynthesis." *The Plant Cell* 7 (7):1001–13. <https://doi.org/10.1105/tpc.7.7.1001>.
- Wiens, D., and B. Barlow. 1975. "Permanent Translocation Heterozygosity and Sex Determination in East African Mistletoes." *Science* 187 (4182). American Association for the Advancement of Science:1208–9. <https://doi.org/10.1126/science.187.4182.1208>.

- Wilson, D. 1975. "Plant Remains from the Graveney Boat and the Early History of *Humulus Lupulus* L. in W. Europe." *New Phytologist* 75:627–48.
- Woods, J., and D. Gent. 2016. "Susceptibility of Hop Cultivars to Downy Mildew: Associations with Chemical Characteristics and Region of Origin." *The American Phytopathological Society* 17 (1):42–48.
- Xin, Z., and J. Chen. 2012. "A High Throughput DNA Extraction Method with High Yield and Quality." *Plant Methods* 8 (1). *Plant Methods*:26. <https://doi.org/10.1186/1746-4811-8-26>.
- Zhang, D., K. Easterling, N. Pitra, M. Coles, E. Buckler, H. Bass, and P. Matthews. 2017. "Non-Mendelian Single-Nucleotide Polymorphism Inheritance and Atypical Meiotic Configurations Are Prevalent in Hop." *The Plant Genome* 10 (3):0. <https://doi.org/10.3835/plantgenome2017.04.0032>.

8 Supplementary data

8.1 Sample list

Table 12: Sample list including sample type, treatment, sample weight and replicate downy mildew scoring rates of experiment 1.

Genotype	Sample ID	Type	Treatment	Weight (mg)	DM Scoring1	DM Scoring2	DM Scoring3
1	118	Sample	Mock	147.84	3	3	3
1	295	Sample	Infected	149.11	3	3	3
2	13	Sample	Mock	155.25	3	5	5
2	399	Sample	Infected	143.72	3	5	5
3	196	Sample	Mock	149.5	5	7	5
3	249	Sample	Infected	145.82	5	7	5
4	28	Sample	Mock	152.95	9	9	7
4	108	Sample	Infected	151.1	9	9	7
5	136	Sample	Mock	156.26	5	7	5
5	275	Sample	Infected	148.2	5	7	5
6	168	Sample	Infected	159.93	3	3	3
6	359	Sample	Mock	155.78	3	3	3
7	57	Sample	Mock	148.55	5	5	7
7	367	Sample	Infected	153.8	5	5	7
8	365	Sample	Mock	146.95	5	7	5
8	410	Sample	Infected	147.57	5	7	5
10	98	Sample	Infected	146.71	5	7	7
10	324	Sample	Mock	151.42	5	7	7
11	182	Sample	Infected	149.42	5	7	5
11	251	Sample	Mock	152.77	5	7	5
12	87	Sample	Infected	157.47	5	5	7
12	104	Sample	Mock	153.22	5	5	7
13	259	Sample	Infected	157.4	3	3	3
13	383	Sample	Mock	148.66	3	3	3
14	24	Sample	Mock	150.55	5	5	7
14	40	Sample	Infected	145.84	5	5	7
15	52	Sample	Mock	159.84	3	5	5
15	113	Sample	Infected	150.62	3	5	5
16	86	Sample	Mock	149	3	5	7

16	413	Sample	Infected	146.71	3	5	7
17	46	Sample	Mock	152.99	5	5	7
17	287	Sample	Infected	147.44	5	5	7
18	42	Sample	Mock	153.76	5	7	5
18	119	Sample	Infected	147.1	5	7	5
19	34	Sample	Mock	151.53	3	5	5
19	190	Sample	Infected	150.49	3	5	5
20	107	Sample	Infected	150.48	3	7	5
20	294	Sample	Mock	147.74	3	7	5
21	247	Sample	Infected	145.44	5	5	5
21	385	Sample	Mock	149.5	5	5	5
22	230	Sample	Infected	147.72	3	3	3
22	342	Sample	Mock	161.45	3	3	3
23	97	Sample	Infected	152.27	3	5	7
23	129	Sample	Mock	160.38	3	5	7
23	222	Sample	Infected	151.67	5	7	5
23	235	Sample	Mock	156.52	5	7	5
23	296	Sample	Mock	160.64	5	5	5
23	370	Sample	Infected	148.99	5	5	5
24	70	Sample	Mock	151.68	3	5	5
24	349	Sample	Infected	147.71	3	5	5
25	208	Sample	Mock	146.88	7	7	7
25	264	Sample	Infected	155.85	7	7	7
26	7	Sample	Infected	151.43	7	7	9
26	54	Sample	Mock	150.48	7	7	9
27	245	Sample	Mock	151.82	7	9	9
27	292	Sample	Infected	149.05	7	9	9
28	111	Sample	Mock	152.5	7	7	9
28	226	Sample	Infected	157.4	7	7	9
29	303	Sample	Mock	148.63	5	5	7
29	340	Sample	Infected	145.26	5	5	7
30	8	Sample	Mock	154.86	5	7	5
30	343	Sample	Infected	144.71	5	7	5
31	121	Sample	Infected	152.51	9	9	9
31	298	Sample	Mock	155.29	9	9	9
32	253	Sample	Mock	146.8	3	3	5
32	355	Sample	Infected	159.96	3	3	5
33	237	Sample	Infected	151.57	7	7	7

33	363	Sample	Mock	151.8	7	7	7
34	242	Sample	Mock	146.83	7	9	9
34	327	Sample	Infected	156.96	7	9	9
35	69	Sample	Mock	155.53	7	7	7
35	258	Sample	Infected	153.42	7	7	7
36	39	Sample	Infected	153.39	5	5	7
36	143	Sample	Mock	156.36	5	5	7
37	148	Sample	Infected	151.52	5	5	5
37	351	Sample	Mock	151.18	5	5	5
38	268	Sample	Infected	148.12	7	7	9
38	297	Sample	Mock	150.53	7	7	9
39	6	Sample	Infected	149.47	3	5	5
39	123	Sample	Mock	149.12	3	5	5
40	193	Sample	Mock	147.5	5	7	5
40	243	Sample	Infected	149.28	5	7	5
41	146	Sample	Infected	153.16	5	7	7
41	311	Sample	Mock	147.78	5	7	7
42	105	Sample	Infected	161.97	7	7	7
42	282	Sample	Mock	158.4	7	7	7
43	95	Sample	Infected	149.49	9	9	9
43	390	Sample	Mock	149.5	9	9	9
44	75	Sample	Infected	147.74	7	7	9
44	374	Sample	Mock	157.96	7	7	9
45	173	Sample	Infected	160.2	9	9	7
45	203	Sample	Mock	148.77	9	9	7
46	94	Sample	Infected	153.4	9	7	9
46	267	Sample	Mock	149.41	9	7	9
47	2	Sample	Mock	147.27	7	7	5
47	140	Sample	Infected	154.88	7	7	5
48	63	Sample	Mock	148.42	3	5	7
48	114	Sample	Infected	145.41	5	5	5
48	170	Sample	Mock	151.38	5	7	5
48	179	Sample	Infected	158.4	5	5	5
48	354	Sample	Mock	148	5	5	5
48	386	Sample	Infected	156.48	5	5	5
49	220	Sample	Infected	151.25	7	7	7
49	381	Sample	Mock	143.26	7	7	7
50	83	Sample	Infected	151.45	7	7	7

50	89	Sample	Mock	146.81	7	7	7
51	215	Sample	Mock	148.4	7	7	7
51	338	Sample	Infected	152.95	7	7	7
52	30	Sample	Mock	155.99	7	5	9
52	49	Sample	Infected	147.44	7	5	9
53	183	Sample	Infected	154.86	5	5	5
53	227	Sample	Mock	147.39	5	5	5
54	48	Sample	Mock	156.88	5	5	5
54	314	Sample	Infected	151.58	5	5	5
55	191	Sample	Infected	152.52	5	7	7
55	318	Sample	Mock	158.75	5	7	7
56	67	Sample	Infected	153.72	3	5	5
56	414	Sample	Mock	147.64	3	5	5
57	23	Sample	Infected	158.37	3	3	3
57	134	Sample	Mock	151.9	3	3	3
58	157	Sample	Infected	161.45	5	5	5
58	283	Sample	Mock	151.9	5	5	5
59	289	Sample	Infected	152.85	5	5	5
59	329	Sample	Mock	148.05	5	5	5
60	271	Sample	Infected	149.16	1	3	3
60	364	Sample	Mock	148.76	1	3	3
61	130	Sample	Mock	149.93	3	5	5
61	233	Sample	Infected	146.92	3	5	5
62	125	Sample	Mock	149.52	7	7	7
62	278	Sample	Infected	151.37	7	7	7
63	133	Sample	Mock	154.98	5	7	7
63	398	Sample	Infected	153.82	5	7	7
64	59	Sample	Mock	154.87	5	5	7
64	210	Sample	Infected	150.19	5	5	7
65	53	Sample	Infected	146.05	5	7	7
65	224	Sample	Mock	158.47	5	7	7
66	15	Sample	Infected	164.21	7	5	7
66	209	Sample	Mock	147.57	7	5	7
67	132	Sample	Mock	158	3	3	3
67	194	Sample	Infected	154.33	3	3	3
68	22	Sample	Mock	152.92	5	5	7
68	88	Sample	Infected	156.43	5	5	7
69	33	Sample	Infected	152.45	1	3	3

69	38	Sample	Mock	150.77	1	3	3
70	156	Sample	Mock	150.46	7	7	5
70	171	Sample	Infected	160.56	7	7	5
71	85	Sample	Infected	151.48	5	3	3
71	200	Sample	Mock	147.87	5	3	3
72	139	Sample	Mock	153.1	5	5	5
72	187	Sample	Infected	153.2	5	5	5
73	65	Sample	Mock	149.7	5	7	5
73	272	Sample	Infected	150.39	5	7	5
74	323	Sample	Mock	148.01	7	5	7
74	387	Sample	Infected	152.09	7	5	7
75	35	Sample	Infected	150.26	7	9	9
75	135	Sample	Mock	152.7	3	5	7
75	166	Sample	Mock	145.36	5	7	5
75	188	Sample	Infected	151.46	9	9	7
75	345	Sample	Infected	147.01	7	7	7
75	406	Sample	Mock	162.31	5	5	5
76	138	Sample	Mock	146.29	7	5	5
76	154	Sample	Infected	152	7	5	5
77	47	Sample	Mock	147.6	3	5	7
77	55	Sample	Infected	145.5	9	7	7
77	189	Sample	Infected	159.33	7	7	7
77	234	Sample	Mock	153.24	5	7	5
77	280	Sample	Infected	163.24	7	7	7
77	394	Sample	Mock	152.8	5	5	5
78	25	Sample	Infected	147.08	7	7	9
78	90	Sample	Mock	145.64	3	5	7
78	142	Sample	Infected	150.23	7	7	7
78	246	Sample	Mock	157	5	7	5
78	319	Sample	Mock	152.37	5	5	5
78	360	Sample	Infected	156.51	9	9	7
79	62	Sample	Mock	150.97	5	5	7
79	404	Sample	Infected	159.5	5	5	7
80	32	Sample	Mock	157.21	5	5	3
80	99	Sample	Infected	154.87	5	5	3
81	153	Sample	Mock	149.78	7	5	7
81	223	Sample	Infected	155.91	7	5	7
82	131	Sample	Mock	148.06	3	3	5

82	257	Sample	Infected	152.4	3	3	5
83	9	Sample	Mock	165	5	5	7
83	141	Sample	Infected	145.92	5	5	7
84	212	Sample	Infected	148.98	5	5	5
84	312	Sample	Mock	149.15	5	5	5
85	216	Sample	Infected	158.27	7	7	7
85	335	Sample	Mock	153.54	7	7	7
86	26	Sample	Mock	159.46	5	5	5
86	395	Sample	Infected	159.95	5	5	5
87	17	Sample	Mock	153.2	7	5	5
87	152	Sample	Infected	148.78	7	5	5
88	4	Sample	Infected	153.46	5	7	7
88	91	Sample	Mock	153.7	5	7	7
89	106	Sample	Mock	154.25	9	7	7
89	352	Sample	Infected	150.96	9	7	7
90	304	Sample	Infected	145.27	5	5	7
90	380	Sample	Mock	149.67	5	5	7
91	100	Sample	Infected	145.99	7	5	5
91	240	Sample	Mock	154.73	7	5	5
92	328	Sample	Infected	148.12	1	3	5
92	391	Sample	Mock	148.1	1	3	5
93	288	Sample	Infected	148.5	3	3	7
93	384	Sample	Mock	152	3	3	7
94	348	Sample	Mock	146.86	5	7	7
94	366	Sample	Infected	152.5	5	7	7
95	50	Sample	Mock	145.95	1	5	5
95	58	Sample	Infected	155.4	1	5	5
96	12	Sample	Mock	149.88	5	5	7
96	302	Sample	Infected	144.07	5	5	7
97	128	Sample	Mock	150.09	9	7	7
97	411	Sample	Infected	149.54	9	7	7
98	16	Sample	Infected	151.31	5	7	5
98	192	Sample	Mock	147.64	5	7	5
99	27	Sample	Mock	146.63	3	5	7
99	71	Sample	Infected	154.48	9	7	7
99	186	Sample	Mock	147.75	5	7	5
99	206	Sample	Infected	147.4	5	5	5
99	300	Sample	Mock	146.52	5	5	5

99	397	Sample	Infected	148.74	5	5	5
100	117	Sample	Infected	152.07	3	3	3
100	299	Sample	Mock	153.3	3	3	3
101	115	Sample	Infected	152	9	9	7
101	150	Sample	Mock	147.62	9	9	7
102	68	Sample	Mock	150.53	5	3	3
102	256	Sample	Infected	156.6	5	3	3
103	178	Sample	Mock	145.35	1	1	3
103	412	Sample	Infected	152.42	1	1	3
104	80	Sample	Infected	166.23	5	5	5
104	102	Sample	Mock	155.33	5	5	5
105	213	Sample	Infected	145.95	3	5	5
105	221	Sample	Mock	149.75	3	5	5
106	101	Sample	Mock	157.72	5	7	5
106	241	Sample	Infected	167.73	5	7	5
107	160	Sample	Infected	155.43	5	5	5
107	254	Sample	Mock	160.67	5	5	5
108	144	Sample	Mock	151.78	7	7	5
108	265	Sample	Infected	146.05	7	7	5
109	195	Sample	Mock	153.09	1	3	3
109	270	Sample	Infected	145.96	1	3	3
110	330	Sample	Infected	156.44	5	3	5
110	336	Sample	Mock	143.86	5	3	5
111	197	Sample	Infected	148.91	5	3	5
111	293	Sample	Mock	146	5	3	5
112	255	Sample	Infected	147.7	3	5	5
112	350	Sample	Mock	155.51	3	5	5
113	180	Sample	Infected	149.91	7	5	5
113	362	Sample	Mock	148.8	7	5	5
114	1	Sample	Infected	159.66	9	7	7
114	18	Sample	Mock	150	9	7	7
115	43	Sample	Mock	151.8	5	5	7
115	239	Sample	Infected	155.05	5	5	7
116	167	Sample	Mock	150.23	7	5	7
116	361	Sample	Infected	152.82	7	5	7
117	401	Sample	Mock	146.59	7	7	7
117	408	Sample	Infected	152.35	7	7	7
118	176	Sample	Mock	152.43	9	7	7

118	277	Sample	Infected	161.54	9	7	7
119	315	Sample	Infected	153.46	3	3	3
119	377	Sample	Mock	152.68	3	3	3
120	112	Sample	Infected	143.61	5	5	3
120	403	Sample	Mock	148.93	5	5	3
121	382	Sample	Mock	147.1	3	3	5
121	409	Sample	Infected	158.99	3	3	5
122	145	Sample	Mock	150.22	7	7	5
122	305	Sample	Infected	151.25	7	7	5
123	74	Sample	Infected	157.06	5	5	3
123	228	Sample	Mock	150.35	5	5	3
124	185	Sample	Infected	151.47	3	5	5
124	388	Sample	Mock	146	3	5	5
125	82	Sample	Mock	149.15	3	5	5
125	332	Sample	Infected	163.52	3	5	5
126	353	Sample	Infected	143.69	5	5	5
126	379	Sample	Mock	147.91	5	5	5
127	60	Sample	Infected	154.83	7	5	5
127	199	Sample	Mock	154.4	7	5	5
128	103	Sample	Mock	157.67	7	7	7
128	250	Sample	Infected	156.29	7	7	7
129	92	Sample	Infected	148.91	7	7	9
129	175	Sample	Mock	150.33	7	7	9
130	262	Sample	Infected	153.7	5	5	7
130	313	Sample	Mock	156.38	5	5	7
131	73	Sample	Infected	157.99	7	5	5
131	158	Sample	Mock	160.23	7	5	5
132	66	Sample	Mock	150.23	3	3	3
132	372	Sample	Infected	151.2	3	3	3
133	11	Sample	Infected	147.38	5	5	7
133	307	Sample	Mock	151.95	5	5	7
134	122	Sample	Mock	151.92	3	3	5
134	236	Sample	Infected	165.76	3	3	5
135	177	Sample	Mock	150	5	5	5
135	334	Sample	Infected	147.14	5	5	5
136	198	Sample	Mock	158.22	5	3	5
136	204	Sample	Infected	154.34	5	3	5
137	217	Sample	Mock	152.46	5	5	5

137	326	Sample	Infected	159.19	5	5	5
138	231	Sample	Mock	149.52	5	5	5
138	371	Sample	Infected	160.86	5	5	5
139	149	Sample	Mock	167.68	1	3	3
139	347	Sample	Infected	152.23	1	3	3
140	45	Sample	Mock	148	7	5	7
140	93	Sample	Infected	161.65	7	5	7
141	172	Sample	Infected	147.71	9	7	7
141	405	Sample	Mock	154.45	9	7	7
142	14	Sample	Mock	159.07	7	5	7
142	164	Sample	Infected	158.35	7	5	7
143	5	Sample	Mock	156.47	5	3	5
143	260	Sample	Infected	152.56	5	3	5
144	19	Sample	Infected	144.78	7	7	7
144	229	Sample	Mock	152.09	7	7	7
145	77	Sample	Infected	149	7	5	7
145	376	Sample	Mock	157	7	5	7
146	281	Sample	Mock	145.64	7	5	5
146	357	Sample	Infected	150.36	7	5	5
147	64	Sample	Infected	152.73	5	3	5
147	358	Sample	Mock	150.3	5	3	5
148	3	Sample	Infected	161.86	9	7	9
148	269	Sample	Mock	153.6	9	7	9
149	306	Sample	Mock	148.8	5	3	5
149	402	Sample	Infected	161.87	5	3	5
150	252	Sample	Infected	146.97	7	5	7
150	261	Sample	Mock	152.95	7	5	7
151	218	Sample	Mock	149.39	9	7	7
151	396	Sample	Infected	149.68	9	7	7
152	10	Sample	Mock	149.7	9	5	7
152	373	Sample	Infected	156.36	9	5	7
153	238	Sample	Mock	147.7	7	7	7
153	393	Sample	Infected	158.13	7	7	7
154	116	Sample	Mock	154.65	3	3	5
154	161	Sample	Infected	147.95	3	3	5
155	79	Sample	Mock	149.18	5	5	7
155	356	Sample	Infected	159.12	5	5	7
156	284	Sample	Infected	165.68	9	9	9

156	389	Sample	Mock	165.54	9	9	9
157	96	Sample	Mock	150.37	5	3	5
157	286	Sample	Infected	150.88	5	3	5
158	291	Sample	Infected	146.85	5	5	3
158	316	Sample	Mock	147.3	5	5	3
159	84	Sample	Infected	153.08	3	3	5
159	263	Sample	Mock	145.48	3	3	5
160	110	Sample	Infected	146.3	7	5	5
160	181	Sample	Mock	153.66	7	5	5
161	159	Sample	Infected	151.72	5	5	7
161	266	Sample	Mock	150	5	5	7
162	29	Sample	Infected	158.76	7	7	7
162	72	Sample	Mock	153.99	7	7	7
163	341	Sample	Mock	151.01	5	5	7
163	375	Sample	Infected	148.24	5	5	7
164	207	Sample	Infected	148.15	1	1	3
164	331	Sample	Mock	150.24	1	1	3
165	76	Sample	Infected	145.88	1	3	3
165	378	Sample	Mock	148.88	1	3	3
166	320	Sample	Mock	156.29	3	3	3
166	321	Sample	Infected	148.18	3	3	3
167	225	Sample	Infected	144.68	5	5	7
167	301	Sample	Mock	157.6	5	5	7
168	184	Sample	Mock	153.37	9	7	9
168	407	Sample	Infected	153.99	9	7	9
169	202	Sample	Infected	156.04	3	5	7
169	308	Sample	Mock	147	3	5	7
170	37	Sample	Mock	152.32	7	7	7
170	127	Sample	Infected	149.84	7	7	7
171	219	Sample	Infected	147.47	5	5	5
171	369	Sample	Mock	153	5	5	5
172	165	Sample	Infected	148.63	3	5	5
172	339	Sample	Mock	149.25	3	5	5
173	36	Sample	Mock	152.58	7	7	7
173	344	Sample	Infected	166.14	7	7	7
174	201	Sample	Infected	153.93	5	7	7
174	279	Sample	Mock	147.79	5	7	7
175	126	Sample	Mock	152.29	7	7	7

175	163	Sample	Infected	150.36	7	7	7
176	81	Sample	Mock	150.98	3	7	5
176	325	Sample	Infected	153.08	3	7	5
177	61	Sample	Infected	149.19	3	3	3
177	214	Sample	Mock	149.35	3	3	3
178	120	Sample	Mock	150.1	5	5	5
178	285	Sample	Infected	158.52	5	5	5
179	51	Sample	Infected	160.74	5	7	5
179	333	Sample	Mock	146.67	5	7	5
180	147	Sample	Mock	149.61	7	7	7
180	248	Sample	Infected	149.98	7	7	7
181	44	Sample	Mock	146.2	5	7	5
181	244	Sample	Infected	153.1	5	7	5
182	41	Sample	Mock	150	7	5	5
182	337	Sample	Infected	155.11	7	5	5
183	20	Sample	Mock	145.94	7	5	7
183	56	Sample	Infected	148.49	7	5	7
184	174	Sample	Mock	159.99	5	7	5
184	400	Sample	Infected	151.2	5	7	5
185	205	Sample	Mock	151.98	5	3	3
185	211	Sample	Infected	150.22	5	3	3
186	151	Sample	Mock	161.85	7	5	5
186	162	Sample	Infected	153.23	7	5	5
187	310	Sample	Mock	154.24	7	5	7
187	346	Sample	Infected	149.53	7	5	7
188	31	Sample	Mock	149.38	7	7	5
188	322	Sample	Infected	156.38	7	7	5
189	273	Sample	Mock	150.6	3	5	5
189	392	Sample	Infected	159.7	3	5	5
190	78	Sample	Infected	148.43	9	5	7
190	317	Sample	Mock	150.7	9	5	7
191	124	Sample	Mock	149.6	5	5	5
191	169	Sample	Infected	154.7	5	5	5
192	232	Sample	Mock	147.12	7	7	7
192	290	Sample	Infected	151.91	7	7	7
193	137	Sample	Infected	153.42	5	7	7
193	276	Sample	Mock	158.56	5	7	7
Blank	415	Blank	Blank	150			

Blank	416	Blank	Blank	150			
Blank	417	Blank	Blank	150			
Blank	418	Blank	Blank	150			
Pool	21	Pool	Pool	152.45			
Pool	109	Pool	Pool	147.76			
Pool	155	Pool	Pool	153.77			
Pool	274	Pool	Pool	147.75			
Pool	309	Pool	Pool	149.2			
Pool	368	Pool	Pool	151.85			

8.2 Authentic standards

Table 13: List of authentic standards analyzed in the study.

No.	Name	Purity	Sum formula	MW	Monoisotopic Mass	rt Standard_pos	rt Standard_neg
1	Xanthohumol	pure	C21H22O5	354.39638	354.146724	137.3	133.8
2	Humulones salt	mix	C21H30O5	362.4599	362.209324	158.2	151.4
3	Lupulones salt	mix	C26H38O4	414.57752	414.27701	183.8	176.7
4	Caffeic acid	pure	C9H8O4	180.15742	180.042259	NA	NA
5	Phenylalanine	pure	C9H11NO2	165.18914	165.078979	8.5	NA
6	Naringenin	pure	C15H12O5	272.25278	272.068473	81.9	NA
7	Naringenin-7-o-glucoside	pure	C21H22O10	434.39338	434.121297	82.2	75.6
8	Epigallo-catechin	pure	C15H14O7	306.26746	306.073953	NA	NA
9	Valine	pure	C5H11NO2	117.14634	117.078979	NA	NA
10	Quercetin	pure	C15H10O7	302.2357	302.042653	94	87.8
11	Ferulic acid	pure	C10H10O4	194.184	194.057909	67.5	60.9
12	Rutin	pure	C27H30O16	610.5175	610.153385	76.7	71.8
13	Isoferulic acid	pure	C10H10O4	194.184	194.057909	69.4	NA
14	Epigallocatechin gallate	pure	C22H18O11	458.3717	458.084911	59.4	NA
15	4-coumaric-acid	pure	C9H8O3	164.15802	164.047344	55.1	50
16	Trans-cinnamic acid	pure	C9H8O2	148.15862	148.052429	87.8	NA
17	(-)-epigallocatechin gallate	pure	C22H18O11	458.3717	458.084911	59.4	NA
18	(-)-epicatechin	pure	C15H14O6	290.268	290.079038	58.5	54.3
19	Metalaxyl	mix	C15H21NO4	279.33	279.147058	NA	NA
20	(-)- epigallocatechin	pure	C15H14O7	306.26746	306.073953	NA	NA
21	Gallic acid	pure	C7H6O5	170.11954	170.021523	NA	NA
22	Kaempferol	pure	C15H10O6	286.2363	286.047738	104.3	98
23	Scopolin	pure	C16H18O9	354.31	354.095082	57.3	52.5
24	N6-Isopentenyladenine	pure	C10H13N5	203.24	203.1170955	59.5	NA
25	cis -Zeatin	pure	C10H13N5O	219.24	219.1120101	30	NA
26	trans -Zeatin	pure	C10H13N5O	219.24	219.1120101	24.1	NA
27	Dihydrozeatin	pure	C10H15N5O	221.26	221.1276601	30	NA
28	N6 -Isopentenyladenosine	pure	C15H21N5O4	335.36	335.1593542	72.9	NA
29	cis -Zeatin riboside	pure	C15H21N5O5	351.36	351.1542688	54.3	NA
30	trans -Zeatin riboside	pure	C15H21N5O5	351.36	351.1542688	52.2	NA
31	Dihydrozeatinriboside	pure	C15H23N5O5	353.17	353.1699189	53.2	NA
32	trans -Zeatin -O -glucoside	pure	C16H23N5O6	381.38	381.1648335	33	NA
33	trans -Zeatin -9 -glucoside	pure	C16H23N5O6	381.387	381.1648335	37.5	NA
34	trans -Zeatin -O -glucoside riboside	pure	C21H31N5O10	513.51	513.2070922	53.2	NA
35	L-Phenylalanin	pure	C6H11NO2	165.15	165.078979	8.5	NA
36	Giberrellic acid	pure	C19H22O6	346.37	346.141638	67.8	69.2
37	Kinetin	pure	C10H9N	215.21	215.080704	42.9	NA
38	L-Tyrosine	pure	C9H11NO3	181.19	181.073898	NA	NA
39	Riboflavin (B2)	pure	C17H20N4O6	376.4	376.138275	62	NA
40	Thiamin	pure	C12H17CIN4OS	300.81	300.081146	NA	NA
41	Salicylsäure	pure	C7H6O3	138.12	138.031694	NA	53.2
42	(-)-Jasmonic Acid	pure	C12H18O3	210.27	210.125594	NA	96
43	(-)-Jasmonic Acid Methyl Ester	pure	C13H20O3	224.3	224.2961	NA	NA
44	(+)-Abscisic acid	pure	C15H20O4	264.32	264.136159	NA	88.8
45	Indole-3-acetic acid	pure	C10H9NO2	175.18	175.063329	NA	66.4

8.3 MS/MS spectra of DMR correlated phenylpropanoids

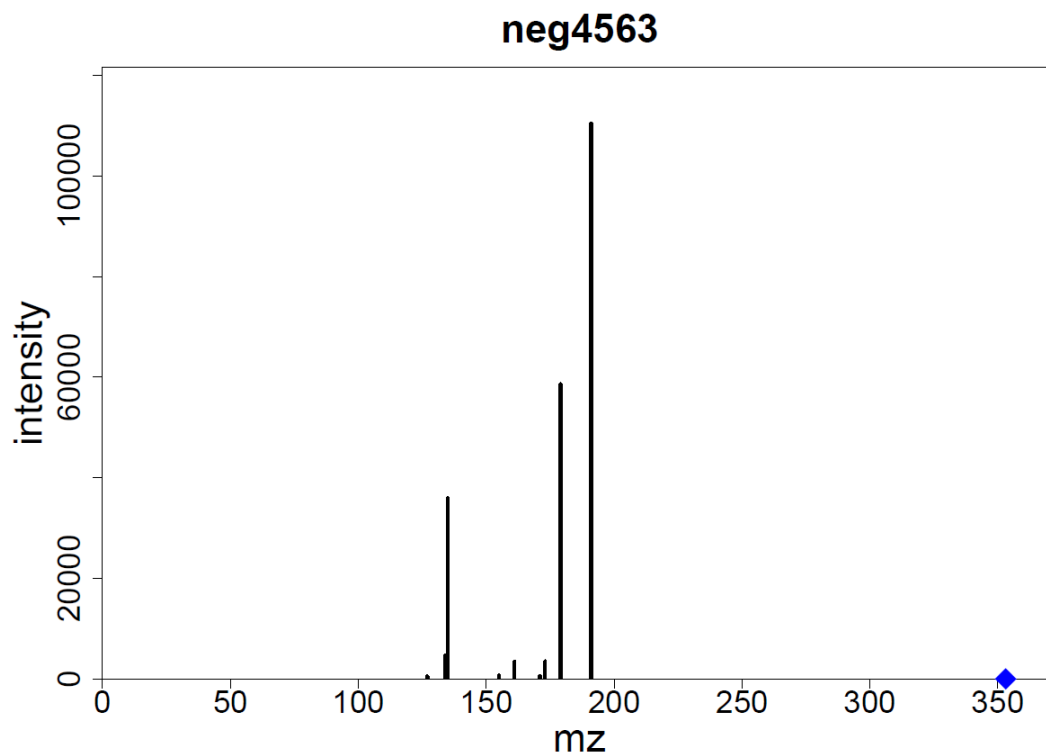


Figure 32: MS/MS spectrum of mass ID neg4563, $m/z=353.09$

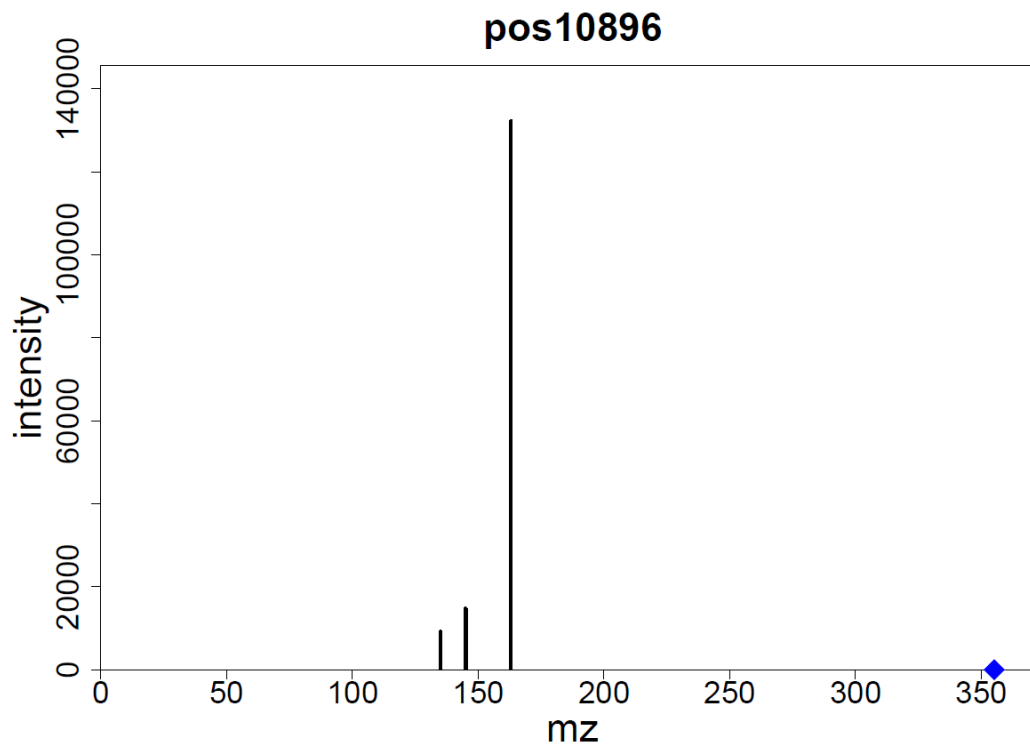


Figure 33: MS/MS spectrum of mass ID pos10896, $m/z=355.10$

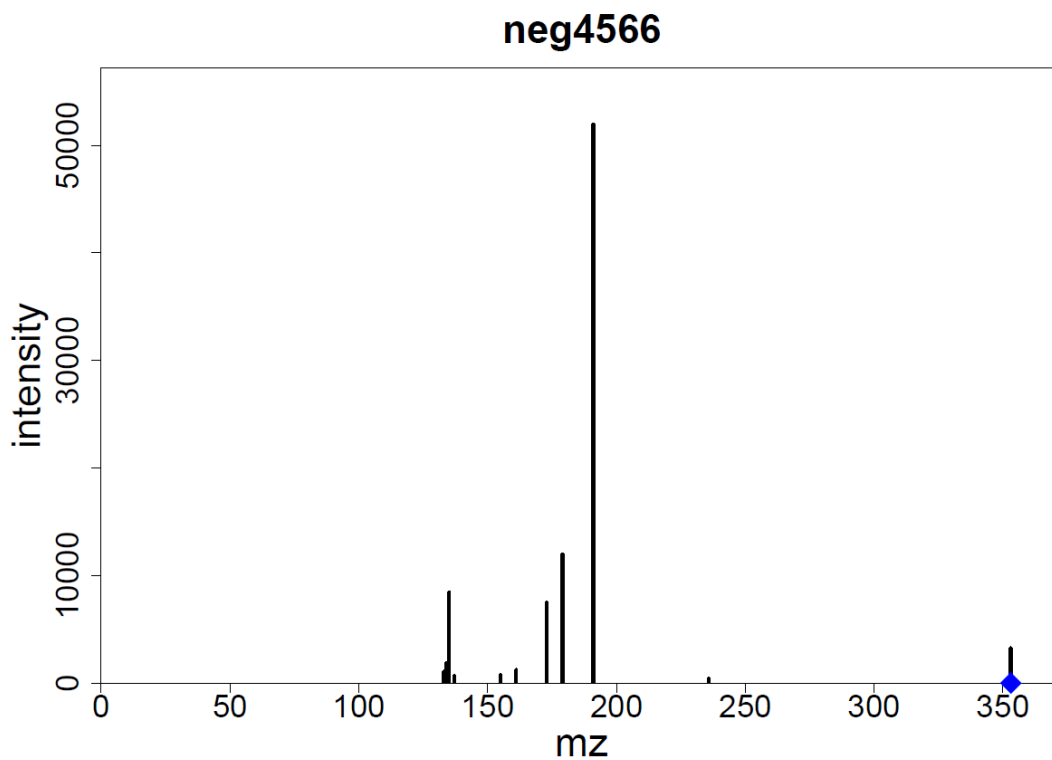


Figure 34: MS/MS spectrum of mass ID neg4566, $m/z= 353.09$

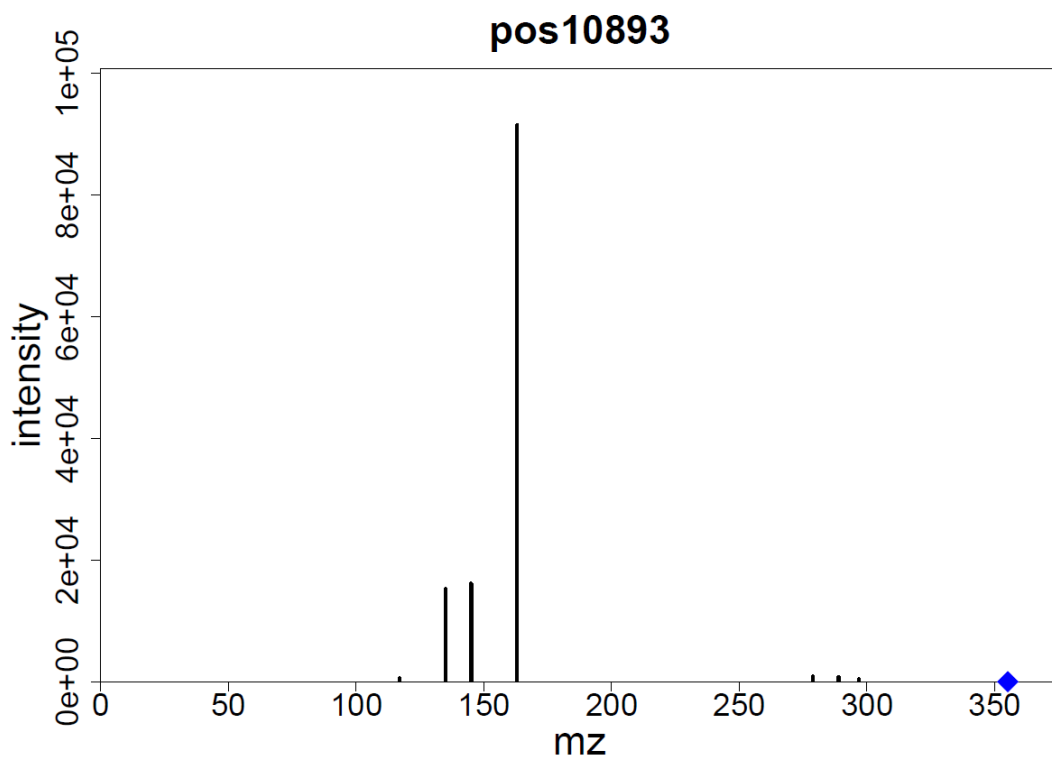


Figure 35: MS/MS spectrum of mass ID pos10893, $m/z= 355.10$

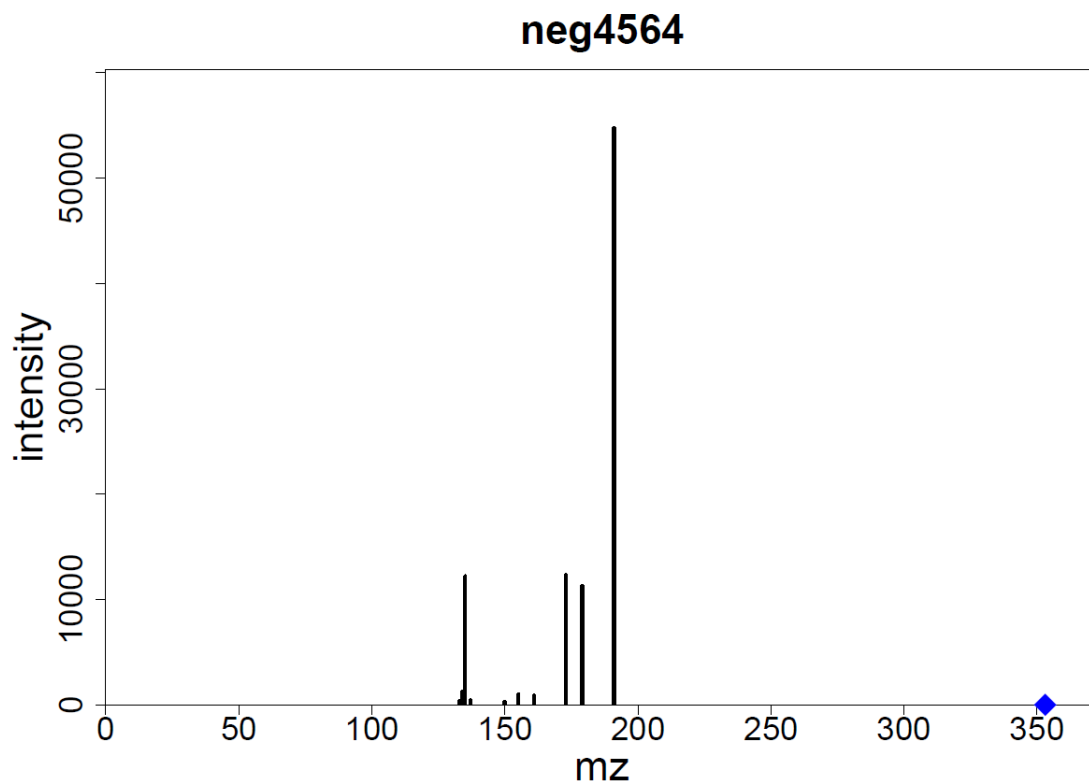


Figure 36: MS/MS spectrum of mass ID neg4564, $m/z= 353.09$

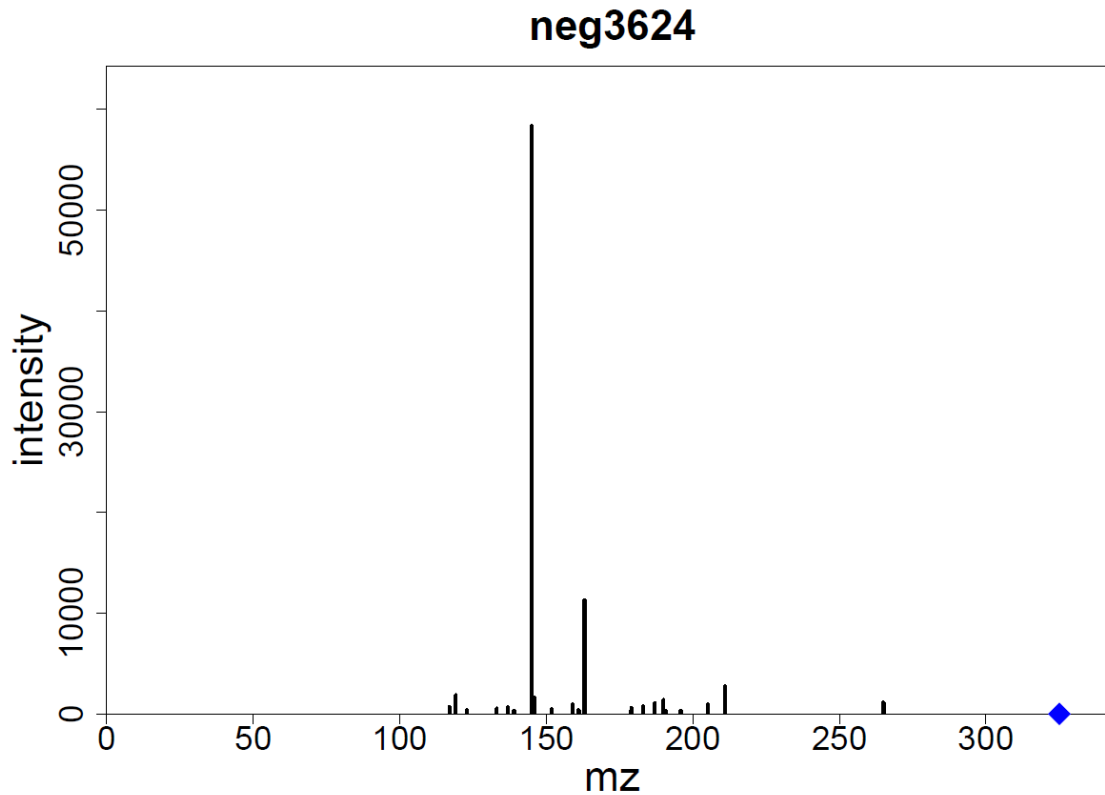


Figure 37: MS/MS spectrum of mass ID neg3624, $m/z= 325.09$

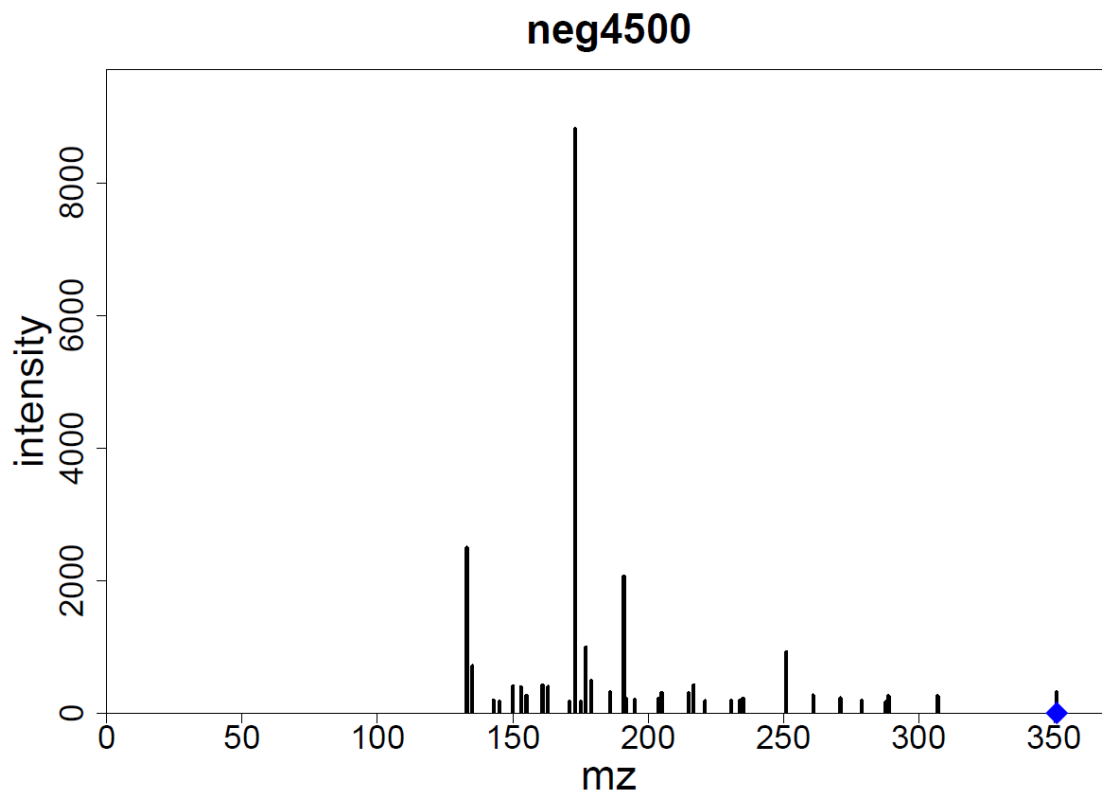


Figure 38: MS/MS spectrum of mass ID neg4500, $m/z= 351.07$

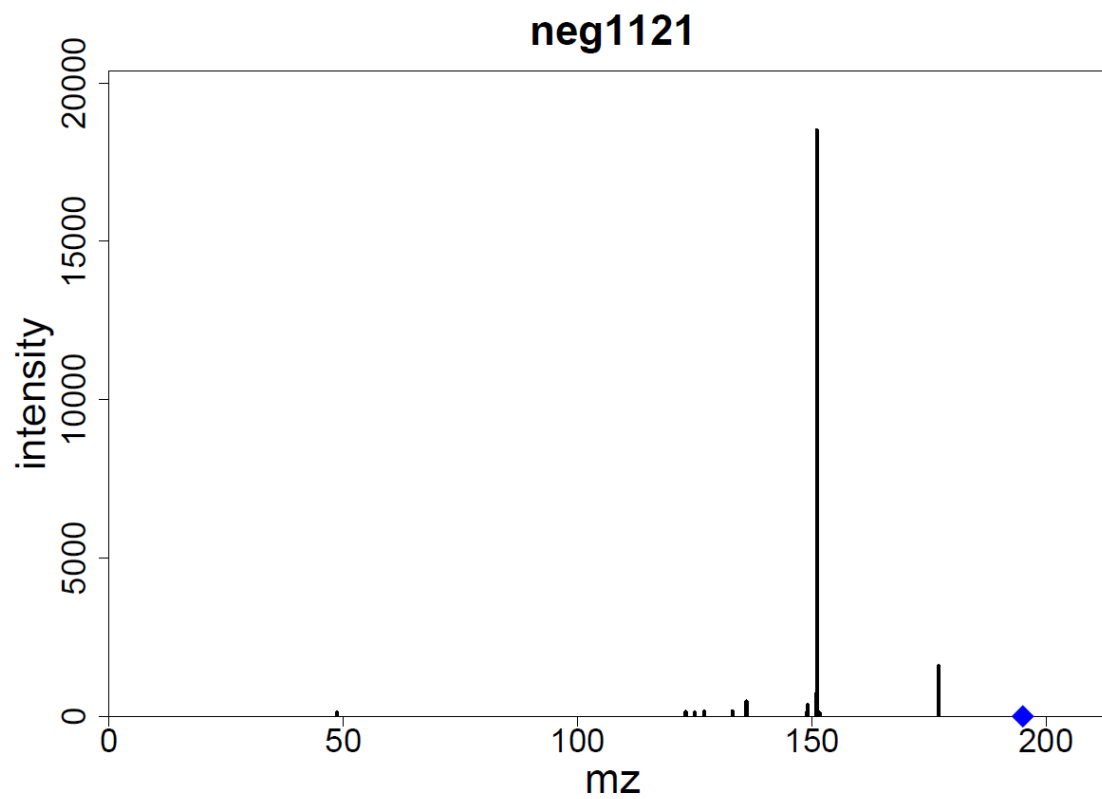


Figure 39: MS/MS spectrum of mass ID neg1121, $m/z= 195.06$

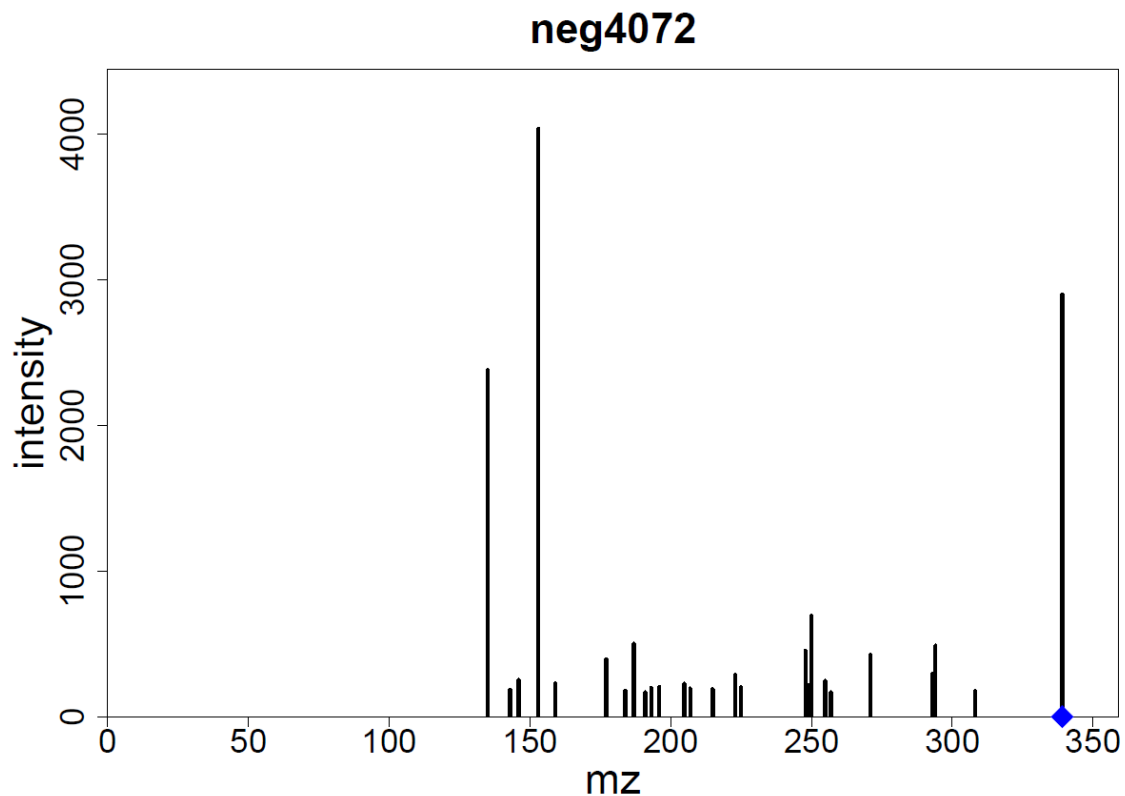
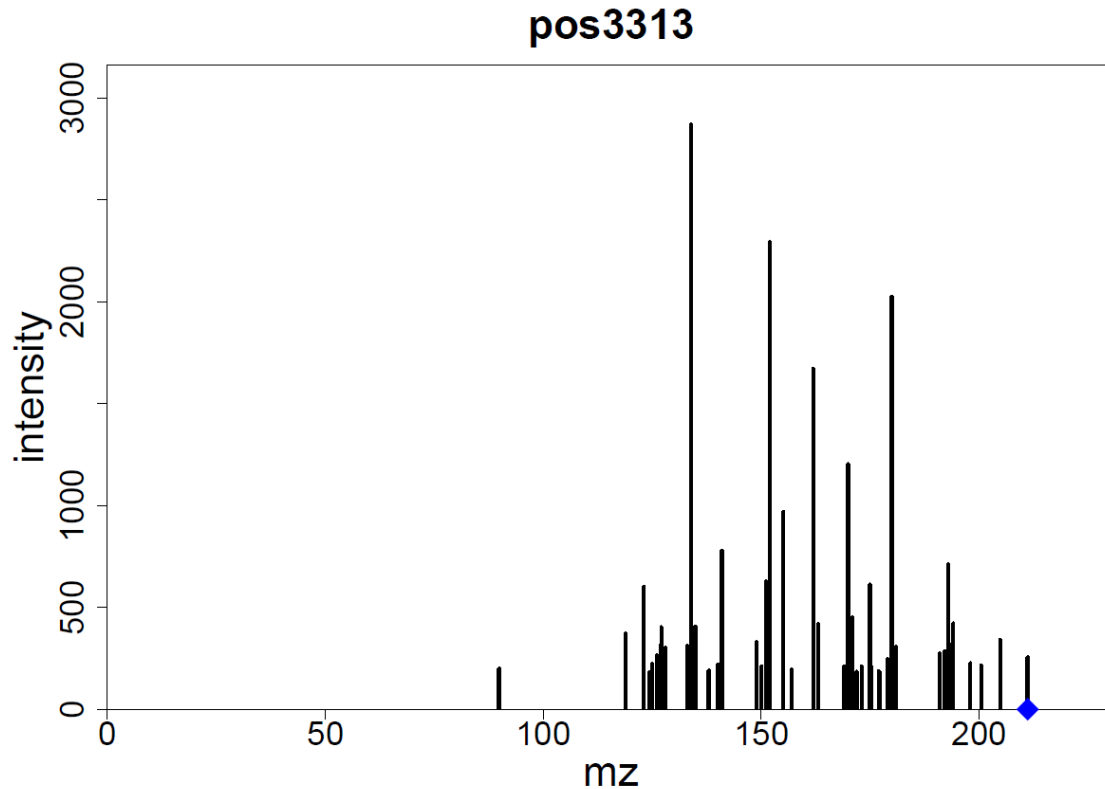
Figure 40: MS/MS spectrum of mass ID neg4072, $m/z= 195.07$ Figure 41: MS/MS spectra of mass ID pos3313, $m/z= 211.10$

Table 14: *m/z* intensities of MS/MS spectra of DMR correlated phenylpropanoids

Compound	Mass-ID	<i>m/z</i> intensity	Compound	Mass-ID	<i>m/z</i> intensity
Coniferyl aldehyde	pos3313	89.8389 200	Chlorogenic acid	neg4563	127.0394 562
		118.919 372			134.0374 4736
		122.9418 574			135.0449 36006
		123.0453 602			155.0349 792
		124.4209 184			161.024 3490
		124.9449 224			171.0298 580
		125.9863 266			173.0455 3508
		127.0399 320			179.035 58650
		127.0743 404			191.0563 110470
		127.9657 302			
		133.1001 312	Chlorogenic acid	neg4566	133.0292 1092
		133.8956 2872			134.0376 1874
		134.8919 406			135.0451 8462
		137.947 188			137.0236 670
		138.0551 190			155.0348 770
		140.0634 220			161.0236 1234
		140.9524 778			173.0459 7506
		148.9415 330			179.0349 11974
		150.0675 212			191.0564 51962
		151.0385 628			235.9002 418
	353.0876 3260				
	Chlorogenic acid	neg4564	133.029 388		
151.8944 384			134.0367 1264		
151.9063 2294			135.0448 12214		
155.0344 970			137.0227 476		
156.958 196			149.9093 300		
161.9019 1672			155.0363 1026		
163.0371 418			161.0233 868		
169.0493 210			173.0455 12354		
169.9169 1204			179.0353 11302		
170.914 450			191.0164 338		
171.8661 186	191.0564 54780				
173.002 212					
	<i>cis-/trans-β-D-Glucosyl-2-hydroxycinnamic acid</i>	neg3624	117.0335 716		
174.9233 614			119.0504 1866		
175.0731 274			122.9697 400		
175.1472 210			133.0643 546		
176.9382 188			136.9489 660		
177.078 184			138.9636 318		
178.9011 246			145.0154 780		
179.4555 192			145.0295 58416		
179.9135 2024			145.942 1610		
180.9338 308			151.9088 458		
190.9041 276			159.0449 984		
192.1027 286			160.912 374		
192.9323 712					

		192.9749 324		161.062 392
		194.0453 422		163.0237 674
		197.9595 226		163.0399 11306
		200.4546 216		178.9787 332
		204.8291 342		179.0555 600
		211.0736 256		182.9547 756
Chlorogenic acid	pos10893	117.033 586		187.0406 1084
		135.044 15304		189.9315 1390
		145.0281 16160		190.9217 296
		163.039 91526		195.8972 318
		278.8966 866		205.0492 960
		288.8929 786		210.9221 296
		296.9076 490		210.9502 2784
Chlorogenic acid	pos10896	135.0437 9148		265.0726 1142
		145.0281 14804	Fraxin	neg4500
		163.0387 132306		133.0296 2496
		355.1017 1060		135.0444 710
				142.9913 194
				145.0294 168
				150.0318 408
				153.0182 390
				155.0339 260
				161.023 418
				163.0404 396
				170.9596 168
				173.0453 8818
				175.0437 170
				177.0181 992
				179.0336 482
				186.025 314
				191.0564 2060
				191.9212 212
				195.03 206
				203.9324 216
				204.9934 308
				215.0568 300
				216.8461 420
				221.0592 184
				230.8271 186
				233.8401 182
				235.0589 218
				251.1135 922
				261.0347 268
				271.0609 226
				278.8806 186
				287.8914 172
				288.8933 258
				307.0773 258
				351.0307 312

4-Coumaryl alcohol	neg1121	48.6672 116
		123.0805 150
		125.0247 118
		127.0755 156
		133.0635 162
		136.0546 472
		148.9845 132
		149.061 358
		151.0039 738
		151.0765 18514
		151.2822 102
		151.6355 112
		177.056 1588
Sinapoyl malate/ Ci- choriin/Escu- lin	neg4072	135.0086 2380
		135.0816 180
		142.9327 186
		145.9388 254
		153.0188 4036
		158.9886 232
		177.0193 310
		177.0557 396
		183.8583 180
		186.9385 502
		190.963 168
		193.0546 198
		195.8994 206
		204.877 228
		206.9581 194
		214.9375 190
		222.8711 286
		224.9246 204
		247.8904 454
		248.8722 218
		250.0032 692
		254.9297 248
		256.8868 168
270.9291 424		
293.0288 296		
293.9933 488		
308.109 176		
339.0721 2898		

8.4 Sequence BLAST of DMR association markers

Table 15: Candidate genes on 'Shinshu Wase' scaffolds containing SNPs in LD with DMR Markers S3_50054921, S3_50054946, S3_50054950 in target organism *Arabidopsis thaliana* (Lamesch et al. 2012).

Scaffold	SNP	bp	Gene start	Gene stop	DMR p-value	E value	BLAST Match	target sequence ID	Protein	Involved in
LD153786	S3_50054950	12269	2064	5395	1.99E-08	1.00E-22	71%	gi 75161393 sp Q8VY07.1 EPN1_ARATH	Clathrin interactor EPSIN 1	EPSIN1 plays an important role in the vacuolar trafficking of soluble proteins at the trans-Golgi network via its interaction with gamma-ADR, VT111, VSR1, and clathrin. Associated with actin filaments and with the Golgi complex. Expressed in most tissues. The mRNA is cell-to-cell mobile.
LD156984	S3_165602689	25893	18796	19092	1.62E-06	4.00E-17	69%	gi 401036 sp P31843.1 RRPO_OENBE	RNA-directed DNA polymerase homolog	Reverse transcriptase homolog
LD132727	S1_38257074	59291	39196	50045	2.95E-06	2.00E-50	88%	gi 82055772 sp Q6XKE6.1 POLG_PVCV2	Genome polyprotein	Encodes presumably for at least four polypeptides: Movement protein (MP), capsid protein (CP), Protease (PR), and reverse transcriptase (RT)
LD149633	S2_344467036	22442	5139	6471	4.03E-06	8.00E-29	43%	gi 75215428 sp Q9XGM8.1 MGAT1_ARATH	Alpha-1,3-mannosyl-glycoprotein 2-beta-N-acetylglucosaminyltransferase	Encodes N-acetyl glucosaminyl transferase I, the first enzyme in the pathway of complex glycan biosynthesis.

LD140310	S1_656189702	21429	1470	2795	5.18E-06	3.00E-79	99%	gi 25453190 sp O23044.1 PER3_ARATH	Peroxidase 3	Removal of H ₂ O ₂ , oxidation of toxic reductants, biosynthesis and degradation of lignin, suberization, auxin catabolism, response to environmental stresses such as wounding, pathogen attack and oxidative stress
LD135333	S1_306003303	38206	64820	65488	5.85E-06	3.00E-38	26%	gi 75207660 sp Q9STE1.1 PP333_ARATH	Pentatricopeptide repeat-containing protein At4g21300	Tetratricopeptide repeat (TPR)-like superfamily protein
LD135889	S1_351372048	7779	43461	48658	6.06E-06	0	97%	gi 322510063 sp Q5G1S8.2 PP241_ARATH	Pentatricopeptide repeat-containing protein At3g18110, chloroplastic	Embryo development ending in seed dormancy
LD174130	S5_36779694	14112	9900	10046	7.56E-06	2.00E-11	9%	gi 73917789 sp Q9LXS6.1 CISY2_ARATH	Citrate synthase 2, peroxisomal	Peroxisomal citrate synthase required for the fatty acid respiration in seedlings, citrate being exported from peroxisomes into mitochondria during respiration of triacylglycerol (TAG). Indeed, complete respiration requires the transfer of carbon in the form of citrate from the peroxisome to the mitochondria.
LD176271	S5_82396152	13664	8366	8725	8.41E-06	2.00E-23	76%	gi 45477045 sp P92523.1 M860_ARATH	Uncharacterized mitochondrial protein AtMg00860	DNA/RNA polymerases superfamily protein
LD158113	S3_203217310	22283	17445	18876	1.17E-05	4.00E-64	57%	gi 75274240 sp Q9LUJ2.1 PP249_ARATH	Pentatricopeptide repeat-containing protein At3g22690	RNA modification, photosystem I assembly, photosystem II assembly, regulation of chlorophyll biosynthetic process, response to cold, response to high light intensity, thylakoid membrane organization
LD144550	S2_109756582	4565	38214	38588	1.23E-05	8.00E-30	89%	gi 401036 sp P31843.1 RRPO_OENBE	RNA-directed DNA polymerase homolog	Catalytic activity

LD140724	S1_680682070	44430	29034	29393	1.51E-05	6.00E-31	40%	gi 55976603 sp Q9LK95.1 MYB21_ARATH	Transcription factor MYB21	Gibberellic acid mediated signaling pathway, jasmonic acid mediated signaling pathway, red, far-red light phototransduction, regulation of transcription, DNA-templated, response to jasmonic acid, stamen development, stamen filament development
LD159889	S3_260034319	17313	5744	7363	1.61E-05	1.00E-95	62%	gi 264664533 sp COLGU5.1 Y5457_ARATH	Probable LRR receptor-like serine/threonine-protein kinase At5g45780	Anther development, homeostasis of number of meristem cells, phosphorylation, protein phosphorylation, transmembrane receptor protein tyrosine kinase signaling pathway
LD145270	S2_145385812	26171	7823	8500	1.68E-05	7.00E-61	93%	gi 45477041 sp P92519.1 M810_ARATH	Uncharacterized mitochondrial protein AtMg00810	DNA/RNA polymerases superfamily protein
LD142126	S1_762106818	31472	5262	12692	1.93E-05	2.00E-16	54%	gi 75146711 sp Q84JS6.1 KNAT6_ARATH	Homeobox protein knotted-1-like 6	Meristem maintenance, regulation of transcription, DNA-templated
LD132499	S1_3594487	81581	46213	48462	1.99E-05	0	100%	gi 122166805 sp Q09X17.1 PSAA_MORIN	Photosystem I P700 chlorophyll a apoprotein A1	PsaA and PsaB bind P700, the primary electron donor of photosystem I (PSI), as well as the electron acceptors A0, A1 and FX. PSI is a plastocyanin-ferredoxin oxidoreductase, converting photonic excitation into a charge separation, which transfers an electron from the donor P700 chlorophyll pair to the spectroscopically characterized acceptors A0, A1, FX, FA and FB in turn. Oxidized P700 is reduced on the luminal side of the thylakoid membrane by plastocyanin.

LD175939	S5_75368029	6036	3198	6321	2.03E-05	4.00E-74	98%	gij75161264 sp Q8VWZ7.1 C76B6_CATRO	Geraniol 8-hydroxylase	Hydroxylase involved in the biosynthesis of hydroxygeraniol, a precursor of the terpenoid indole alkaloids such as vinblastine and vincristine. Also able to hydroxylate in vitro nerol and to catalyze 3'-hydroxylation of the flavanone naringenin to form eriodictyol. No activity with apigenin, kaempferol, p-coumaric acid and ferulic acid as substrates
LD146174	S2_189158271	9522	1846	2211	2.18E-05	5.00E-54	74%	gij2851508 sp Q43291.2 RL211_ARATH	60S ribosomal protein L21-1	Translation protein SH3-like family protein
LD192590	S7_1574207	5813	5599	6238	2.47E-05	3.00E-29	88%	gij45477041 sp P92519.1 M810_ARATH	Uncharacterized mitochondrial protein AtMg00810	DNA/RNA polymerases superfamily protein
LD158867	S3_227723771	5132	4208	4873	2.61E-05	6.00E-60	92%	gij45477041 sp P92519.1 M810_ARATH	Uncharacterized mitochondrial protein AtMg00810	DNA/RNA polymerases superfamily protein
LD150129	S2_365162646	29886	8009	8329	2.61E-05	7.00E-38	22%	gij75249447 sp Q93Z00.1 TCP14_ARATH	Transcription factor TCP14	Cell proliferation, inflorescence development, regulation of defense response, regulation of seed germination, regulation of transcription, DNA-templated, response to abscisic acid, response to cytokinin, response to gibberellin
LD176733	S5_91802326	1938	10884	12020	2.88E-05	1.00E-82	46%	gij75334039 sp Q9FLW0.1 Y5241_ARATH	Probable receptor-like protein kinase At5g24010	Protein autophosphorylation
LD133123	S1_89744369	62150	6437	28241	2.92E-05	9.00E-31	93%	gij45477041 sp P92519.1 M810_ARATH	Uncharacterized mitochondrial protein AtMg00810	DNA/RNA polymerases superfamily protein

LD142521	S2_2448148	19024	12695	13628	2.94E-05	1.00E-17	36%	gi 75216958 sp Q9ZVC9.2 FRS3_ARATH	Protein FAR1-RELATED SEQUENCE 3	Regulation of transcription, DNA-templated, response to red or far red light
LD143980	S2_80659580	42274	24975	26927	2.97E-05	0	100%	gi 193806277 sp POC7R4.1 PP110_ARATH	Pentatricopeptide repeat-containing protein At1g69290	
LD141764	S1_741351487	36186	46011	46562	3.01E-05	1.00E-82	99%	gi 122166794 sp Q09X06.1 YCF4_MORIN	Photosystem I assembly protein Ycf4 (chloroplast) [Morus indica]	Seems to be required for the assembly of the photosystem I complex
LD141760	S1_741133195	40251	2663	3601	3.15E-05	7.00E-80	79%	gi 94707155 sp Q9ZUM9.3 ASHR2_ARATH	Histone-lysine <i>N</i> -methyltransferase ASHR2	Histone methyltransferase
LD139021	S1_575536215	22728	21735	23765	3.84E-05	0	95%	gi 75171206 sp Q9FK93.1 PP406_ARATH	Pentatricopeptide repeat-containing protein At5g39680	RNA modification, embryo development ending in seed dormancy
LD133647	S1_148044612	81183	77727	83844	4.23E-05	3.00E-75	100%	gi 75337549 sp Q9SR52.1 UREA_ARATH	Urease	nitrogen compound metabolic process, urea catabolic process
LD144059	S2_84773001	85441	59319	60476	4.53E-05	0	81%	gi 122224630 sp Q14FG1.1 PSBC_POPAL	Photosystem II CP43 reaction center protein	One of the components of the core complex of photosystem II (PSII). It binds chlorophyll and helps catalyze the primary light-induced photochemical processes of PSII. PSII is a light-driven water: plastoquinone oxidoreductase, using light energy to abstract electrons from H ₂ O, generating O ₂ and a proton gradient subsequently used for ATP formation

LD133857	S1_170275910	68321	2839	15680	4.62E-05	2.00E-131	100%	gi 75270141 sp Q53UH4.1 DUSKY_IPONI	Anthocyanidin 3-O-glucoside 2"-O-glucosyltransferase	Glycosyltransferase that mediates the glucosylation of anthocyanidin 3-O-glucosides to yield anthocyanidin 3-O-sophorosides. 3-O-sophoroside derivatives are required for the bright blue or red color of flowers
LD164023	S4_44897839	8054	2968	5272	4.97E-05	4.00E-54	67%	gi 75161525 sp Q8VYR3.1 TBL2_ARATH	Protein trichome birefringence-like 2	Encodes a member of the TBL (TRICHOME BIREFRINGENCE-LIKE) gene family containing a plant-specific DUF231 (domain of unknown function) domain. TBL gene family has 46 members, two of which (TBR/AT5G06700 and TBL3/AT5G01360) have been shown to be involved in the synthesis and deposition of secondary wall cellulose, presumably by influencing the esterification state of pectic polymers.
LD143588	S2_60196838	38730	526	2149	5.00E-05	2.00E-43	71%	gi 75213627 sp Q9SZL8.1 FRS5_ARATH	Protein FAR1-RELATED SEQUENCE 5	Regulation of transcription, DNA-templated, response to red or far red light
LD195724	S7_43369589	5227	281	826	5.02E-05	2.00E-17	30%	gi 125987635 sp P0C2F6.1 RNHX1_ARATH	Putative ribonuclease H protein At1g65750	Transposable_element_gene
LD137557	S1_476588588	30049	7078	12931	5.07E-05	7.00E-119	100%	gi 2494076 sp P93338.1 GAPN_NICPL	NADP-dependent glyceraldehyde-3-phosphate dehydrogenase	Important as a means of generating NADPH for biosynthetic reactions
LD168081	S4_153839718	6707	8836	13214	5.13E-05	1.00E-70	88%	gi 75181688 sp Q9M0Y3.1 ENT3_ARATH	Equilibrative nucleotide transporter 3	Encodes an equilibrative nucleoside transporter AtENT3. Mutations of this locus allow mutants to grow on uridine analogue fluorouridine.
LD132686	S1_32428922	123951	93871	95617	5.27E-05	4.00E-68	45%	gi 75248718 sp Q8W3Z1.1 BAMS_BETPL	Beta-amyrin synthase	Oxidosqualene cyclase converting oxidosqualene into beta-amyrin, generating five rings and

										eight asymmetric centers in a single transformation
LD148564	S2_298437343	30242	3419	4696	5.34E-05	2.00E-82	93%	gi 75206916 sp Q9SND9.1 Y3028_ARATH	Uncharacterized acetyltransferase At3g50280	Transferase activity, transferase activity, transferring acyl groups other than amino-acyl groups
LD141241	S1_711081052	38904	48191	51652	5.34E-05	4.00E-55	66%	gi 75207472 sp Q9SS90.1 RGLG1_ARATH	E3 ubiquitin-protein ligase RGLG1	Abscisic acid-activated signaling pathway, auxin metabolic process, cytokinin metabolic process, negative regulation of response to water deprivation, positive regulation of abscisic acid-activated signaling pathway, protein K63-linked ubiquitination
LD175346	S5_62802663	10441	3815	4921	5.46E-05	1.00E-18	58%	gi 125987635 sp POC2F6.1 RNHX1_ARATH	Putative ribonuclease H protein At1g65750	Transposable_element_gene
LD163285	S4_23621368	14949	18706	21468	5.61E-05	5.00E-31	94%	gi 75313305 sp Q9SD81.1 GDPD6_ARATH	Glycerophosphodiester phosphodiesterase GDPD6	Glycerol metabolic process, lipid metabolic process
LD136192	S1_375235060	65220	17143	17427	6.19E-05	7.00E-12	55%	gi 45477042 sp P92520.1 M820_ARATH	Uncharacterized mitochondrial protein AtMg00820	DNA/RNA polymerases superfamily protein
LD152259	S2_452226735	752	8246	12829	6.43E-05	8.00E-63	47%	gi 306531058 sp Q9M2T1.2 AP3BA_ARATH	AP3-complex subunit beta-A	Encodes PAT2, a putative beta-subunit of adaptor protein complex 3 (AP-3) that can partially complement the corresponding yeast mutant. Mediates the biogenesis and function of lytic vacuoles.
LD133565	S1_139357852	93787	85758	87613	6.59E-05	1.00E-90	39%	gi 75202765 sp Q9SCV1.1 BGA11_ARATH	Beta-galactosidase 11	Carbohydrate metabolic process

LD133734	S1_157098219	3034	76660	84467	6.63E-05	7.00E-50	92%	gi 44887921 sp Q94A76.2 GORK_ARATH	Potassium channel GORK	Ion transmembrane transport, ion transport, potassium ion transmembrane transport, regulation of ion transmembrane transport, response to abscisic acid, response to cold, response to jasmonic acid, response to water deprivation
LD137981	S1_506116632	37940	12387	13879	7.24E-05	0	90%	gi 5921932 sp Q42600.1 C84A1_ARATH	Ferulate-5-hydroxylase	Lignin biosynthetic process, oxidation-reduction process, phenylpropanoid biosynthetic process, response to UV-B
LD133909	S1_175533163	51059	36824	37312	7.46E-05	9.00E-90	70%	gi 122166793 sp Q09X05.1 CEMA_MORIN	Chloroplast envelope membrane protein (chloroplast) [Morus indica]	May be involved in proton extrusion. Indirectly promotes efficient inorganic carbon uptake into chloroplasts
LD134568	S1_239300846	108714	67053	68753	7.57E-05	2.00E-65	72%	gi 75213627 sp Q9SZL8.1 FRS5_ARATH	Protein FAR1-RELATED SEQUENCE 5	Regulation of transcription, DNA-templated, response to red or far red light
LD137218	S1_452195649	19019	36669	37433	7.66E-05	6.00E-19	31%	gi 75213095 sp Q9SWG3.1 FAR1_ARATH	Protein FAR-RED IMPAIRED RESPONSE 1	Far-red light signaling pathway, positive regulation of circadian rhythm, positive regulation of transcription, DNA-templated, red or far-red light signaling pathway, response to far red light, response to red or far red light
LD186101	S6_62372088	3436	2924	3563	7.84E-05	2.00E-17	84%	gi 45477041 sp P92519.1 M810_ARATH	Uncharacterized mitochondrial protein AtMg00810	DNA/RNA polymerases superfamily protein
LD180108	S5_157986106	2781	9467	10016	7.89E-05	3.00E-28	43%	gi 75338958 sp Q9ZSA8.1 DLO1_ARATH	Protein DMR6-LIKE OXYGENASE 1	Defense response to oomycetes, leaf senescence, oxidation-reduction process, response to bacterium, response to fungus, response to oomycetes, response to salicylic acid, salicylic acid catabolic process, secondary metabolic process

LD153337	S3_33002210	3751	20927	22204	8.66E-05	8.00E-138	94%	gi 75273965 sp Q9LSF1.1 OXI1_ARATH	Serine/threonine-protein kinase OXI1	Defense response, protein phosphorylation, response to oxidative stress, response to wounding
LD149073	S2_320518853	1819	12065	13504	8.79E-05	2.00E-105	98%	gi 75215431 sp Q9XGN4.1 GOLS1_AJURE	Galactinol synthase 1	Major galactinol synthase mainly involved in the biosynthesis of storage raffinose family oligosaccharides (RFOs) that function as osmoprotectants. May promote plant stress tolerance.
LD151637	S2_427612202	8993	2307	3160	8.82E-05	2.00E-42	76%	gi 75267749 sp Q9ZPE4.1 FBW2_ARATH	F-box protein FBW2	SCF-dependent proteasomal ubiquitin-dependent protein catabolic process, negative regulation of gene expression, posttranscriptional regulation of gene expression, protein ubiquitination, response to abscisic acid, ubiquitin-dependent protein catabolic process
LD141186	S1_707886568	38725	35433	36975	9.02E-05	7.00E-65	93%	gi 38605591 sp Q8LNZ5.1 XTHB_PHAAN	Probable xyloglucan endotransglucosylase/hydrolase protein B	Catalyzes xyloglucan endohydrolysis (XEH) and/or endotransglycosylation (XET). Cleaves and religates xyloglucan polymers, an essential constituent of the primary cell wall, and thereby participates in cell wall construction of growing tissues (By similarity)

9 Paper manuscript, patent application and presentations

Paper manuscript

Feiner A., Pitra N., Matthews P., Pillen, K., Wessjohann, L., Riewe, D.: Downy mildew resistance is genetically mediated by prophylactic production of phenylpropanoids in hops., submitted.

Patent application

Applicant: Simon H. Steiner, Hopfen, GmbH, Mainburg, Germany

European Patent Office: submitted on 13.12.2018

Title: Uses of compositions comprising at least one phenylpropanoid as antioomycotic agents.

Presentations

International Hop Growers' Convention (IHGC), St. Stefan am Walde, Austria

Feiner A., Zhang D., Matthews P., Riewe D., 2017: Metabolome-genome-wide association study of downy mildew resistance in hops (*Humulus lupulus* L.) reveals metabolite interaction, *Proceedings of the Scientific-Technical Commission*

Young Scientists Symposium (YSS), Bitburg/Trier, Germany

Feiner A., Zhang D., Matthews P., Pillen K., Wessjohann L., Riewe D., 2018: An untargeted metabolomics approach for identification of protective compounds against downy mildew in hops

12th Plant Science Student Conference (PSSC), Gatersleben, Germany

Feiner A., Zhang D., Matthews P., Pillen K., Wessjohann L., Riewe D., 2018: Metabolome-genome-wide association study of downy mildew resistance in hops (*Humulus lupulus* L.) dissects metabolic interaction

10 Danksagung

An erster Stelle möchte ich Prof. Dr. Klaus Pillen als meinem Doktorvater und Prof. Dr. Ludger Wessjohann als meinem Mentor sehr herzlich für die Betreuung und Möglichkeit danken, meine Promotion gemeinsam mit der Martin-Luther-Universität Halle/Wittenberg und dem Leibniz-Institut für Pflanzenbiochemie anfertigen zu können. Für die Übernahme des Drittgutachtens möchte ich mich recht herzlich bei Prof. Dr. Gerd Weber bedanken.

Ein besonderer Dank gilt Dr. David Riewe, der mir bei allen fachlichen Fragen zur Seite stand, für die hervorragende Zusammenarbeit bei der Anfertigung des Studiendesigns, der metabolischen Messungen bis hin zur Auswertung und der Darstellung der Daten und Lesen dieser Arbeit. Ebenfalls danke ich Janine Wiebach für die Mithilfe bei der Auswertung der metabolischen Daten sowie Andrea Apelt für ihre Mühen bei der Aufbereitung und Extraktion der Blattproben.

Dr. Lore Westphal und Annegret Laub möchte ich für die Mithilfe bei den Infektionsexperimenten danken, ohne deren Hilfe ich die Pflanzen im Phytoschrank nicht anziehen, infizieren und beproben hätte können. Dr. Andrea Porzel und Dr. Norbert Arnold danke ich für die guten fachlichen Gespräche und Ratschläge. Dr. Peter Darby danke ich besonders für die Zusendung der Pilzsporen, ohne welche die Infektion nicht stattfinden hätte können. Des Weiteren möchte ich mich bei ihm für das Lesen dieser Arbeit bedanken. Ich danke auch Dr. John Henning für seine Ratschläge bei der Erstellung der genetischen Karten.

Der Firma Simon H. Steiner, Hopfen, GmbH möchte ich für die Finanzierung dieses Projektes danken. Hierbei möchte ich mich vor allem bei den Geschäftsführern Pascal Piroué und Joachim Gehde für das ständige Vertrauen und Unterstützung meiner Arbeit bedanken. Dr. Paul Matthews möchte ich für das Mentoring innerhalb des Unternehmens und für seine fachlichen Ratschläge danken. Dr. Dong Zhang und Nicholi Pitra waren bei der Auswertung der genetischen Daten eine sehr große Hilfe, wofür ich mich sehr bedanken möchte.

Ein besonderer Dank gilt meiner Familie, besonders meinen Eltern, die mir das Studium und diesen Werdegang ermöglicht haben. Mein letzter und größter Dank gilt jedoch meiner Ehefrau Stefanie, für die unendliche Geduld, das Verständnis und unermüdliche Motivation in allen Situationen, die ich während dieser Promotion durchlaufen habe. Du warst stets meine größte Unterstützung und dafür bin ich Dir überaus dankbar.

11 Curriculum vitae

■ Personal data

Name: Alexander Eduard Feiner
 Date of birth: 19.08.1985
 Place of birth: Mainburg
 Nationality: German

■ Scientific education

Since 01/2014 External PhD student at Martin-Luther University Halle/Wittenberg and Leibniz-Institute of Plant Biochemistry, Halle (Saale)
 Thesis title: Genetic and metabolic analysis of downy mildew resistance in hops (*Humulus lupulus* L.)
 Supervisor: Prof. Dr. Klaus Pillen

10/2010-10/2012 Technical University München/Weihenstephan
 Degree: M.Sc. Agricultural Management

10/2005 – 03/2010 University of Applied Science Weihenstephan
 Degree: Engineer of Agriculture (Diploma)

09/1996 – 06/2005 Gabelsberger Gymnasium Mainburg
 Degree: A-Level (German: Abitur)

■ Work experience

Since 11/2012 Permanent employee at Simon H. Steiner, Hopfen, GmbH, Mainburg, Germany, Department Biotechnology and Biological Science

04/2010 – 10/2010 Internship Hopsteiner Breeding Program, Yakima, Washington State, USA

03/2009 – 03/2010 Internship at the Association of German Hop Growers, Wolnzach, Germany

10/2006 – 03/2007 Internship at Farm Franz Hauner, Stadlhof, Germany

12 Eidesstattliche Erklärung

Ich erkläre an Eides statt, dass ich die Arbeit selbstständig und ohne fremde Hilfe verfasst, keine anderen als die von mir angegebenen Quellen und Hilfsmittel benutzt und die den benutzten Werken wörtlich oder inhaltlich entnommenen Stellen als solche kenntlich gemacht habe.

Datum

Unterschrift des Antragstellers